



<https://theses.gla.ac.uk/>

Theses Digitisation:

<https://www.gla.ac.uk/myglasgow/research/enlighten/theses/digitisation/>

This is a digitised version of the original print thesis.

Copyright and moral rights for this work are retained by the author

A copy can be downloaded for personal non-commercial research or study,
without prior permission or charge

This work cannot be reproduced or quoted extensively from without first
obtaining permission in writing from the author

The content must not be changed in any way or sold commercially in any
format or medium without the formal permission of the author

When referring to this work, full bibliographic details including the author,
title, awarding institution and date of the thesis must be given

Enlighten: Theses

<https://theses.gla.ac.uk/>
research-enlighten@glasgow.ac.uk

A Thesis

entitled

"KINETIC STUDIES BY NUCLEAR MAGNETIC RESONANCE"

Submitted in part fulfilment of the
requirements for admittance to the degree of

Doctor of Philosophy

in

The University of Glasgow

by

David Dewar MacNicol, B.Sc.

University of Glasgow

October, 1965.

ProQuest Number: 10984226

All rights reserved

INFORMATION TO ALL USERS

The quality of this reproduction is dependent upon the quality of the copy submitted.

In the unlikely event that the author did not send a complete manuscript and there are missing pages, these will be noted. Also, if material had to be removed, a note will indicate the deletion.



ProQuest 10984226

Published by ProQuest LLC (2018). Copyright of the Dissertation is held by the Author.

All rights reserved.

This work is protected against unauthorized copying under Title 17, United States Code
Microform Edition © ProQuest LLC.

ProQuest LLC.
789 East Eisenhower Parkway
P.O. Box 1346
Ann Arbor, MI 48106 – 1346

ACKNOWLEDGEMENTS

I wish to record my sincere thanks to Professor J. C. D. Brand for his constant guidance and encouragement during the course of this work.

I should also like to thank Dr. B. D. Batts and Dr. A. L. Porte for very helpful discussions, and Dr. R. Wallace for assistance with the computing. It is also a pleasure to thank Mr. A. A. Leven, Mrs. F. Lawrie, Mrs. M. Lawson and Mr. J. H. Gall for their very capable technical assistance.

Finally, I am indebted to the Department of Scientific and Industrial Research for financial assistance in the form of a Research Studentship.

CONTENTS

<u>CHAPTER I.</u>	<u>Introduction</u>	
1.1	General	1
1.2	Proton-transfer Reactions . . .	3
1.3	Hindered Internal Rotation ..	9
<u>CHAPTER II.</u>	<u>Theoretical</u>	
2.1	General	12
2.2	Nature of the Chemical Shift and Spin-Spin Coupling	20
2.3	Relaxation Processes	25
2.4	The Bloch Equations	29
2.5	Collapse of Signals by Exchange between Different Chemical Positions	33
2.6	Collapse of Spin Multiplets by Exchange Processes	49
2.7	Relation to Chemical Kinetics ..	56
<u>CHAPTER III.</u>	<u>Historical</u>	
3.1	Proton Transfer Reactions involving Solvent Participation	63
3.2	Internal Rotation about Bonds with Partial Double Bond Character	86

<u>CHAPTER IV.</u>		<u>Experimental and Results</u>	
4.1	Materials		98
4.2	Preparation of Solutions		100
4.3	Instrumental		101
4.4	Measuring Techniques		105
4.5	Infrared and Ultraviolet Spectra		108
4.6	Proton Magnetic Resonance		
	Results for		
	p-Nitroso-N,N-dimethylaniline ..		110
4.7	Proton Magnetic Resonance		
	Results for the Conjugate Acid		
	of p-Nitroso-N,N-dimethylaniline		116
4.8	Results for Proton Transfer in		
	Aqueous Dioxane		120
4.9	Determination of Association		
	Constants by Proton Magnetic		
	Resonance Spectroscopy		121
4.10	Kinetic Results for Proton		
	Transfer in Aqueous Dioxane ..		128
<u>CHAPTER V.</u>		<u>Discussion</u>	
5.1	Hindered Internal Rotation ..		139
5.2	Proton Exchange in Aqueous		
	Dioxane		144
	Glossary of Symbols for Chapters IV and V ..		152
	References		153
	Relevant Publications		164

CHAPTER I

INTRODUCTION

Chapter I Introduction

1.1 General

1.2 Proton-transfer Reactions

1.3 Hindered Internal Rotation

INTRODUCTION

1.1. General

High-resolution nuclear magnetic resonance (NMR) spectroscopy provides a powerful and direct method for the investigation of chemical reaction mechanisms in solution. The importance of the method lies not only in the fact that it gives data on the chemical kinetics of systems which are in chemical equilibrium, but that it also allows a detailed microscopic picture of the nature of solvent participation in chemical reaction mechanisms to be built up.

The method, which will be described in detail in Chapter 2, is based on the sensitive dependence of NMR spectra of systems in chemical equilibrium on dynamic processes which affect the exchange of nuclei possessing a magnetic moment among two or more states of different electronic environment. All nuclei, except those with even number values of both the mass number A and the charge number Z , possess a magnetic moment. This interchange of nuclear environments may be brought about either by actual chemical exchange processes such as intermolecular or interionic exchange of atoms, groups of atoms, or electrons, or by

/intramolecular

intramolecular processes such as hindered rotation and ring inversion. Thus apart from the very valuable kinetic and mechanistic information which can be derived from NMR spectra about reactions involving chemical exchange, the kinetic dependence of NMR spectra also provides a method, in certain cases, for the investigation of such phenomena as hindered rotation and ring inversion in molecules.

It is important to distinguish clearly between the above application of NMR for obtaining information about rapid rate processes occurring in systems in equilibrium and the conventional use of NMR to handle kinetic problems, in which the NMR spectrometer is simply used as an analytical tool. The change in concentration with time for one or more components in the reacting system being measured from the corresponding changes in spectrum intensity. The latter technique is generally applied to comparatively slow reaction rates which can often be measured by other spectroscopic or kinetic techniques but which are sometimes conveniently determined by NMR.

1.2. Proton-transfer Reactions

The kinetics and reaction mechanisms of fast proton transfer reactions involving oxygen and nitrogen acids and bases have been studied extensively in water and also in a few other solvents of relatively high dielectric constant and have been reviewed recently by de Maeyer and Kustin.² On the other hand comparatively few studies^{2,3,4,5,6} have been carried out to investigate the detailed microscopic nature of proton transfer processes in solvents of low dielectric constant. The aim of a large part of this thesis is to derive a more fundamental understanding of the detailed nature of fast proton transfer reactions occurring in solvents of low dielectric constant. Fast reactions in this context are reactions with half-times between about 10^{-1} and 10^{-11} seconds.

In considering protolytic, or proton transfer reactions, that is, reactions involving the movement of a proton without any attendant electrons from one molecule or ion to another, it is convenient to define acids and bases after the Bronsted concept⁷, namely, an acid is a species having a tendency to lose a proton, and a base is a species having a tendency to

/add

add a proton. It is important to realise however that owing to the extremely small size of the proton which has a radius of the order of 10^{-13} cm. compared with 10^{-8} cm. for other common ions it exerts an enormous polarizing power on any molecule or ion in the neighbourhood and for this reason will not be found occurring free in solution. The free proton is, in fact, encountered only in a vacuum or in a very dilute gas.

It is well known that most reactions between acids and bases take place extremely rapidly but it has nevertheless proved possible to obtain a large amount of kinetic information about this type of reaction.

There are a few known acid-base reactions, notably the neutralisation of the nitroparaffins by various bases such as hydroxyl⁸ and ethoxide⁹ ions and amines¹⁰ which are slow enough to be followed by conventional means such as by measuring the change in conductivity as the reaction proceeds. Slower acid-base reactions have also been extensively studied by measuring the rate of hydrogen isotope exchange and reviews of this method of investigating acid-base reactions have been written by Wiberg¹¹ and

/Westheimer.¹²

Westheimer¹².

Until recently, however, most information about the rates of acid-base reactions was derived from observations of catalysis by acids and bases¹³, in which formation of a primary product, produced by the gain or loss of a proton by a molecule (the substrate), is detected by means of its further reaction such as rearrangement, decomposition, or reaction with some other species. This kind of observation is limited to fairly slow reactions, and also to those in which gain or loss of a proton is accompanied by a considerable structural change.

In the last fifteen years a number of very powerful new methods have been developed which allow the direct observation of acid-base reactions not involving any subsequent chemical change. Among the most powerful and widely applicable of these are NMR spectroscopy, polarography¹⁴, and the relaxation methods which have been reviewed by Eigen¹⁵. Interesting kinetic information can, in some cases, also be obtained from studies of fluorescence¹⁶, for example, information about the acid-base behaviour of β -naphthol in an electronically excited state.

Especially important among the relaxation methods

/for

for the study of acid-base phenomena are ultrasonic absorption and the electric impulse, high-frequency alternating field, and temperature jump methods. In the relaxation methods the position of the chemical equilibrium is slightly perturbed by a rapid change in some external parameter such as electric field, pressure or temperature, and the rate at which the system changes to its new equilibrium state is studied either by direct observation or by its interaction with the perturbing agent. Such systems are usually characterised by a relaxation time τ which is the time needed for the system to traverse a fraction $1/k$ of its path to the new equilibrium. For chemical systems τ is equal to the reciprocal of a first-order velocity constant and is of the same order of magnitude as the half-time of the reaction. Some of the highest velocity constants known for reactions occurring in solution have been measured by these methods, for example, the velocity constant for the reaction $H^+ + OH^- \longrightarrow H_2O$ was found, by the electric impulse method,¹⁷ to be $1.3(\pm 0.2) \times 10^{11} M^{-1} \text{sec.}^{-1}$ which corresponds closely with the theoretical expression for the rate of encounter of two ions of opposite charge.¹⁸

Another modern technique, deserving of mention, for the study of acid-base reactions is based on the broadening of Raman spectra caused by proton-transfer. This technique can be used for very fast reactions with half-times between 10^{-11} and 10^{-14} seconds, and Kreevoy and Mead¹⁹ have used this method to investigate proton transfer in buffers of CF_3COOH and CF_3CO_2^- . They estimate that the rate constant for the recombination of proton and anion is of the order of $3 \times 10^{11} \text{M}^{-1} \text{sec.}^{-1}$. This is faster than the calculated diffusion rate and may be caused by the fact that, after dissociation, some protons recombine with the anion without ever diffusing away into the solution.

NMR spectroscopy, and especially proton magnetic resonance (PMR) spectroscopy, gives a particularly powerful method of investigating fast proton transfer reactions since the NMR spectrum shows directly which protons are exchanging as well as allowing evaluation of the absolute rates of the exchange processes.

Although a number of methods are available, at the present time (1965), for the study of the kinetics of fast proton transfer reactions, the choice of NMR to study protolytic reactions in media of low dielectric constant is well founded since no other known kinetic

/method

method gives as deep an insight into the detailed microscopic nature of solvent participation in chemical reaction mechanisms.

1.3. Hindered Internal Rotation

The study of the magnitude and origin of the forces interfering with free internal rotation in molecules has interested physical chemists for many years. Hindered internal rotation can be classified broadly, for convenience, as torsion of one part of a molecule relative to the remainder about double bonds, about single bonds with varying degrees of double bond character and about single bonds.

In the case of rotation about double bonds in for example, ethylene derivatives, the rate of rotation is sufficiently slow to permit the separation of isomers by ordinary chemical techniques. Here the ease of rotation is greatly reduced by the fact that internal rotation involves the uncoupling of the π electrons of the double bond. In contrast, the potential barriers hindering rotation about single bonds are comparatively low amounting to only a few thousand calories in most circumstances. Much work has been directed to the determination of barrier heights opposing internal rotation about single bonds and an account of the various methods available is given by Wilson.²⁰

Between the above two extreme cases rotation may

/occur

occur about bonds with partial double bond character and various physical methods including NMR spectroscopy, ultrasonic absorption, infra-red spectroscopy and ultra-violet spectroscopy have been employed to study this type of system. Most of the quantitative investigations of barrier height for rotation about bonds with partial double bond character refer to non-aromatic molecules, for example, N,N-dimethylnitrosamine,^{21, 22} alkyl nitrites,^{22, 23, 24} amides,²⁵⁻³⁰ incl. and butadiene, glyoxal and their derivatives.^{31, 32} Barriers to internal rotation in aromatic compounds have been comparatively neglected. It is well known, of course, that the Ar-X bond has considerable double bond character when X is an unsaturated group or has lone pair electrons but the hindering potential is established for only very few compounds, notably some aromatic aldehydes,^{33, 34} and nitro compounds.³⁵ It will therefore be the object of part of this thesis to investigate further the magnitude and origin of the forces leading to hindered rotation in aromatic compounds.

C H A P T E R I I

THEORETICAL

Chapter II Theoretical

2.1 General

2.2 Nature of the Chemical Shift and Spin-Spin
Coupling

2.3 Relaxation Processes

2.4 The Bloch Equations

2.5 Collapse of Signals by Exchange between
Different Chemical Positions2.6 Collapse of Spin Multiplets by Exchange
Processes.

2.7 Relation to Chemical Kinetics

THEORETICAL

2.1 General

Many atomic nuclei possess spin angular momenta in much the same fashion as does the electron. The maximum measurable component of the angular momentum P of a nucleus is given by

$$P = \hbar I \quad (2-1)$$

where \hbar is Planck's constant divided by 2π and I is the nuclear spin quantum number which must be zero, integral or half integral. Nuclei which possess non-zero spin angular momenta also possess a magnetic moment which is always parallel to the angular momentum vector. Thus, if μ is the maximum observable component of the magnetic moment, we can write

$$\mu = \gamma \hbar I \quad (2-2)$$

where γ is a scalar quantity known as the nuclear magnetogyric ratio.

According to quantum electrodynamics the absolute value of the magnetic moment μ_a is given by

$$\mu_a = \gamma \hbar \sqrt{I(I + 1)} \quad (2-3)$$

It is of interest to note that the values of nuclear spin I show certain regular features which may be expressed in terms of the charge number Z and the mass number A . These are, when A is odd, I is half

/integral

integral, but when A and Z are even, I is equal to zero and finally, when A is even but Z is odd, the spin I is integral. Nuclei with spin $I = 0$ have no magnetic resonance spectra, and it can be seen from the above rules that such commonly occurring nuclei C^{12} and C^{16} fall into this class. Common nuclei which possess spin $\frac{1}{2}$ are H^1 , F^{19} and P^{31} . Apart from possessing a magnetic moment, some nuclei also possess an electrical quadrupole moment which is also related to the spin. The electrical quadrupole moment is a measure of the non-sphericity of the electric charge distribution within the nucleus, that is, whether it is drawn out into a cigar shape or flattened into a plate form. An important rule for which there is strong theoretical backing³⁶ is that only nuclei with I greater or equal to unity possess electrical quadrupole moments. NMR experiments on nuclei with $I = \frac{1}{2}$ therefore are not complicated by direct interaction of the nuclear spin with the electrical environment. A common nucleus which does possess an electrical quadrupole moment is N^{14} which has $I = 1$. The interaction of this quadrupole moment with electric field gradients in, for example liquids can be an important factor governing the nature of the NMR spectrum.

/When

When a nucleus is placed in a magnetic field H_0 the energy of the system relative to that in zero magnetic field becomes

$$-\mu_a \cdot H_0 = -\gamma \hbar \sqrt{I(I+1)} H_0 \cos \theta \quad (2-4)$$

where θ is the angle between μ_a and H_0 . Quantum mechanics shows that θ cannot take on all possible values but only those leading to values of the component of $\sqrt{I(I+1)}$ along the H_0 axis, m , of I , $I - 1$, $I - 2$, $-I + 1$, $-I$. Thus

$$\cos \theta = \frac{m}{\sqrt{I(I+1)}} \quad (2-5)$$

and since there are $2I + 1$ allowed values of the magnetic quantum number m , a nucleus of spin I will have $2I + 1$ distinct states, the energy levels of which become separated in a magnetic field H_0 , and which are

$$-\gamma \hbar I H_0, -\gamma \hbar (I - 1) H_0, \dots, \gamma \hbar (I - 1) H_0, \gamma \hbar I H_0 \quad (2-6)$$

These energy levels are equally spaced, the separation between them being $\gamma \hbar H_0$. This splitting of energy levels in a magnetic field may be referred to as nuclear Zeeman splitting, because it is analogous to the magnetic splitting of electronic levels.

Initially, for the sake of clarity, only NMR experiments on nuclei with spin $I = \frac{1}{2}$ will be considered and later transitions occurring between the energy levels of nuclei with $I = \frac{1}{2}$ such as N^{14} ($I = 1$)

/and

and O^{17} ($I = 5/2$) will be discussed where these become significant.

For nuclei with $I = \frac{1}{2}$ two nuclear spin energy levels exist and are $-\gamma\hbar H_0/2$ and $+\gamma\hbar H_0/2$

$$\begin{array}{rcl}
 & & \text{Energy} \\
 & & +\gamma\hbar H_0/2 \\
 H_0 = 0 & \begin{array}{l} \text{---} \\ \text{---} \end{array} & \begin{array}{l} m = -\frac{1}{2} \\ m = +\frac{1}{2} \end{array} \\
 & & -\gamma\hbar H_0/2
 \end{array} \quad (2-7)$$

Using equation (2-2) the difference in energy between the levels, $\gamma\hbar H_0$, can also be expressed as $\mu H_0/I$. These two energy levels are, of course, degenerate in the absence of a magnetic field.

The basis of NMR experiments is to induce transitions between nuclear Zeeman levels by the absorption or emission of energy quanta. The frequency of radiation ν required can be found by the Bohr frequency condition

$$h\nu = \frac{\mu H_0}{I} \quad (2-8)$$

and, by equation (2-2)

$$\nu = \frac{\gamma H_0}{2\pi} \quad (2-9)$$

Thus the frequency is proportional to the applied field. If one substitutes, as typical values, μ for /the proton

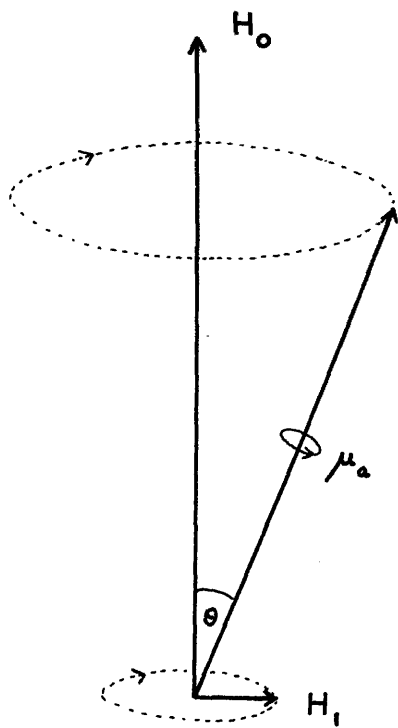


Figure 2-1.

the proton (1.42×10^{-23} erg gauss⁻¹) and $H_0 = 14,000$ gauss, the appropriate frequency is about 60 Mc. sec.⁻¹ which can be conveniently produced by radiofrequency (rf) techniques.

In order to excite transitions between nuclear energy levels in the magnetic resonance experiment it is necessary to supply radiation of the appropriate frequency with the magnetic vector circularly polarised in a plane perpendicular to the steady magnetic field. This requirement of circular polarisation can be explained by a classical argument as follows. If a magnetic dipole μ_a is placed in a magnetic field H_0 , as shown in Figure 2-1, the dipole precesses about the direction of the applied field. The rate of precession is given by the well-known Larmor angular frequency relationship,³⁷

$$\omega_0 = \gamma H_0 \quad (2-10)$$

Suppose now that an additional small magnetic field H_1 is applied at right angles to H_0 , in the plane containing μ_a and H_0 . The dipole will experience a couple $\mu_a \times H_1$ tending to increase the angle θ between μ_a and H_0 . If the small field H_1 is made to rotate about H_0 as axis in synchronism with the

/precession

precession of the dipole, this couple will cause the angle θ to increase steadily. If, on the other hand H_1 rotates with an angular frequency different from the Larmor precessional frequency, or in the opposite sense, the couple $\mu_a \times H_1$ will vary in magnitude and direction according to the relative phases of the two motions and will merely produce small perturbations of the precessional motion with no net effect. A resonance therefore occurs when the angular frequency $2\pi\nu$ of the rotating field is equal to the angular frequency of the Larmor precession ω_0 , namely when

$$2\pi\nu = 2\pi\nu_0 = \omega_0 = \gamma H_0 \quad (2-11)$$

Comparison of equations (2-11) and (2-9) shows that this classical resonance condition agrees exactly with that derived from quantum theory. Moreover, it can be seen that as with the quantum theory³⁸, so also classically a condition for the observation of resonance is that the electromagnetic radiation be circularly polarised with the magnetic vector rotating in a plane perpendicular to the magnetic field.

Although the generation of a high-frequency rotating magnetic field is quite practicable, it is usually much simpler to provide a linearly oscillating magnetic field. This is adequate for most purposes

/since

since a linearly oscillating field of amplitude $2H_1$ can be regarded as a superposition of two equal fields of amplitude H_1 rotating with equal angular velocities in opposite directions (the phases being appropriate). The component rotating in the direction opposite to the Larmor precession will have little effect on the resonance.

It is important to note that a detailed consideration of transition probabilities shows that, in general, transitions between neighbouring levels are the only ones that can be induced by an oscillating magnetic field. This statement is relevant, of course, only for nuclei with spin number $I = \frac{1}{2}$ since there are only two allowed levels for nuclei with $I = \frac{1}{2}$.

In a typical NMR experiment the precessional frequency of the nuclei is changed by varying the applied magnetic field, keeping the oscillator frequency constant. At some value of the field the nuclear precession frequency becomes equal to the frequency of the rotating field vector produced by the oscillator and resonance occurs.

There are two experimental schemes for observing
/the absorption

the absorption of energy of a nuclear spin system -
the nuclear resonance technique of Purcell,³⁹ and the
nuclear induction technique of Bloch.⁴⁰ Full
discussions of the two experimental approaches are to
be found in the books by Andrew;⁴¹ and Pople,
Schneider and Bernstein.⁴²

2.2. Nature of the Chemical Shift and Spin-Spin Coupling

The information which can be obtained from an NMR spectrum depends critically on the physical state of the sample. Solid samples give rise to what are known as broad-line spectra, the line width being largely dependent on the magnitude of the nuclear dipole-dipole interactions in the solid. Such solid-state spectra give, in certain cases, valuable information about molecular geometry and molecular rotation in crystals and this subject has been treated in detail in the book by Andrew.³⁸

The breadth of lines in the solid-state are dependent on the fact that the nuclei maintain the same orientations relative to one another and to the external field. In liquids and gases, on the other hand, where the molecules are rotating and tumbling about rapidly, the magnetic field at any one nucleus due to the others effectively averages out to zero and the resonance signals become much sharper. This is an example of the general and important phenomenon in resonance experiments in which sufficiently rapid fluctuations of environment show up only as an average.

From what has been said so far all nuclei of the same species in a mobile liquid or gas might be expected to resonate at exactly the same applied field independent of their chemical situation if the frequency ν of the rf field is held constant, according to equations (2-8) and (2-9), since μ and γ are constant for a given nuclear species. Fortunately this turns out not to be the case because the magnetic field at the nucleus of an atom differs by a small amount from the applied field due to an interaction between the applied field and the electrons surrounding the nucleus. This small difference in magnetic field is caused by induced precessional motion of the electrons, and since the induced currents are proportional to the applied field H_0 , the magnitude of the secondary field causing the difference between H_0 and the field at the nucleus H_{local} is also proportional to H_0 . Thus the local magnetic field at the position of the nucleus can be expressed as

$$H_{\text{local}} = H_0(1 - \sigma) \quad (2-12)$$

where σ is a non-dimensional constant independent of H_0 but dependent on the chemical (electronic)

/environment

environment known as the "screening constant" because the local field is usually slightly smaller than the applied field. As a result, resonance will occur in a different part of the spectrum for each chemically distinct position. This displacement of a signal for different chemical environments due to variations in screening constants is referred to as a "chemical shift" δ which is defined by

$$\delta = \frac{H - H_r}{H_r} \quad (2-13)$$

where H is the resonant field of the signal being measured at a fixed frequency and H_r the corresponding field for a second proton signal chosen as a reference signal.

As an example, liquid ethanol, $\text{CH}_3\text{CH}_2\text{OH}$, at room temperature under conditions of moderate resolution (about 1 part in 10^6) shows three signals with intensities approximately in the ratio 3:2:1 in order of decreasing applied magnetic field corresponding to the three chemically distinct proton situations, methyl, methylene and hydroxyl respectively.

Another very important effect which can influence the nature of high-resolution NMR spectra arises from

/an interaction

an interaction between neighbouring nuclear spins which is proportional to the scalar product $I(1) \cdot I(2)$ where $I(1)$ and $I(2)$ are the nuclear spin vectors. Unlike the direct interaction of magnetic dipoles an energy of this sort does not average to zero when the molecules are rotating, so its effect is still observable in the spectra of liquids. The interpretation of these interactions was first given by Ramsay and Purcell,⁴³ who showed that they arise from an indirect coupling mechanism via the electrons in the molecule. The result of this type of spin-spin coupling is to produce more lines in the NMR spectrum than would otherwise be expected, for a given nucleus may experience one of two or more possible small secondary magnetic fields due to a neighbouring nucleus or nuclei.

An example of this is given by the spectrum of liquid ethanol containing a trace of acid under typical high-resolution conditions (1 part in 10^8), such as is reproduced in the book by Jackman.⁴⁴ which shows that the methyl resonance consists of three lines with areas approximately in the ratio 1:2:1

/corresponding

corresponding to the various combinations of possible spin states of the $-\text{CH}_2-$ protons. Similarly, the methylene resonance has fine structure, the approximate relative intensities of the lines being 1:3:3:1 corresponding to the possible arrangements of the spin states of the CH_3- protons. It is interesting to note that no further splitting of the $-\text{CH}_2-$ resonance due to the possible spin states of the hydroxyl proton is observed. This is due to the fact that under the experimental conditions, acid-catalysed proton exchange is sufficiently rapid (see later) to let the methylene protons see only an average of the two possible secondary magnetic fields corresponding to the spin states of the hydroxyl proton. In highly purified ethanol further splitting of the $-\text{CH}_2-$ quartet and the hydroxyl singlet is observed.⁴⁵

2.3. Relaxation Processes

In the absence of such phenomena as chemical exchange processes and nuclear quadrupole coupling the spectral lines obtained in NMR experiments on liquids are usually extremely narrow. The finite broadening of the lines observed is due to a variety of causes and can readily be measured.

The natural line width of any transition is determined by the finite lifetime of the upper state, because of the possibility of spontaneous emission of radiation. The extent of broadening due to this effect has been shown⁴⁶ to be quite negligible compared with other causes.

Of much more importance is the finite lifetime of both states because of the possibility of transitions between them being induced by the other molecular degrees of freedom. This is the spin-lattice or longitudinal relaxation process and is always present. Consider an assembly of nuclear spins (with $I = \frac{1}{2}$) which is initially not in a magnetic field so that the populations of the two spin states are equal. If a steady magnetic field H_0 is now applied the nuclei will tend to populate the quantum states according to the Boltzmann distribution law.

/It is

It is convenient to define a time T_1 , the spin-lattice relaxation time, which is the time required to reduce the difference between the excess population in the lower state and its equilibrium value by a factor h . T_1 is therefore a measure of the rate at which the spin system comes into thermal equilibrium with the other degrees of freedom.

The order of magnitude of the broadening due to spin-lattice relaxation can be estimated from the uncertainty principle $\Delta E \Delta t \approx \hbar$ where ΔE is the uncertainty in energy and Δt the uncertainty in time. Since $\Delta E = h\Delta\nu$, the uncertainty in frequency of absorption is $1/2\pi\Delta t$. Thus the line width measured on a frequency scale, owing to spin-lattice relaxation will be of the order $1/T_1$. Spin-lattice relaxation occurs by a variety of mechanisms, the most universal of which is via the direct interaction of neighbouring magnetic dipoles, which varies as the nuclei move relative to one another. Spin-lattice relaxation is discussed in detail in the book by Pople, Schneider and Bernstein.⁴⁷

When the line width is larger than that due to spin-lattice relaxation it is convenient to define another characteristic time, the transverse relaxation

time T_2 , in terms of the line shape function $g(\nu)$ such that

$$T_2 = \frac{1}{2}[g(\nu)]_{\max} \quad (2-14)$$

Such a further increase in line width can be caused by the interaction of magnetic dipoles in solids and in highly viscous liquids where the nuclei stay in the same relative positions for a long time for here nuclei must be treated as being in a variety of fields because of the local magnetic field due to neighbouring dipoles. In mobile liquids and gases, however, the magnetic fields effectively average out and T_1 and T_2 become approximately equal.

A further cause of broadening is the variation of the static magnetic field H_0 over the dimensions of the sample. This instrumental limitation means that the observed spectrum will be broadened because it is really a superposition of spectra from molecules in different parts of the sample and in many cases the inhomogeneity of the applied magnetic field is the most important factor governing T_2 .

High-resolution NMR signals can also be broadened by the effect known as saturation,⁴⁸ the magnitude of the effect increasing with the amplitude of the applied oscillating magnetic field. Often such signal

/distortion

distortion can be avoided by using a sufficiently low power level.

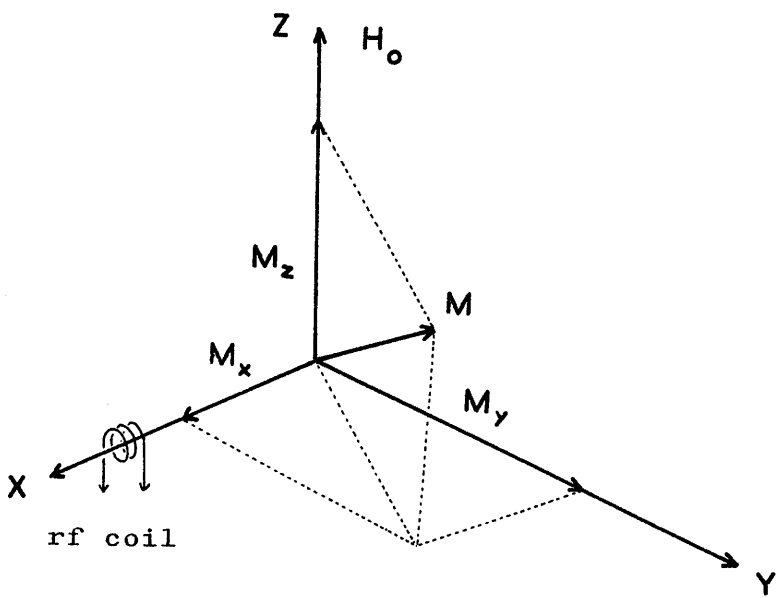


Figure 2-2.

2.4. The Bloch Equations.

In his original formulation of the behaviour of nuclear moments in variable magnetic fields, Bloch⁴⁹ used a set of macroscopic or phenomenological equations for the variation of the components of the total magnetic moment M per unit volume. M is given in terms of cartesian coordinates as (M_x, M_y, M_z) and the significance of the axes in a typical nuclear resonance experiment employing the "single-coil system" is shown in Figure 2-2. The Z axis (here the vertical direction) is taken along the magnetic field axis, while the X axis coincides with the axis of the sample tube and the axis of the single coil. This coil acts both as oscillator and receiver. The vector M is subjected to the oscillator field which, as has been said already, can be regarded as being resolved into two vectors of length H_1 rotating with angular velocities ω in opposite directions in the X, Y plane with phase relationships such as to give no net field along Y .

It can be shown⁵⁰ that the rate of change of $M_x, M_y,$ and M_z with time are given by the Bloch equations in the form

$$\frac{dM_x}{dt}$$

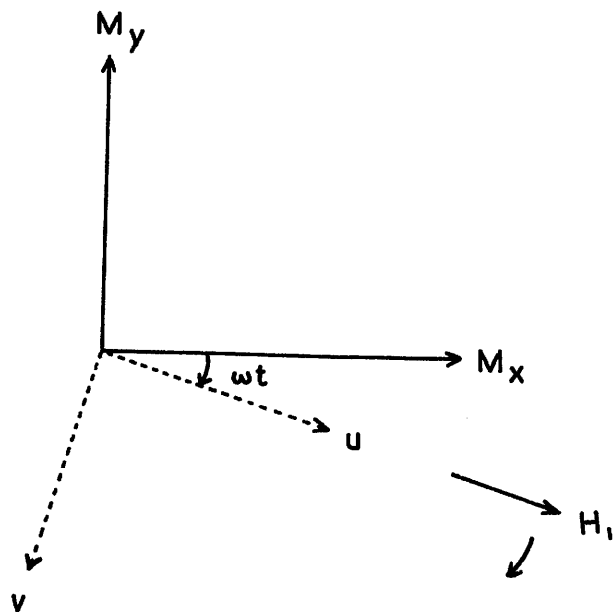


Figure 2-3.

$$\frac{dM_x}{dt} = \gamma(M_y H_0 + M_z H_1 \sin\omega t) - \frac{M_x}{T_2} \quad (2-15)$$

$$\frac{dM_y}{dt} = \gamma(M_z H_1 \cos\omega t - M_x H_0) - \frac{M_y}{T_2} \quad (2-16)$$

$$\frac{dM_z}{dt} = \gamma(-M_x H_1 \sin\omega t - M_y H_1 \cos\omega t) - \frac{M_z - M_0}{T_1} \quad (2-17)$$

In equation (2-17) M_0 represents the equilibrium value of M_z . Bloch introduced T_2 , the transverse relaxation time, into these equations to describe the rate at which the individual nuclei get out of phase due to fluctuations and relaxation effects, that is, the rate at which the components M_x and M_y will decay to zero. This definition of T_2 is consistent with the definition given earlier in equation (2-14).

The Bloch equations (2-15) to (2-17) take a simpler form if, instead of being referred to fixed axes X, Y and Z, they are referred to a set of axes rotating with the applied rf field H_1 . This means that a new set of axes is defined rotating with the angular velocity $-\omega$ about the Z axis. The components of M along and perpendicular to the direction of H_1 , u and v, are shown in Figure 2-3. The relations between the components are

$$/u =$$

$$u = M_x \cos \omega t - M_y \sin \omega t \quad (2-18)$$

$$v = -M_x \sin \omega t - M_y \cos \omega t \quad (2-19)$$

Substituting equations (2-18) and (2-19) in the Bloch equations (2-15) to (2-17) a new set of equations for the three components u , v , and M_z referred to rotating axes is produced

$$\frac{du}{dt} + \frac{u}{T_2} + (\omega_0 - \omega)v = 0 \quad (2-20)$$

$$\frac{dv}{dt} + \frac{v}{T_2} - (\omega_0 - \omega)u + \gamma H_1 M_z = 0 \quad (2-21)$$

$$\frac{dM_z}{dt} + \frac{M_z - M_0}{T_1} - \gamma H_1 v = 0 \quad (2-22)$$

To discuss the magnetic resonance absorption experiment the steady state solution of the Bloch equations is required in which M_z is constant and the transverse components rotate with the applied rf field H_1 . This solution is easily obtained from equations (2-20) to (2-22) by putting all time derivatives equal to zero. Hence,

$$u = M_0 \frac{\gamma H_1 T_2^2 (\omega_0 - \omega)}{1 + T_2^2 (\omega_0 - \omega)^2 + \gamma^2 H_1^2 T_1 T_2} \quad (2-23)$$

and

$$v = -M_0 \frac{\gamma H_1 T_2}{1 + T_2^2 (\omega_0 - \omega)^2 + \gamma^2 H_1^2 T_1 T_2} \quad (2-24)$$

The out-of-phase component v , given by equation (2-24), is proportional to the absorption intensity, so that if the oscillating magnetic field is small, that is $H_1 \ll 1/\gamma\sqrt{T_1 T_2}$, the absorption mode for a slow passage experiment is given by a line shape function $g(\nu)$ such that

$$g(\nu) = \frac{2T_2}{1 + 4\pi^2 T_2^2 (\nu_0 - \nu)^2} \quad (2-25)$$

Equation (2-25) describes a Lorentzian curve, the width at half-height $\Delta\nu_{\frac{1}{2}}(\text{c. sec.}^{-1})$ is equal to $1/T_2\pi$. In practice, line shapes are not always well approximated by the Lorentz-type curve. This, of course, represents a limitation of the original phenomenological equations.

2.5. Collapse of Signals by Exchange between Different Chemical Positions

A necessary condition for the applicability of the NMR method of measuring rates to a specific system is that the nuclei involved in the exchange can be in at least two different "environments", characterised by different local magnetic fields, and accordingly different Larmor frequencies of the nuclei. The exchange process will transfer nuclei from one environment to another, with an accompanying switch of their resonance frequency to a different value. It is thus possible to follow the exchange reaction because the nuclei are "labelled" by their Larmor frequency. The experimentally determined quantity is the increase in line width in the NMR spectrum caused by these frequency exchanges.

Qualitatively the changes observed in the NMR spectrum of a system involving, for example, intermolecular exchange of nuclei as its exchange rate is increased gradually from zero to a high value are as follows. A gradual broadening of the resonance lines involved in the exchange will be observed initially until the individual lines overlap and a single broad line is observed. On continued increase of exchange

/rate

rate this line will narrow, and at very fast rates a single sharp line at the centre of gravity of the contributing lines is observed. The first stage of broadened individual lines is often called "lifetime broadening", since the broadening can be considered as arising from the finite time a nucleus stays in a definite frequency state. The second stage in which there is a single collapsed line is referred to as "exchange narrowing". In this case, the exchange is fast enough for an averaging of the individual resonance frequencies to occur and the width of the observed line decreases with increasing exchange rate. Analogous spectral changes take place in the case of hindered rotations and ring inversions in molecules.

The quantitative description of the effect of exchange processes occurring in liquids is best developed by suitable modification of the Bloch equations which were introduced in Section 2.4. This approach was first used by Gutowsky, McCall and Slichter⁵¹ and was later presented in a simplified form by McConnell.⁵²

In considering exchange events it is most convenient to refer the Bloch equations to the rotating coordinate frame already described in

Section 2.4. If the oscillating field H_1 is not too large, the polarization M_z is not appreciably altered from its equilibrium value M_0 and the equations for u and v become

$$\frac{du}{dt} + \frac{u}{T_2} + (\omega_0 - \omega)v = 0 \quad (2-26)$$

$$\frac{dv}{dt} + \frac{v}{T_2} - (\omega_0 - \omega)u = -\gamma H_1 M_0 \quad (2-27)$$

Equations (2-26) and (2-27) are the real and imaginary parts of a complex equation and a complex moment can be defined as

$$G = u + iv \quad (2-28)$$

the equation for G is

$$\frac{dG}{dt} + \left[\frac{1}{T_2} - i(\omega_0 - \omega) \right] G = -i\gamma H_1 M_0 \quad (2-29)$$

The Bloch equations in their simplest form apply to the macroscopic moment M when all nuclei are acted on by the same field H_0 . Consider the case of two chemically distinct positions with different screening constants, neither of the positions being involved in spin-spin coupling. There will now be two possible fields and hence two corresponding Larmor frequencies denoted by ω_A and ω_B . If no exchange of nuclei occurs between A and B positions there will be two independent macroscopic moments, with complex components obeying

/the equations

the equations

$$\frac{dG_A}{dt} + \alpha_A G_A = -i\gamma H_1 M_{oA} \quad (2-30)$$

$$\frac{dG_B}{dt} + \alpha_B G_B = -i\gamma H_1 M_{oB} \quad (2-31)$$

where α_A and α_B are complex quantities defined by

$$\alpha_A = T_{2A}^{-1} - i(\omega_A - \omega) \quad (2-32)$$

$$\alpha_B = T_{2B}^{-1} - i(\omega_B - \omega) \quad (2-33)$$

T_{2A} and T_{2B} being the transverse relaxation times of nuclei in the two positions in absence of exchange.

The equations in their present form take no account of the possibility of exchange between A and B positions. Initially a procedure similar to that proposed by McConnell⁵² to allow for exchange will be considered.

Suppose that nuclei remain in one position until they make a sudden rapid jump to another so that the nuclear precession during the jump can be neglected. It is clear that under these conditions a nuclear exchange between positions of the same type will have no effect, hence such exchanges will be neglected and only exchanges between positions of type A and B will be considered.

/It will

It will be assumed that while a nucleus is in an A position, there is a constant probability τ_A^{-1} per unit time of its making a jump to a B position. τ_A is then the mean lifetime for a stay on A sites. Another corresponding time τ_B can be defined for the lifetime of B positions. The fractional populations of A and B sites P_A and $P_B (= 1 - P_A)$ are then related to τ_A and τ_B by

$$P_A = \frac{\tau_B}{\tau_A + \tau_B} \quad P_B = \frac{\tau_A}{\tau_A + \tau_B} \quad (2-34)$$

by considerations of detailed balancing.

The modified Bloch equations proposed by McConnell⁵² are

$$\frac{dG_A}{dt} + \alpha_A G_A = -i\gamma H_1 M_{oA} + \tau_B^{-1} G_B - \tau_A^{-1} G_A \quad (2-35)$$

$$\frac{dG_B}{dt} + \alpha_B G_B = -i\gamma H_1 M_{oB} + \tau_A^{-1} G_A - \tau_B^{-1} G_B \quad (2-36)$$

Equations (2-35) and (2-36) differ from equations (2-30) and (2-31) only by the addition of terms to allow for the exchange. Thus $\tau_B^{-1} G_B$ in equation (2-35) represents the rate of increase of G_A due to transfer of magnetization from B to A sites. Similarly $\tau_A^{-1} G_A$ is the corresponding rate of loss. It should be noted that equations (2-35) and (2-36) are valid

/only

only for a small rf field (no appreciable saturation) and that in the more general form given by McConnell⁵² this requirement is not present.

The solutions of equations (2-35) and (2-36) corresponding to slow passage conditions is obtained by putting

$$\frac{dG_A}{dt} = \frac{dG_B}{dt} = 0 \quad (2-37)$$

The equations can then be solved for G_A and G_B , noting that

$$M_{oA} = P_A M_o \quad M_{oB} = P_B M_o \quad (2-38)$$

the total complex moment is given by

$$G = G_A + G_B = -i\gamma H_1 M_o \frac{\tau_A + \tau_B + \tau_A \tau_B (\alpha_A P_B + \alpha_B P_A)}{(1 + \alpha_A \tau_A)(1 + \alpha_B \tau_B) - 1} \quad (2-39)$$

This equation was first derived by Gutowsky, McCall and Slichter⁵¹ using a more complicated argument.

The intensity of absorption at frequency ω is then proportional to the imaginary part of G .

Before mentioning the general case some important special cases will be considered, the first of which is that of slow exchange or "lifetime broadening".

When τ_A and τ_B are sufficiently large compared with the inverse of the separation $(\omega_A - \omega_B)^{-1}$, the spectrum will consist of distinct signals in the

/vicinity

vicinity of the frequencies ω_A and ω_B . For example, if the radiofrequency ω is close to ω_A , and thus far away from ω_B , G_B is effectively zero and the solution becomes

$$G \approx G_A \approx -i\gamma H_1 M_0 \frac{P_A \tau_A}{1 + \alpha_A \tau_A} \quad (2-40)$$

and the imaginary part of this is

$$v = -\gamma H_1 M_0 \frac{P_A T_{2A}'}{1 + (T_{2A}')^2 (\omega_A - \omega)^2} \quad (2-41)$$

a broadened signal centred at ω_A with width given by the parameter

$$T_{2A}'^{-1} = T_{2A}^{-1} + \tau_A^{-1} \quad (2-42)$$

There will, of course, be a corresponding signal centred on ω_B .

This shows that the exchange leads to an additional broadening of the individual signals. If $T_{2A}'^{-1}$ and T_{2A}^{-1} are known τ_A can be found by means of equation (2-42). $T_{2A}'^{-1}$ can often be conveniently determined by measurement of the width at half height $\Delta\nu_{\frac{1}{2}}$ (in c.sec.⁻¹) of the exchange broadened resonance centred on ω_A recorded under conditions of slow passage and negligible saturation, since $T_{2A}'^{-1} = \pi\Delta\nu_{\frac{1}{2}}$. It should be emphasised that a sufficiently low rf

power must be employed for, as has been indicated in Section 2.3., saturation can lead to significant distortion of signal shape.

It is also important to point out that a sufficiently slow sweep rate must be used, otherwise a series of characteristic oscillations or "wiggles" appear after the signal and the signal is broadened by distortion. It has been shown by Jacobsohn and Wangsness⁵³ that "wiggles" and the accompanying signal distortion broadening are not present at all if a sweep rate $d\nu/dt$ (c.sec.⁻²) of less or equal to $1/8\pi T_2^2$ is used to sweep through a signal characterised by transverse relaxation time T_2 .

Hence, in order to obtain accurate values of T_{2A}^{-1} by the slow passage method, a condition is $d\nu/dt \leq 1/8\pi T_{2A}^2$. T_{2A}^{-1} , the reciprocal of the transverse relaxation time of nuclei in A sites in absence of exchange, often corresponds to the field inhomogeneity and can be calculated from the decay envelope of the "wiggles" following a fast sweep through a suitable sharp resonance line such as is produced by the six equivalent protons of acetone (the C^{13} satellite lines do not have any significant effect on this type of measurement). T_{2A}^{-1} may also /be determined

be determined by the slow passage line width method bearing in mind the above conditions concerning the sweep rate and the rf power.

This procedure for obtaining exchange rates is valid, provided the broadening is not large enough to cause appreciable overlap of the signals.

The second special case is that of rapid exchange or "exchange narrowing". In the limit of this case τ_A and τ_B are small and equation (2-39) reduces to

$$G = -i\gamma H_1 M_0 \frac{\tau_A + \tau_B}{\alpha_A \tau_A + \alpha_B \tau_B} = - \frac{i\gamma H_1 M_0}{P_A \alpha_A + P_B \alpha_B} \quad (2-43)$$

The imaginary part is

$$v = -\gamma H_1 M_0 \frac{T_2'}{1 + T_2'^2 (P_A \omega_A + P_B \omega_B - \omega)^2} \quad (2-44)$$

representing a single resonance line centred on a mean frequency

$$\omega_{\text{mean}} = P_A \omega_A + P_B \omega_B \quad (2-45)$$

However, if the exchange is not quite rapid enough to give complete collapse, the signal centred on ω_{mean} will have a larger width than that given by equation (2-46). This case can be conveniently dealt with using the treatment of Piette and Anderson.²³

They define quantity τ such that

$$\frac{1}{\tau} = \frac{1}{\tau_A} + \frac{1}{\tau_B} \quad (2-47)$$

and their relationship for fast exchange is of the form

$$\frac{1}{T_2'} = \frac{1}{T_2} + \frac{\nabla \tau T_2}{(\tau + T_2)} \quad (2-48)$$

$$\approx \frac{1}{T_2} + \nabla \tau \quad \text{when } T_2 \gg \tau \quad (2-49)$$

$$\text{where } \nabla = \langle \omega^2 \rangle - \langle \omega \rangle^2 \quad (2-50)$$

$$\text{with } \langle \omega \rangle = \sum_A P_A \omega_A \quad \text{and } \langle \omega^2 \rangle = \sum_A P_A \omega_A^2 \quad (2-51)$$

For the case of two lines ∇ is given by

$$\nabla = \frac{P_A^2 P_B^2 (\omega_A - \omega_B)^2 (\tau_A + \tau_B)^2}{\tau_A \tau_B} \quad (2-52)$$

Hence, in this case, equation (2-49) becomes

$$\frac{1}{T_2'} = \frac{1}{T_2} + P_A^2 P_B^2 (\omega_A - \omega_B)^2 (\tau_A + \tau_B) \quad (2-53)$$

It is assumed in this treatment that T_2 is unchanged between sites A and B.

It should be pointed out, perhaps, that the requirement that $\tau \ll T_2$ is readily met for the values of T_2 normally obtained experimentally, except when the chemical shift of the collapsing signals is very small (that is, of the order of two or three cycles per second).

$1/\tau_A$ and $1/\tau_B$

τ_A and τ_B can be found, in this case, by means of equations (2-53) and (2-34) since $1/T_2'$ and $1/T_2$ can be measured by the methods already described in connection with the slow exchange case. It should be noted, however, that the value of $(\omega_A - \omega_B)$ is also required and so must be known or estimated.

Another case of considerable importance arises when the fractional population of one type of site, say A, tends to unity, that is the number of B sites is extremely small compared with the number of A sites. Thus the lifetime τ_B becomes extremely small compared with τ_A and in this case equation (2-39) reduces to

$$G \approx -i\gamma H_1 M_0 \frac{\tau_A}{\alpha_A \tau_A} \quad (2-54)$$

the imaginary part of which is

$$v = -\gamma H_1 M_0 \frac{T_{2A}}{1 + T_{2A}^2 (\omega_A - \omega)^2} \quad (2-55)$$

This represents an unbroadened signal centred on ω_A , so that if one of the populations is extremely small compared with the other any contribution to line width due to the collapse of the chemical shift is negligible.

This may be put on a more quantitative basis by

/considering

considering Meiboom's dominant line approximation,⁵⁴ which applies when fractional population of one type of site is close to unity. For the case of exchange occurring between two sites, A and B, with $P_B \ll 1$, and a low rf power, the broadening of the dominant line Δ will be given to a very good approximation by

$$\Delta = \frac{1}{T_1'} - \frac{1}{T_2} = \tau \frac{P_B \delta^2}{1 + \tau^2 \delta^2} \quad (2-56)$$

where δ is the chemical shift in radians per second between the two types of sites and τ has the same significance as in equation (2-47). It is useful to look at the maximum possible broadening of the dominant line. This can be done by re-writing equation (2-56) as

$$\tau^2(\delta^2 \Delta) - \tau(P_B \delta^2) + \Delta = 0 \quad (2-57)$$

For slow rates of exchange the dominant line will be sharp, then with increasing exchange rate the dominant line will first broaden and finally sharpen up again. At high rates of exchange the dominant line will again be sharp. Clearly there will be two possible values of τ for each value of the broadening, except at the maximum broadening where the two values of τ are coincident. Since equation (2-57) has the form $ax^2 + bx + c = 0$, the condition for equal roots is $b^2 = 4ac$ and hence the condition for maximum broadening is

$$/P_B^2 \delta^4$$

$$P_B^2 \delta^4 = 4\delta^2 \Delta^2 \quad (2-58)$$

that is, the maximum possible broadening Δ_{\max} is given by

$$\Delta_{\max} = \frac{P_B \delta}{2} \quad (2-59)$$

The Meiboom dominant line approximation⁵⁴ also provides a convenient method for investigating exchange processes when the nuclei in the species of low concentration are coupled to a nucleus possessing a nuclear quadrupole moment, for instance N^{14} .

Consider the case for protons attached to nitrogen. The NH protons are split into a 1:1:1 triplet by spin-spin interaction with the N^{14} nucleus, the NH coupling constant being J . However, the quadrupolar relaxation of the N^{14} nucleus, with characteristic time T^1 , has some effect on the dominant line and this is allowed for by using an effective coupling constant J_{eff} instead of J where

$$J_{\text{eff}} = \frac{JT^1}{(T^1 + \tau)} \quad (2-60)$$

In the absence of exchange there would be four relevant lines, the major line of intensity $1 - P_B$ and resonance frequency ω_0 and three NH lines, each

/of intensity

of intensity $P_B/3$ whose frequencies differ from ω_0 by $\delta - J_{\text{eff}}$, δ , and $\delta + J_{\text{eff}}$ radians per second respectively. δ is the chemical shift of the NH protons relative to the protons with the large fractional population. The expression for the broadening of the dominant line Δ in presence of exchange with small P_B is then

$$\Delta = \frac{1}{T_2'} - \frac{1}{T_2} = \quad (2-61)$$

$$= \frac{P_B \tau}{3} \left[\frac{(\delta - J_{\text{eff}})^2}{1 + (\delta - J_{\text{eff}})^2 \tau^2} + \frac{\delta^2}{1 + \delta^2 \tau^2} + \frac{(\delta + J_{\text{eff}})^2}{1 + (\delta + J_{\text{eff}})^2 \tau^2} \right]$$

Equation (2-61) has been used by Grunwald and Price^{2,3} to study proton exchange of amines in acetic acid.

The transition from a spectrum of two lines to one line occurs when the lifetimes τ_A and τ_B are of the order of $(\omega_A - \omega_B)^{-1}$. The full expression for the intensity of absorption in this intermediate range is obtained from the imaginary part of the general expression for the complex moment G (equation (2-39)).

Gutowsky and Holm²⁷ give a general expression which reduces for the case with $P_A = P_B = \frac{1}{2}$ and $T_{2A}^{-1} = T_{2B}^{-1} = 0$ to give a line shape function $g(\nu)$ of the form

$$/g(\nu)$$

$$g(\nu) = K \frac{\tau(\nu_A - \nu_B)^2}{[\frac{1}{2}(\nu_A + \nu_B) - \nu]^2 + 4\pi^2\tau^2(\nu_A - \nu)^2(\nu_B - \nu)^2} \quad (2-62)$$

where K is a normalising constant. This treatment requires that the width of the signals in absence of exchange is small compared with their separation. It turns out that the actual shape of this function depends only on the product $\tau|\nu_A - \nu_B|$. This function describes with increasing rate of exchange, the broadening of the individual signals, the drawing together of the two maxima, coalescence to form a single peak when τ reaches the intermediate value

$$\tau = \frac{\sqrt{2}}{2\pi(\nu_A - \nu_B)} \quad (2-63)$$

and the final sharpening up of the signal at the mean position.

In obtaining average lifetimes by means of the general exchange expression it is often most convenient to set up equations describing the line shapes and to solve them numerically for various values of τ , T_2 and so on. The observed spectra are then compared with the calculated spectra and when identity is found τ is read directly. The comparison of the observed spectra is facilitated by plotting characteristic parameters of the calculated line shapes

/such

such as the ratio of maximum to minimum intensity, or the half width of the coalesced lines as a function of τ . This approach has been used in the case of equal⁵⁵ and unequal⁵⁶ doublets, triplets,⁵⁵ and quadruplets.⁵⁷

Another convenient method for the measurement of τ in some cases depends on obtaining analytical solutions of the appropriate exchange equations to give τ in terms of measureable quantities. This method has been used by Gutowsky and Holm²⁷ and Takeda and Stejskal⁵⁸ in the case of equal and unequal doublets, the separation of the doublet being expressed as a function of τ so that peak separation measurements allow determination of τ values. This method applies, of course, only when the peaks are separate, that is before the coalescence point.

2.6. Collapse of Spin Multiplets by Exchange Processes

Section 2.5 was concerned with the collapse of signals arising from nuclei in different chemical positions, that is, collapse of a chemical shift. It is also frequently found that the components of a spin multiplet may be partly or completely collapsed by similar mechanisms.

The collapse of spin multiplets can be caused by the exchange of nuclei between identical molecules. This effect was demonstrated by Arnold⁵⁹ for the hydroxyl protons of ethanol, which show a triplet spectrum (due to coupling with the methylene protons) in absence of exchange but collapse to a singlet if the exchange rate is increased by the addition of acid.

For simplicity first consider the case where species A and B are coupled through spin-spin interaction (J), and assume that both A and B have $I = \frac{1}{2}$. The spectrum, in the absence of exchange, will consist of four lines⁶⁰ and the separations and intensities will be determined by the ratio J/δ , where δ is the chemical shift. Suppose that $\delta \gg J$ so that the spectrum consists of two well separated doublets of almost equal intensity. Next assume that only one of the nuclei, say A, undergoes exchange. This will
/modulate

modulate the spin-spin interaction of B at random at a rate $\frac{1}{2}\tau$ where 2τ is the mean lifetime of A in a given state. It is very important to note that if A undergoes chemical exchange its mean lifetime between exchanges is τ since it has a probability of one half of preserving its spin state in each exchange process. The two resonances belonging to B will thus behave in the same manner as if they belonged to two different chemical species which are exchanging so that the theoretical treatment for an equal doublet given in Section 2.5 applies to a good approximation.

It is of interest to look briefly at a more rigorous treatment, such as is considered by Grunwald and coworkers⁶¹ for the case of the exchange of the hydroxyl protons of methanol. In absence of exchange the methyl protons of methanol give rise to a doublet due to coupling with the hydroxyl proton. With increasing proton exchange rate, the components of the doublet will broaden and then fuse together to give a single line which will finally sharpen up.

The rate of proton spin inversion can be characterised by a time τ , defined as

$$\frac{1}{\tau} \equiv 2 \times \frac{\text{rate of spin inversion of the OH group}}{[\text{MeOH}]} \quad (2-64)$$

/There

There are two contributions to the spin inversion rate: chemical exchange, and spontaneous inversion. The latter can be characterised by the relaxation time T_1 of the OH protons. Hence

$$\frac{1}{\tau} = \frac{1}{T_1} + \frac{R}{[\text{MeOH}]} \quad (2-65)$$

where R is the rate of proton exchange.

It should be noted that although equation (2-64) contains the factor two, this factor cancels out in equation (2-65) because of a factor of one half in the relation between T_1 and the transition probability⁶² and also the probability of one half, mentioned above, that exchange leads to spin inversion.

Consider the case when the CH_3 - resonance is a single peak. Here the width of the exchange broadened line provides a suitable measure for the exchange rate. In the limiting case of fast exchange, so that $(1/T_2' - 1/T_2) \ll J$, the relationship to τ is given by^{63,64}

$$\frac{1}{T_2'} - \frac{1}{T_2} = \frac{J^2 \tau}{4} \left(1 + \frac{1}{1 + \delta^2 \tau^2} \right) \quad (2-66)$$

where δ is the chemical shift (in radians per second) between the two kinds of protons causing the spin splitting J, that is, in the case the chemical shift

/between

between the CH_3^- and OH protons.

The last factor in equation (2.66) is a quantum correction. This factor is absent in the corresponding "classical" expression^{51,52} derived from the Bloch equations.

Another effect of considerable importance in some cases can arise from spin-spin splitting of a proton resonance by O^{17} (spin $I = 5/2$) which is only partially averaged out by proton exchange. This effect can produce significant increases in line width in molecules containing the OH grouping such as water⁵⁴ and methanol⁶⁵ even for the natural abundance of O^{17} which is 0.037%.

Consider the case of water with its normal ratio of oxygen isotopes. In absence of proton exchange the theoretical PMR spectrum would consist of one very intense line corresponding to the species H_2O^{16} and H_2O^{18} , the nuclear spins of O^{16} and O^{18} being zero, and six lines of very low intensity corresponding to the six possible states of the O^{17} nuclear spin which are $\pm 1/2$, $\pm 3/2$, $\pm 5/2$ assuming that the PMR spectrum was measured at a temperature at which the longitudinal relaxation time of O^{17} is sufficiently long.

/According

According to the treatment of Meiboom⁵⁴ which makes a correction for the quadrupole relaxation of O^{17} , the extent of the broadening $B(O^{17})$ of the water resonance for conditions of low rf power can be expressed as

$$B(O^{17}) = \frac{3.7}{3} \times 10^{-4} \tau \sum \frac{n^2 (J_{\text{eff}})^2}{1 + (nJ_{\text{eff}}\tau)^2} \quad (2-67)$$

where $n = 1/2, 3/2, 5/2$.

and

$$J_{\text{eff}} = \frac{J^1 T^1}{T^1 + \tau} \quad (2-68)$$

in which J^1 is the O^{17} -H coupling constant, T^1 the relaxation time of O^{17} in water, and τ the average lifetime between successive exchanges, that is, the average time a proton is bonded to a specific oxygen atom. J_{eff} is an effective coupling constant which makes allowance for the relaxation of the O^{17} nucleus.

A detailed study of the kinetics of fast proton transfer processes occurring in water has been carried out by Meiboom⁵⁴ by measuring the broadening of the proton resonance (of natural water and O^{17} enriched water) and the O^{17} resonance (of water enriched with O^{17}) as a function of pH.

It is of interest to note that it is generally true that maximum exchange broadening occurs in the case of collapse of a chemical shift δ (radians per second) when

$$\tau\delta \approx 1 \quad (2-69)$$

where the significance of τ is given by equation (2-47). In the case of collapse of fine structure arising from spin-spin interaction J (radians per second) maximum exchange broadening occurs when

$$\tau J \approx 1 \quad (2-70)$$

where τ is the average residence time between exchange events.

Hence the range of mean lifetimes measureable by the above techniques is seen to depend on δ or J and can be roughly estimated by substitution of typical values of δ and J in the appropriate relationships given above. Thus, if protons are concerned, the measureable mean lifetimes are normally between 1 and 10^{-3} seconds approximately, a difficult range to measure by other means. Values of δ and J are fixed by molecular parameters, apart from the variation of δ , which is small in practice, made possible by changing the magnetic field strength, so that in order to bring the mean lifetimes into the measureable range where

/kinetic

kinetic effects on the line shapes are observable it is often necessary to carefully adjust the chemical or physical conditions of the system, such as solvent, pH, temperature or concentration.

2.7. Relation to Chemical Kinetics

The mean lifetime of nuclei in A sites between exchanges τ_A can be evaluated from the NMR spectrum as already described and is related to the conventional rate constant k by the expression

$$\frac{1}{\tau_A} = \frac{1}{[A]} \frac{d[A]}{dt} = k[A]^{a-1}[B]^b \dots \quad (2-71)$$

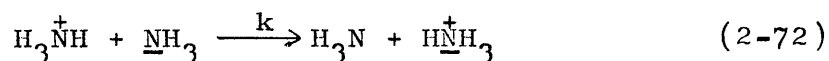
where $a, b \dots$ are the orders of the reaction with respect to the concentrations of A, B The orders of reaction a, b, \dots can be determined by a series of experiments in which τ_A is measured as a function of the concentrations of A, B When the reaction is unimolecular and of the first order, as is usually assumed for hindered rotations and ring inversion, $1/\tau_A$ is the rate constant.

In relating mean lifetimes to the chemical rate constants considerable care must be taken to introduce the proper statistical factors where necessary. It has already been stressed in Section 2.6 that for the case of two species A and B coupled through spin-spin interaction (J) for the case $\delta \gg J$ (both nuclei with $I = \frac{1}{2}$) that if the mean lifetime of nuclei in a particular spin state is denoted by 2τ , then the mean lifetime between exchange events which is of more

/direct

direct chemical interest is given by τ since the probability of chemical exchange bringing about a change in spin state is equal to one half. Evaluation of the conventional rate constant on a basis of the rate of interchange of spin states and neglecting the above statistical consideration would lead to a value of the rate constant which was half the **true** value.

Another example of the necessity of introducing the appropriate statistical factor is afforded by the proton transfer reaction between NH_4^+ and NH_3 studied by Emerson, Grunwald and Kromhout,⁶⁶ namely



This reaction was studied by measuring the broadening of the proton triplet in the NH_4^+ spectrum, and applying the slow exchange equation,

$$\frac{1}{T_2'} = \frac{1}{T_2} + \frac{1}{\tau_{I_z}} \quad (2-73)$$

where τ_{I_z} is the mean lifetime that a proton is bonded to nitrogen of a given spin state (I_z), the other terms having their usual significance.

In application of equation (2-71) to the evaluation of the conventional rate constant k , $1/\tau_{I_z}$ must be replaced by $4.3/2.1/\tau_{I_z}$ to give the true value
/of k

of k . The factor 4 enters because τ_{I_z} measures the mean lifetime of one proton, and the factor $3/2$ takes into account transfers which take place between N atoms in the same spin state and so leave no mark in the spectrum.

If the rate of a reaction has been studied over a range in temperature, the free energy of activation ΔG^\ddagger , the heat of activation ΔH^\ddagger , and the entropy of activation ΔS^\ddagger for the process can be obtained from transition state theory by means of the equation⁶⁷

$$k = \frac{\kappa kT}{h} e^{-\Delta H^\ddagger/RT} e^{\Delta S^\ddagger/R} \quad (2-74)$$

where k is Boltzmann's constant, h is Planck's constant, and κ is the transmission coefficient, that is, the fraction of forward-moving transition state molecules that actually become product. Equation (2-74) can be expressed in an equivalent form as

$$\log_{10} \frac{k}{T} = \log_{10} \frac{\kappa k}{h} + \frac{\Delta S^\ddagger}{2.303R} - \frac{\Delta H^\ddagger}{2.303RT} \quad (2-75)$$

so that if $\log_{10} \frac{k}{T}$ is plotted against $1/T$ ($^{\circ}\text{K}^{-1}$), the resulting straight line will have slope $(-\Delta H^\ddagger/2.303R)$ and intercept $(\log_{10} \frac{\kappa k}{h} + \frac{\Delta S^\ddagger}{2.303R})$. Thus ΔH^\ddagger and ΔS^\ddagger can be determined provided a reasonable estimate

/of the transmission

of the transmission coefficient κ can be made. The value of the free energy of activation ΔG^\ddagger at any temperature is then conveniently given by equation (2-76)

$$\Delta G^\ddagger = \Delta H^\ddagger - T\Delta S^\ddagger \quad (2-76)$$

If the value of the rate constant is known at only one temperature, as is frequently the case for hindered rotation and ring inversion studies where a single rate constant is obtained at the temperature of coalescence of the lines, the free energy of activation at this temperature can be found by means of the equation

$$k = \frac{\kappa kT}{h} e^{-\Delta G^\ddagger/RT} \quad (2-77)$$

Often the quantities which are computed from measurements of the temperature dependence of reaction rate are the parameters A and E_a of the Arrhenius equation

$$k = A e^{-E_a/RT} \quad (2-78)$$

Comparison of equation (2-78) with the transition state equation (2-74) shows that the Arrhenius equation is only an approximation, in as much as it represents, by the constant A , a number of quantities which actually depend on temperature. However, in general these

/quantities

quantities vary much more slowly with temperature than does the factor $e^{-E_a/RT}$ and it is usual to accept the Arrhenius activation energy E_a as an approximation to the energy of activation, and to take the logarithm of the Arrhenius frequency factor A as an approximate measure of the entropy of activation.

E_a and A can be obtained from the slope and intercept of a plot of $\log_{10}k$ against $1/T(^{\circ}K^{-1})$, the slope being $-E_a/2.303R$ and the intercept $\log_{10}A$.

To conclude this section the kinetic order of a reaction with respect to the solvent will be briefly discussed. Consider a reaction in which an acid molecule HA reacts with n solvent molecules SH such that $n + 1$ protons are transferred. Let the rate of proton exchange associated with this reaction be $d[HA]/dt$ in the acid and $d[SH]/dt$ in the solvent. Then, $d[SH]/dt$ is equal to n times $d[HA]/dt$ since n solvent molecules exchange a proton every time one HA molecule exchanges a proton. Conversely, if both $d[SH]/dt$ and $d[HA]/dt$ can be measured, the ratio is n which can thereby be found.

It must be shown, of course, that the measurements apply to the same reaction and a necessary, though not sufficient, condition is that the two rates follow

/identical

identical rate laws. For example, CH_3NH_3^+ reacts with CH_3NH_2 in aqueous solution by two distinct processes, both of which follow the rate law,

rate = $k[\text{CH}_3\text{NH}_3^+][\text{CH}_3\text{NH}_2]$ but only one of which involves water molecules.⁵⁷

If proton exchange involves several processes in parallel, the rate laws for $d[\text{HA}]/dt$ and $d[\text{SH}]/dt$ will be sums consisting of several distinct kinetic terms. In this case the number of solvent molecules participating in each reaction will be equal to the ratio of the rate constants for the corresponding kinetic terms.⁶⁵

In favourable cases the kinetic NMR method as described above allows evaluation of both $d[\text{HA}]/dt$ and $d[\text{SH}]/dt$ and so provides a means of determining the number of solvent molecules participating in any given process. Such cases will be considered in detail in Chapter 3.

CHAPTER III

HISTORICAL

Chapter III Historical

- 3.1 Proton Transfer Reactions involving Solvent
Participation
- 3.2 Internal Rotation about Bonds with Partial
Double Bond Character

3.1. Proton Transfer Reactions involving Solvent

Participation

Comprehensive reviews have been written recently by de Maeyer and Kustin¹ and Albery⁶⁸ which contain good general accounts of the study of proton transfer processes in solution, and, as recently as this year (1965), the Faraday Society held a general discussion meeting⁶⁹ entitled "The Kinetics of Proton Transfer Processes." The use of NMR to study proton transfer and other reactions in solution has been reviewed by Loewenstein and Connor.⁷⁰

In this section particular emphasis will be placed on proton transfer reactions involving solvent participation since a general review of this topic is not available, although very recently a general discussion of solvent participation in proton transfer reactions of amines and their conjugate acids has been presented in a paper by Grunwald and Cocivera.⁵

The first published report of the use of the PMR method to study the detailed kinetics of proton exchange was concerned with aqueous solutions of methylammonium ion.⁷¹ Since then these studies have been extended to a number of amines and other compounds

/in a variety

in a variety of hydroxylic solvents covering a wide range of dielectric constant, though, as has been said already, comparatively few detailed studies in solvents of low dielectric constant have been carried out.

The most extensive measurements in this field are related to the study of amines and the results for methylamine^{71,57,72,2,3} will be considered first since these are well suited to illustrate the kind of information which can be obtained. In the original studies^{71,57} carried out by Grunwald, Loewenstein and Meiboom proton transfer processes in acidic aqueous solutions of methylamine in which the methylamine existed essentially in the form of the cation CH_3NH_3^+ were investigated. When the pH is less than about unity the proton spectrum gives no indication of proton exchange and consists of, on going from high to low magnetic field, a sharp quadruplet from CH_3 , the splitting being the result of spin-spin interaction with the protons of the NH_3^+ group, then a sharp single line from water, and finally a triplet from NH_3^+ , the splitting being due to spin-spin coupling with the N^{14} nucleus. It might be expected that each component of the NH_3^+ triplet would be split into a quadruplet due to

/spin-spin

spin-spin coupling with the CH_3 protons. However, each of the triplet components is broadened due to quadrupole relaxation of the N^{14} nucleus (spin $I = 1$) and the superposed quadruplet structure becomes almost invisible. If the pH of the solution is increased, proton exchange becomes important, and the spectrum changes in a number of ways. With increasing pH, the CH_3 quadruplet first broadens and then coalesces into a singlet which finally sharpens; similarly, the NH_3^+ triplet first broadens and then disappears, while the H_2O singlet first broadens and then sharpens again, simultaneously shifting slightly in the direction of the NH_3^+ frequency. Since the hydrogens of the CH_3 group are certainly not exchanging rapidly under these experimental conditions, all these effects must be due to protolytic exchange on the NH_3^+ group, also involving the water protons. The sharp singlet which at high pH replaces both the NH_3^+ triplet and the water singlet represents an average for both kinds of protons, the exchange between them being now too fast for separate lines to be distinguishable.

It was shown by Grunwald, Loewenstein and Meiboom^{71, 57} that information about the reaction kinetics of the

/exchange

exchange processes could be obtained from the broadening at intermediate acidities in all three components of the spectrum. Matching, as described in Section 2.5, of calculated and observed envelopes of the CH_3 spectra and measurement of the broadening of the components of the NH_3^+ triplet gave two distinct methods of determining the mean lifetime of the NH_3^+ protons between exchanges. The mean lifetime of protons on oxygen before being transferred to nitrogen was determined by measurement of the broadening of the water line in the "lifetime broadening" region and application of the slow exchange approximation, equation (2-42).

By studying the way in which the mean lifetimes of the water and NH_3^+ protons depend upon the pH and the concentration of methylammonium ion, Grunwald and coworkers^{71,57,72} found the major mechanisms for protolysis of methylammonium ion in aqueous solution in the pH range 3-5 to be reactions (3-2) and (3-3) shown below:

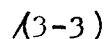
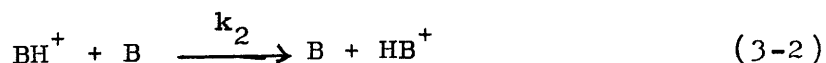
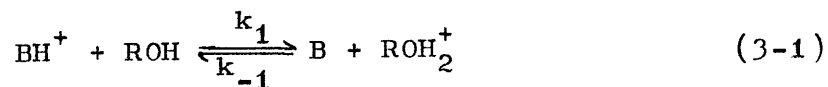
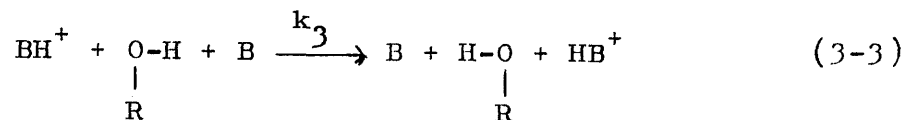


TABLE 3-1

Rate Constants for Proton Transfer^a and Acid Dissociation Constants, Water, 25°C.

BH ⁺	k ₁ (sec. ⁻¹)	10 ⁻¹⁰ k ₋₁ (M ⁻¹ sec. ⁻¹)	k ₂ (M ⁻¹ sec. ⁻¹)	k ₃ (M ⁻¹ sec. ⁻¹)	10 ¹⁰ K _A (M)	ref.
NH ₄ ⁺	24.6	4.3	11.7 x 10 ⁸	0.9 x 10 ⁸	5.68	66
CH ₃ NH ₃ ⁺	-	-	4.0 x 10 ⁸	5.3 x 10 ⁸	0.242	72
(CH ₃) ₂ NH ₂ ⁺	-	-	0.5 x 10 ⁸	9.0 x 10 ⁸	0.168	55, 73
(CH ₃) ₃ NH ⁺	4.7	3.0	0.0 x 10 ⁸	3.4 x 10 ⁸	1.57	74
(CH ₃) ₃ PH ⁺	8	0.5	≤ 1.2 x 10 ²	≤ 1.2 x 10 ²	16	75, 5

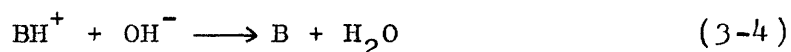
^aThe rate constants in this table apply to reactions (3-1) to (3-3), as indicated in the text, and to dilute solutions.



where, for the case of methylammonium ion in acidic aqueous solution, $\text{BH}^+ \equiv \text{CH}_3\text{NH}_3^+$, $\text{B} \equiv \text{CH}_3\text{NH}_2$,

$\text{ROH} \equiv \text{H}_2\text{O}$, and $\text{ROH}_2^+ \equiv \text{H}_3\text{O}^+$

It should be pointed out that no more than a few percent of the total protolysis of methylammonium ion takes place by a diffusion controlled⁵⁷ process of the type



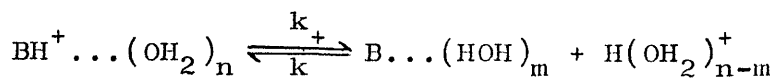
since the hydroxide ion concentration is too low in the acidic region of interest.

In the case of methylammonium ion the rate constant k_1 for acid dissociation was found to be too small for measurement by the kinetic PMR method. Values of k_1 for related compounds have been determined by PMR and are given in table 3-1, together with relevant acid dissociation constants. Also included in table 3-1 are selected values of k_2 and k_3 , the rate constants for reactions of the type (3-2) and (3-3) shown above. The values of the rate constants k_1 , k_2 , and k_3 given in the table all correspond to dilute aqueous solutions at 25°C.

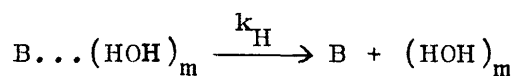
Several interesting trends are apparent from the data given in table 3-1. The values of the rate constant k_{-1} ($= k_1/K_A$) for the reverse process of equilibrium (3-1) suggest the reaction of H_3O^+ with amine takes place at nearly every encounter. Diffusion controlled processes between H_3O^+ and bases are quite common,⁷⁶ but this mechanism is not general and an example of this is given by the reaction between H_3O^+ and $(CH_3)_3P$ which is probably not diffusion controlled (table 3-1). Values of k_1 , in contrast to those of k_{-1} , are quite sensitive to the addition of inert salts and decrease when salt is added.^{66,74,77} Furthermore, addition of strong acids produces a very marked reduction in k_1 , and it has been shown that it is possible, by using sulphuric acid-water mixtures, to reduce k_1 by as much as six orders of magnitude relative to the value in water.^{77,78} A detailed study of this phenomenon has been carried out by Grunwald⁷⁷ and the following mechanism is proposed in which the proton transfer is represented as occurring in two steps,

(a) reversible ionisation to produce an amine-water hydrogen-bonded complex





and (b) breaking of the amine-water hydrogen bond, (3-5)



where $m \geq 1$, $n \geq 2$, and k_H is the rate constant for breaking the $\text{B} \dots (\text{HOH})_m$ hydrogen bond. It is very important to note that the $\text{B} \dots (\text{HOH})_m$ hydrogen bond must be broken during the lifetime of the amine-water complex, or the reversible cycle shown in (3-5a) will lead only to momentary escape of the BH^+ proton and not to exchange. This is similar to a mechanism proposed earlier by Swain and his coworkers for the exchange between $(\text{CH}_3)_3\text{NH}^+$ and methanol solvent.^{79,80}

Kinetic studies have allowed the determination of k_H for certain amines^{77,78} and the values obtained for NH_3 , CH_3NH_2 , and $(\text{CH}_3)_3\text{N}$, in water at 25°C, were 5×10^{11} , 8×10^{10} and 1.1×10^{10} (sec.⁻¹) respectively. It appears therefore that methyl-substitution on nitrogen strengthens the hydrogen bond.

It is noteworthy that the rate constant k_2 for direct proton transfer from BH^+ to B decreases sharply with methyl-substitution on nitrogen (table 3-1).

This could be due to increased steric hindrance or to
/the increased

TABLE 3-2

Rate Constants for Proton Transfer and Acid Dissociation Constants, Methanol, 25°C.

BH ⁺	k ₁ (sec. ⁻¹)	k ₋₁ (M ⁻¹ sec. ⁻¹)	k ₃ (M ⁻¹ sec. ⁻¹)	K _a ^a (M)	ref.
p-CH ₃ C ₆ H ₄ NH ₃ ⁺	2.92 x 10 ³	1.04 x 10 ¹⁰	8.1 x 10 ⁷	2.8 x 10 ⁻⁷	82
(CH ₃) ₃ NH ⁺	0.6	0.5 x 10 ¹⁰	3.25 x 10 ⁸	1.20 x 10 ⁻¹⁰	5
C ₆ H ₅ (CH ₃) ₂ PH ⁺	3.7 x 10 ³	1.3 x 10 ⁸	<10 ⁴	2.8 x 10 ⁻⁵	82

^ameasured in methanol at 25°C

the increased energy of the desolvation step that must precede proton transfer. The rate constant k_3 for the reaction of BH^+ , water and B is not highly sensitive to methyl-substitution, but small changes are observed and these appear to parallel the changes in $1/K_A$ (table 3-1). In the trimethylamine case, Luz and Meiboom,⁸¹ using solvent enriched in oxygen-17, were able to prove the number of solvent molecules involved in this process is one.

Detailed studies by Grunwald and coworkers⁷² on the protolysis of methylammonium ion indicated, in this case, that the most probable rate-determining step for the reaction with rate constant k_3 is proton transfer from a water molecule in the solvation shell of $CH_3NH_3^+$ to a molecule of CH_3NH_2 , to produce the triple ion $CH_3NH_3^+ \cdot OH^- \cdot HNH_2^+CH_3$, the reaction being completed by rapid release of a proton from $CH_3NH_3^+$.

Solvent participation has also been found to play an important role in certain protolytic reactions occurring in methanol as solvent and pertinent data for p-toluidinium and trimethylammonium ion as well as phenyldimethylphosphonium ion are summarised in table (3-2), the rate constants having the same significance

/as before

as before except that they refer to methanol as solvent at 25°C. The magnitudes of k_{-1} suggest that the reaction of CH_3OH_2^+ is diffusion controlled with the amines but not with the phosphine. It has been found that the rate of proton exchange decreases markedly in strong acid.⁸² This phenomenon is similar to that noted in water and can be explained by a two-stage mechanism analogous to (3-5). Values of k_3 are available for p-toluidinium ion and for trimethylammonium ion (table 3-2). In the former case it has been shown by Grunwald and coworkers⁸² that only one methanol molecule undergoes proton exchange in this reaction. The value of k_3 for trimethylammonium ion in methanol is almost identical with that observed in water (tables 3-1 and 3-2). The corresponding reaction for phenyldimethylphosphonium ion is very much slower, the upper limit being $10^4 \text{M}^{-1} \text{sec.}^{-1}$.⁸²

Quite recently Krakower and Reeves⁸³ have investigated proton exchange between methanol and the phenolic proton of o-chlorophenol, the exchange rate being studied as a function of temperature.

An elegant series of studies on the proton transfer processes of benzoic acid and various

/substituted

substituted benzoic acids in methanol has been carried out by Grunwald, Meiboom and coworkers.^{61,65,84,85} In solutions of benzoic acid and sodium benzoate in methanol it was shown⁶⁵ that the rate law for proton exchange between benzoic acid HBz and methanol at 24.8°C is given by equation (3-6) and that for OH-proton exchange involving methanol subspecies is given by equation (3-7).

$$\text{Rate} = 0.71 \times 10^5 [\text{HBz}] + 1.52 \times 10^8 [\text{HBz}][\text{Bz}^-] \quad (3-6)$$

$$\left. \begin{aligned} \text{Rate} = & 1.31 \times 10^5 [\text{HBz}] + 1.21 \times 10^8 [\text{HBz}][\text{Bz}^-] \\ & + 8.79 \times 10^{10} [\text{H}^+] + 1.85 \times 10^{10} [\text{MeO}^-] \end{aligned} \right\} \quad (3-7)$$

Equation (3-6) involves two kinetic terms, one first-order in HBz, the other second-order, that is, first order each in HBz and Bz⁻. Equation (3-7) involves two similar terms, and also an additional term proportional to [H⁺], and one proportional to [MeO⁻]. The reasonable assumption was made that the first-order term in equation (3-6) refers to the same process as that in equation (3-7) so that the number of solvent (methanol) molecules in that process was found to be $(1.31 \times 10^5)/(0.71 \times 10^5)$, or 1.85. A similar assumption for the second-order term lead to

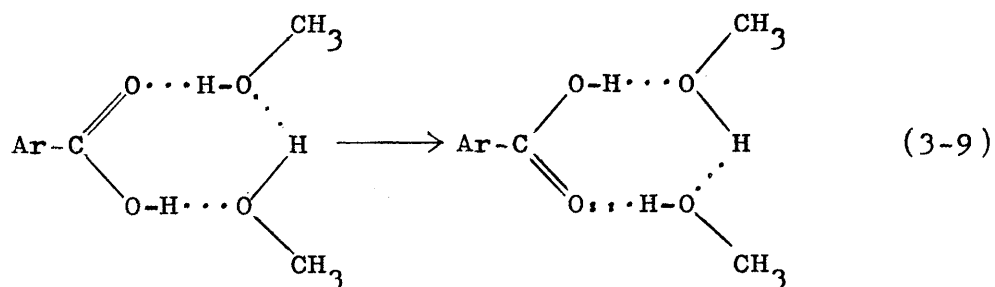
/the conclusion

conclusion that the number of methanol molecules in that process is $(1.52 \times 10^8)/(1.21 \times 10^8)$ or 0.8. Within experimental error these numbers could be exactly 2 and 1 respectively.

The general rate expression⁸⁴ for exchange between a benzoic acid and methanol at 24.8°C has the same form as equation (3-6), that is

$$\text{Rate} = k_I[\text{HA}] + k_{II}[\text{HA}][\text{A}^-] \quad (3-8)$$

The rate constants for various benzoic acids are given in table (3-3). The first process, which involves two methanol molecules, and which corresponds to the first kinetic term $k_I[\text{HA}]$, is thought to take place by a cyclic pathway of the type



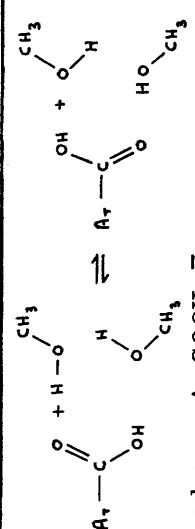
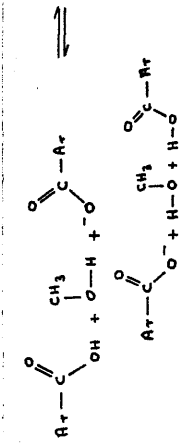
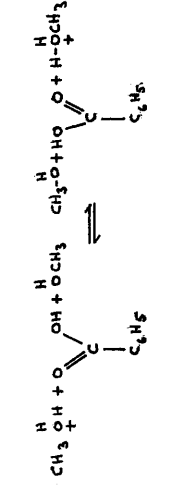
As can be seen from table (3-3), the rate of the process corresponding to the second kinetic term of equation (3-8), which involves one methanol molecule, does not change rapidly with the acid strength of the benzoic acid. This lack of sensitivity of rate

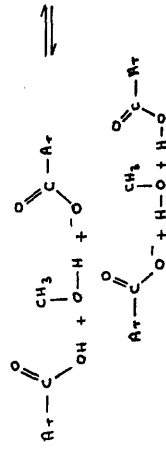
/with acid

TABLE 3-3

Reaction	Rate Constant	Activation Parameters	Conditions	ref.
$\text{CH}_3\text{OH} + \text{CH}_3\text{OH}_2^+ \rightleftharpoons \text{CH}_3\text{OH}_2^+ + \text{CH}_3\text{OH}$	8.8×10^{10} (sec. ⁻¹)	$\Delta H^\ddagger = 2.3$ kcal./mole	methanol, 24.8°C	61
$\text{CH}_3\text{OH} + \text{CH}_3\text{O}^- \rightleftharpoons \text{CH}_3\text{O}^- + \text{CH}_3\text{OH}$	1.85×10^{10} (sec. ⁻¹)		methanol 24.8°C	61
$\begin{array}{c} \text{CH}_3 \\ \\ \text{O} = \text{C} - \text{OH} \\ \\ \text{Ar} \end{array} + \text{H} - \text{O} \begin{array}{c} \text{CH}_3 \\ \\ \text{O} - \text{H} \end{array} \rightleftharpoons \begin{array}{c} \text{OH} \\ \\ \text{Ar} - \text{C} = \text{O} \\ \\ \text{O} - \text{CH}_3 \end{array} + \text{H} - \text{O} \begin{array}{c} \text{CH}_3 \\ \\ \text{O} - \text{H} \end{array}$				65, 84
where $\text{ArCOOH} \equiv$	(sec. ⁻¹)	$\Delta H^\ddagger = 6.53$ kcal./mole	methanol, 24.8°C	
benzoic acid	1.31×10^5	$\Delta S^\ddagger = -14.4_2$ eu	methanol -81.6°C	
benzoic acid	2.2×10^2			
m-nitrobenzoic acid	3.6×10^5		methanol 24.8°C	
p-nitrobenzoic acid	4.5×10^5	$\text{pK}_a = 8.34^b$		
o-nitrobenzoic acid	19×10^5	8.33^b		
3,5-dinitrobenzoic acid	16×10^5	7.56^b 7.38^b		

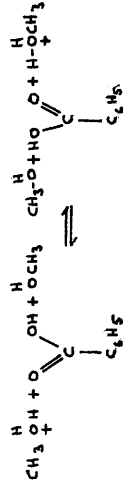
TABLE 3-3

Reaction	Rate Constant	Activation Parameters	Conditions	ref.
$\text{CH}_3\text{OH} + \text{CH}_3\text{OH}_2^+ \rightleftharpoons \text{CH}_3\text{OH}_2^+ + \text{CH}_3\text{OH}$	$8.8 \times 10^{10} \text{ (sec.}^{-1}\text{)}$	$\Delta H^\ddagger = 2.3$ kcal./mole	methanol, 24.8°C	61
$\text{CH}_3\text{OH} + \text{CH}_3\text{O}^- \rightleftharpoons \text{CH}_3\text{O}^- + \text{CH}_3\text{OH}$	$1.8_5 \times 10^{10} \text{ (sec.}^{-1}\text{)}$		methanol 24.8°C	61
 <p>where $\text{ArCOOH} \equiv$</p>				
benzoic acid	(sec.^{-1}) 1.31×10^5	$\text{pK}_a =$ 9.41^b	methanol, 24.8°C	65,84
benzoic acid	2.2×10^2	$\Delta H^\ddagger = 6.53$ kcal./mole $\Delta S^\ddagger = -14.4_2$ eu	methanol -81.6°C	
m-nitrobenzoic acid	3.6×10^5	8.34^b	methanol, 24.8°C	
p-nitrobenzoic acid	4.5×10^5	8.33^b		
o-nitrobenzoic acid	19×10^5	7.56^b		
3,5-dinitrobenzoic acid	16×10^5	7.38^b		
 <p>where $\text{ArCOOH} \equiv$</p>				
benzoic acid	$1.21 \times 10^8 \text{ (M}^{-1}\text{sec.}^{-1}\text{)}$	$\Delta H^\ddagger = 4.06$ kcal./mole $\Delta S^\ddagger = -7.9_2$ eu	methanol, 24.8°C	65,84
benzoic acid	$1.7 \times 10^6 \text{ (M}^{-1}\text{sec.}^{-1}\text{)}$		methanol, -81.6°C	
m-nitrobenzoic acid	$2.5 \times 10^8 \text{ (M}^{-1}\text{sec.}^{-1}\text{)}$		methanol, 24.8°C	
p-nitrobenzoic acid	$2.7 \times 10^8 \text{ (M}^{-1}\text{sec.}^{-1}\text{)}$			
o-nitrobenzoic acid	$1.8 \times 10^8 \text{ (M}^{-1}\text{sec.}^{-1}\text{)}$			
3,5-dinitrobenzoic acid	$4.1 \times 10^8 \text{ (M}^{-1}\text{sec.}^{-1}\text{)}$			
				
benzoic acid	$2.58 \times 10^8 \text{ (M}^{-1}\text{sec.}^{-1}\text{)}$	$\Delta H^\ddagger = 3.30$ kcal./mole $\Delta S^\ddagger = -9.0$ eu	methanol, 24.8°C	85
benzoic acid	$7.5 \times 10^6 \text{ (M}^{-1}\text{sec.}^{-1}\text{)}$		methanol, -81.6°C	

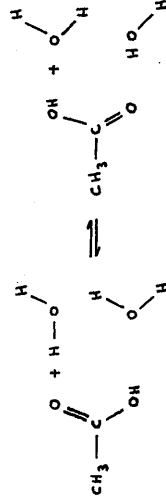


where $\text{ArCOOH} \equiv$

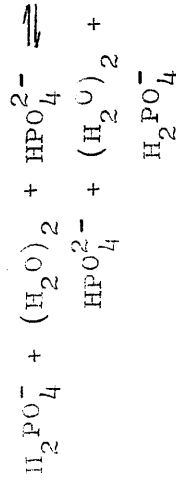
benzoic acid	$1.21 \times 10^8 (\text{M}^{-1} \text{sec.}^{-1})$	$\Delta H^\ddagger = 4.06$ kcal./mole	methanol, 24.8°C	65,84
benzoic acid	$1.7 \times 10^6 (\text{M}^{-1} \text{sec.}^{-1})$	$\Delta S^\ddagger = -7.92$ eu	methanol, -81.6°C	
m-nitrobenzoic acid	$2.5 \times 10^8 (\text{M}^{-1} \text{sec.}^{-1})$			
p-nitrobenzoic acid	$2.7 \times 10^8 (\text{M}^{-1} \text{sec.}^{-1})$		methanol, 24.8°C	
o-nitrobenzoic acid	$1.8 \times 10^8 (\text{M}^{-1} \text{sec.}^{-1})$			
3,5-dinitrobenzoic acid	$4.1 \times 10^8 (\text{M}^{-1} \text{sec.}^{-1})$			



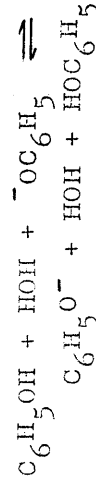
	$2.58 \times 10^8 (\text{M}^{-1} \text{sec.}^{-1})$	$\Delta H^\ddagger = 3.30$ kcal./mole	methanol, 24.8°C	85
	$7.5 \times 10^6 (\text{M}^{-1} \text{sec.}^{-1})$	$\Delta S^\ddagger = -9.0$ eu	methanol, -81.6°C	



	$4.8 \times 10^7 (\text{sec.}^{-1})$	$\Delta H^\ddagger = 3.1$ kcal./mole	water, 25°C	87
		$\Delta S^\ddagger = -13.0$ eu		

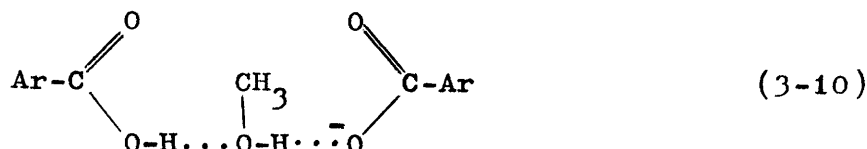


	$1.45 \times 10^9 (\text{M}^{-1} \text{sec.}^{-1})$		water, 25°C	88
--	---	--	-------------	----



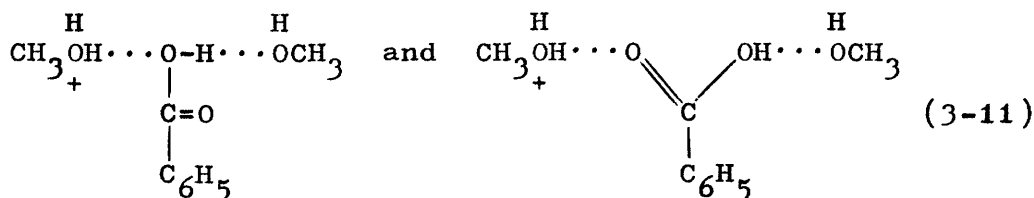
	$7.1 \times 10^8 (\text{M}^{-1} \text{sec.}^{-1})$	$\Delta H^\ddagger = 4.2$ kcal./mole	water, 25°C	89
		$\Delta S^\ddagger = -5.0$ eu		

with acid strength is in good keeping with a push-pull, or concerted, mechanism for this process similar to that envisaged by Swain for the ionisation of alkylammonium ions in methanol.^{79,80}



Rate measurements were also made at -81.6°C , and relevant results are included in table (3-3). It is noteworthy that a third term of the form $k[\text{HBz}]^{\frac{1}{2}}[\text{Bz}^-]^{\frac{1}{2}}$ appears in the kinetic analysis for the exchange between benzoic acid and methanol at low temperature. This term has been shown to be polymolecular in methanol but its mechanism is not yet understood.⁶⁵

In the presence of HCl a different fast concerted mechanism has been found to take place⁸⁵ involving one molecule each of CH_3OH_2^+ , $\text{C}_6\text{H}_5\text{OH}$, and CH_3OH . Kinetic data for this process are given in table (3-3) and two possible mechanisms suggested are



/Feldbauer

Feldbauer and Weller⁸⁶ have investigated, in a similar manner to that described above, the proton transfer processes of acetic acid and formic acids in ethanol as solvent. It was found that the first term of a rate equation of form (3-8) is insignificant for acetic acid, and that the second term is insignificant for formic acid.

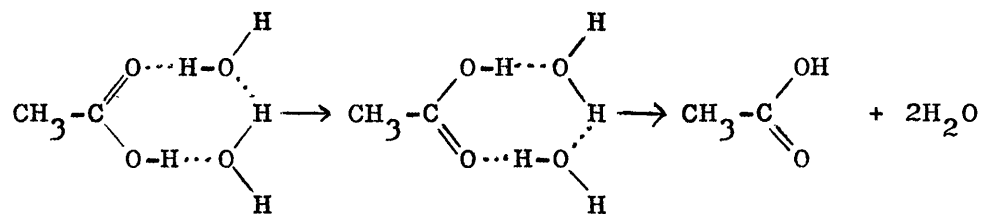
Very valuable kinetic information about proton transfer processes occurring in solution, including ones involving solvent participation has been obtained in a series of studies by Luz and Meiboom,^{81,87,88,89,90} The solvent employed in these studies was O¹⁷-enriched water and exchange rates were determined from the broadening of the PMR line of water.

It has already been mentioned above that in the case of the protolytic reaction of trimethylammonium ion with rate constant k_3 , Luz and Meiboom were able to show⁸¹ the number of participating molecules is one.

In a study of the kinetics of proton exchange in aqueous solutions of acetate buffers, the above workers were able to show⁸⁷ that the main protolytic reaction bringing about proton exchange between the carboxyl group of acetic acid and water, under the conditions of the study, has the mechanism shown below,

/which

which involves the formation of a hydrogen-bonded complex consisting of one acetic acid molecule and two water molecules, and proton transfer within this complex



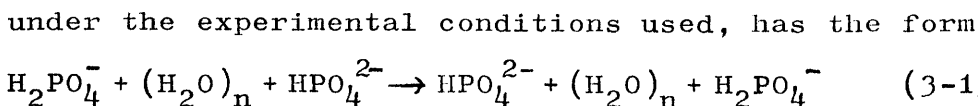
It is of interest to note that this reaction mechanism is analogous to the mechanism of the process corresponding to the first kinetic term of the general rate expression (3-8) for the exchange of benzoic acids in methanol.^{65,84} It should be pointed out, however, that the experimental conditions employed by Luz and Meiboom⁸⁷ were such that the kinetic data obtained do not exclude the possibility that the rate constant of a reaction of the type $\text{AcOH} + \text{OH}_2 + \text{AcO}^- \rightarrow \text{AcO}^- + \text{HOH} + \text{AcOH}$, might be as high as $1 \times 10^8 \text{M}^{-1} \text{sec.}^{-1}$. Kinetic data are given in table (3-3).

The same workers have also carried out studies on the rates and mechanisms of proton exchange in aqueous

/solutions

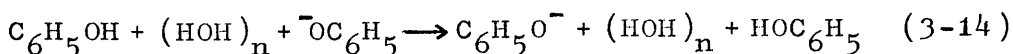
solutions of phosphate buffer,⁸⁸ and aqueous solutions of phenol-sodium phenolate buffer,⁸⁹ Pertinent data are given in table (3-3).

In the study of proton exchange in aqueous solutions of phosphate buffer the predominant exchange reaction involving the buffer components, detected



The second-order rate constant obtained for the above reaction, $1.45 \times 10^9 \text{M}^{-1} \text{sec}^{-1}$ (at 25°C) has been shown⁸⁸ to be consistent with a diffusion controlled mechanism in which the number of intervening solvent (water) molecules is two, that is, $n = 2$ in equation (3-13). Since the proton exchange takes place via two water molecules it is reasonable to suppose that these belong to the hydration shells of the reacting phosphate ions, proton transfer being rapid whenever the hydration shells of the ions come into contact.

In the case of proton exchange in aqueous solutions of phenol-sodium phenolate buffer,⁸⁹ the main protolytic reaction involving the buffer components detected under the experimental conditions used can be represented by an equation of the type



/in which

in which the proton transfer takes place through a chain of n water molecules. The actual number of water molecules, which must be at least one or the reaction would not be detected, could not be determined by the method used in this study and, in the evaluation of the second-order rate constant for this reaction, $7.1 \times 10^8 \text{ M}^{-1} \text{ sec.}^{-1}$ (at 25°C) the assumption is made that n is equal to one. The findings for the analogous reactions between trimethylammonium ion and trimethylamine in aqueous solution⁸¹ and between benzoic acid and benzoate ion in methanol⁶⁵ are referred to by Luz and Meiboom in support of this assumption. Should, in fact, the actual number of participating solvent molecules n be greater than one the true second-order rate constant would be $(7.1 \times 10^8)/n \text{ M}^{-1} \text{ sec.}^{-1}$ rather than $7.1 \times 10^8 \text{ M}^{-1} \text{ sec.}^{-1}$

It is also of interest to note that by using suitable buffer solutions Luz and Meiboom⁹⁰ were able to obtain Arrhenius rate expressions for the elementary processes $\text{H}_2\text{O} + \text{H}_3\text{O}^+ \xrightarrow{k_{11}} \text{H}_3\text{O}^+ + \text{H}_2\text{O}$ and $\text{H}_2\text{O} + \text{OH}^- \xrightarrow{k_{11}} \text{OH}^- + \text{H}_2\text{O}$ and these are respectively $k_{11} = 6.0 \times 10^{11} e^{-2.4/RT}$ and $k_{11} = 1.0 \times 10^{11} e^{-2.1/RT}$ where R is to be taken in $\text{kcal.mole}^{-1} \text{K}^{-1}$.

/A recent

TABLE 3-4

Values of $k_1, k_{-1}, (k_2 + k_3), k_H, k_{\text{intra}}$ ^a and Acid Dissociation Constants
for Amino Acids in Aqueous Solution^b

BH ⁺	k_1 ^c (sec ⁻¹)	$10^{10} \times k_{-1}$ (M ⁻¹ sec ⁻¹)	$10^{10} \times k_H$ (sec ⁻¹)	$(k_2 + k_3)$ (M ⁻¹ sec ⁻¹)	k_{intra} (sec ⁻¹)	$10^{10} \times K_A$ (M)	Temp. (°C)	ref.
HO ₂ CCH ₂ NH ₃ ⁺	370	2.0	0.85	$\sim 2.8 \times 10^8$		186 ^d	23 ± 1	93
CH ₃ O ₂ CCH ₂ NH ₃ ⁺	470	2.5	1.52	2.8×10^8		186	23 ± 1	93
⁻ O ₂ CH ₂ NH ₃ ⁺	~ 5.1			$< 1.6 \times 10^8$	175		23 ± 1	93
HO ₂ CCH ₂ NH ₂ CH ₃ ⁺	110	4.4	1.15			25 ^d	21 ± 1	91,93
CH ₃ O ₂ CCH ₂ NH ₂ CH ₃ ⁺	120	4.8	2.9			25	21 ± 1	92,93
⁻ O ₂ CH ₂ NH ₂ CH ₃ ⁺	~ 4.5			$< 2.0 \times 10^8$	80		21 ± 1	92,93

^aThe significance of these rate constants is given in the test.

^bThe data given are selected from a summary presented in a paper by Sheinblatt and Gutowsky, 93

^cThe values of k_1 apply to dilute aqueous solutions

^dThis value of K_A is taken as equal to the value of K_A for the corresponding methyl ester.

A recent series of investigations has been directed at the elucidation of the protolysis kinetics of the simple amino acids, sarcosine and glycine in acidic aqueous solution.^{91,92,93} A summary of the proton exchange rate constants and the values of the first-order rate constant k_H for breaking the N...HOH hydrogen bond which were obtained in these studies is contained in a paper by Sheinblatt and Gutowsky.⁹³ Pertinent values of k_1 , k_{-1} , k_H , k_{intra} (see below), and the sum of the rate constants k_2 and k_3 selected from this summary are given in table (3-4). The rate constants k_1 , k_{-1} , k_H , k_2 , and k_3 all refer to the nitrogen function and have the same significance as before. Comparison of the results for the amino acids (table (3-4)) with the amine results (tables (3-1) and (3-2)) which have already been discussed shows a marked similarity between the two series. The results for the amino acids have been discussed in detail by Sheinblatt and Gutowsky.⁹³

Of interest, in the present context, is a type of intramolecular protolysis (rate constant, k_{intra}) which was found to occur in the zwitterionic forms of sarcosine⁹² and glycine,⁹³ which involves the net

/transfer

transfer of a proton from a positively charged nitrogen atom to the ionised carboxyl group and in which the proton transfer may occur via one or more participating solvent (water) molecules. An alternative mechanism which is equally well in keeping with the data^{92,93} should be noted, however and this involves the "jump" of a NH_2^+ or NH_3^+ proton to the COO^- group followed by rapid intermolecular exchange of the proton which has arrived in a COOH site. The method used does not allow the determination of which of the alternatives corresponds to the actual mechanism. Before going on to discuss reactions, in which the solvent plays a critical role, occurring in solvents of low dielectric constant, reference should be made to a PMR study carried out by Anbar Loewenstein and Meiboom⁵⁶ on the kinetics of proton exchange between hydrogen peroxide and water in the pH range 2.5 to 6.5. The reaction was found to be both acid and base catalysed. In the acid region, pH 4.5, the reaction involves H_3O^+ and H_2O_2 , while in the less acidic region it was found to involve HO_2^- , H_2O_2 and H_2O . The rate constants for these processes are given in table (3-3). The above workers discuss⁵⁶ various possible detailed microscopic mechanisms for /the latter

TABLE 3-5

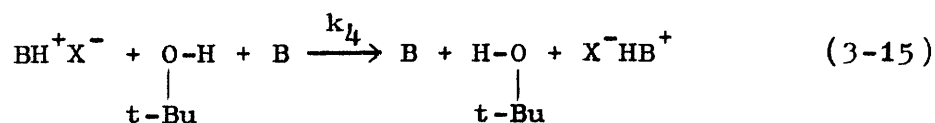
Rate Constants for Reaction (3-15) in t-Butanol 35°C

BH ⁺	anion	k_4 (M ⁻¹ sec. ⁻¹)	$\frac{k_3(\text{H}_2\text{O})^a}{k_4(\text{t-BuOH})}$	ref.
(CH ₃) ₃ NH ⁺	Cl ⁻	1.1 x 10 ⁵	3,500	5
(CH ₃) ₃ NH ⁺	Br ⁻	5.3 x 10 ⁵	740	5
(CH ₃) ₃ NH ⁺	p-toluenesulphonate	7.0 x 10 ⁵	560	5
CH ₃ NH ₃ ⁺	Cl ⁻	2.6 x 10 ⁷	23	5
CH ₃ NH ₃ ⁺	p-toluenesulphonate	2.4 x 10 ⁷	25	5

^aAll data at 35°C

the latter process.

Proton transfer processes occurring in solvents of low dielectric constant (ϵ) are altered by ionic association. Grunwald and Cocivera⁵ have studied the protolytic reactions of methylammonium and trimethylammonium salts in t-butanol ($\epsilon = 12.47$ at 25°C)⁹⁴ and the reactive species was found to be the solvated ion-pair BH^+X^- , rather than the solvated free ion BH^+ . Rate constants for reaction (3-15), given below, have been measured⁵ for several methylammonium and trimethylammonium salts in t-butanol at 35°C , and are listed in table (3-5).

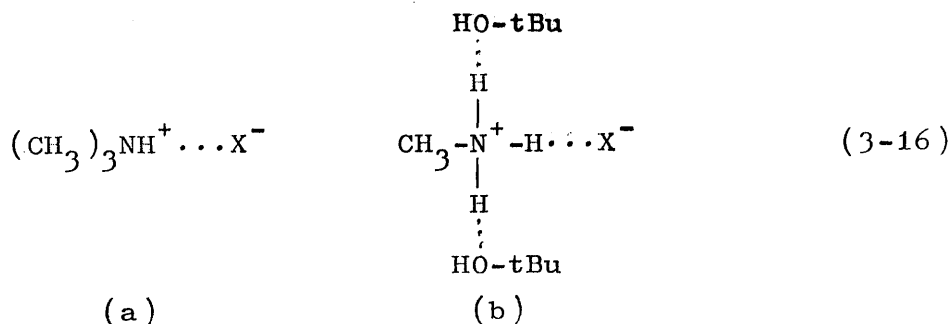


The kinetics of proton exchange was found to be second-order, that is, first-order in ammonium salt and first-order in amine. In the concentration range employed in these studies (10^{-3} - 10^{-1}M) the salts exist largely in the form of ion-pairs.

Inspection of the data in table (3-5) shows a marked contrast between the behaviour of methylammonium

/salts

salts and of trimethylammonium salts. For the former k_4 , the rate constant for reaction (3-15) is quite insensitive to the nature of the anion and is about one-twentieth of k_3 in water. For the latter, k_4 is highly sensitive to the nature of the anion and ranges from 1/3000 to 1/500 of k_3 in water. This contrast in behaviour has been explained by Grunwald and Cocivera⁵ on the basis that the ion-pairs are intimate ion-pairs with anion and cation in direct contact, and possible structures suggested are



In the ion-pair of type (3-16a), it is pointed out, the single NH proton is probably bound to the anion by a strong hydrogen bond and this gives a reason for the low reactivity of the single trimethylammonium NH proton as well as the sensitive dependence of exchange rate with the nature of the anion. On the other hand it is extremely unlikely that all three

/NH protons

TABLE 3-6

First-Order Rate Constants for Proton Exchange of Ammonium Salts with Acetic Acid in Glacial Acetic Acid at 25°C

BH^+X^-	k_5 (sec. ⁻¹)	$10^{10}K_A$ (in water) ^a (M)	ref.
$NH_4^+OAc^-$	6,080	5.69	2,3
$CH_3NH_3^+OAc^-$	230	0.238	2,3
$(CH_3)_3NH^+OAc^-$	945	1.58	2,3
TRIS·H ⁺ OAc ^{-b}	41,000	84.0	2,3
NH_4^+ picrate	30		4
$NH_4^+O_2CCCl_3^-$	2		4
$NH_4^+Cl^-$, $CH_3NH_3^+Cl^-$, $(CH_3)_3NH^+Cl^-$	} too slow to measure		4

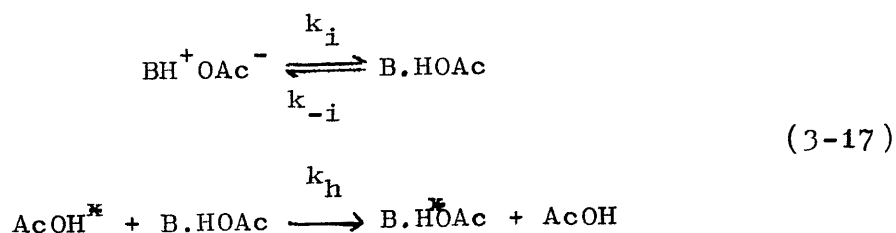
^afor BH^+

^bTRIS = (tris-hydroxymethyl)aminomethane.

of CH_3NH_3^+ are bound to the anion by strong hydrogen bonds, so that one or perhaps two (as shown in a formulation of type (3-16b)) of the NH protons are hydrogen-bonded to solvent molecules and so can react freely by process (3-15).

Recently Grunwald and Price^{2,3} have studied the ionisation and proton exchange of several amines in glacial acetic acid ($\epsilon = 6.22$ at 25°C).⁹⁴ In this solvent medium it was found that the amines studied are almost completely converted to the acetate salts, which exist in solution largely in the form of ion-pairs BH^+OAc^- .^{2,3}

Proton exchange of the amines studied with acetic acid was found to be first-order in the concentration of BH^+OAc^- ^{2,3} and values of the first-order rate constant k_5 for proton exchange of ammonium acetates with acetic acid in glacial acetic acid at 25°C , are given in the upper portion of table (3-6). The exchange mechanism proposed by Grunwald and Price^{2,3} has two steps and is of the form



Inspection of the upper portion of table (3-6) shows that the values of k_5 are nearly proportional to those of the acid dissociation constant K_A of BH^+ in water, that is $d \log k_5 / d \log K_A \approx 1$. The above authors point out that this correlation suggests that the mechanism of proton exchange involves an ionisation step, as suggested in (3-17) above. In the proposed mechanism (3-17), the rate determining step could be either the initial proton transfer (k_i) or the exchange of acetic acid between solvation shell of B and bulk solvent (k_h). Several lines of argument suggest that the second step (k_h) is rate-determining.²³

The effect of changing the anion on the rate of proton exchange has been investigated briefly.^{2,3,4} The rate has been found to be first-order in BH^+X^- and some rate constants (again denoted by k_5) are listed in the lower portion of table (3-6). As can be seen the rate constants are strongly dependent on the nature of the anion and appear to be proportional to its basicity. The basicity of X^- relative to OAc^- was equated to $K_A(HOAc)/K_A(HX)$, and the ratio of K_A values was measured directly in acetic acid, under the conditions of the k_5 measurements.⁴

/It has been

It has been pointed out⁵ that the fact that the values of k_5 of chloride salts are too small to be measured by the PMR method, is consistent with the low basicity of the chloride ion.

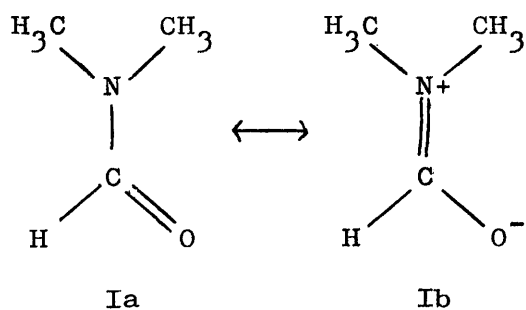
When BH^+Cl^- is added to a solution of BH^+OAc^- , the rate of proton exchange has been found to drop markedly.^{2,3} It has been shown that if it is assumed that such aggregates as $\text{BH}^+\text{OAc}^-\text{BH}^+\text{Cl}^-$ are unreactive in the sense that the reaction rate is too slow to be detected by the PMR technique used in these experiments, then the decrease in rate can be accounted for quantitatively.^{2,3}

3.2. Internal Rotation about Bonds with Partial Double Bond Character

As was pointed out in Chapter I, NMR provides a powerful means of studying hindered internal rotation about bonds with partial double bond character in certain cases. Reviews of this topic have been written by Phillips,⁹⁵ Loewenstein and Connor,⁷⁰ and Pople, Schneider and Bernstein.⁹⁶ The aim of the present section will be to review briefly the NMR studies which have been carried out up to the present which have yielded quantitative information about the nature of the energy barrier for the above type of system.

The first observations of this kind were made in 1955 by Phillips⁹⁷ who studied N,N-dimethylformamide and N,N-dimethylacetamide. The proton spectrum of the former at room temperature was found to consist of a singlet at low field from the formyl proton, and, at higher field, a doublet from the methyl protons. It was found that the splitting of the methyl resonance could not be due to spin-spin coupling since the formyl resonance showed no fine structure and since the separation of the methyl lines depended on the strength of the applied magnetic field.⁹⁷ Phillips
/therefore

therefore deduced that the doublet fine structure of the methyl resonance must arise from the chemical and magnetic non-equivalence of the methyl groups due to hindered rotation about the $-\text{CO}-\text{N}'$ bond of N,N-dimethyl formamide. Lack of ease of rotation about this bond is to be expected due to the resonance stabilised nature of the molecule, since this rotation involves decrease in orbital overlap and hence loss of resonance energy.



The contribution of the zwitterionic canonical form Ib to the true molecular structure will tend to make all the atoms of the molecule lie in one plane except, of course, for the protons of the methyl groups. If the amide group is planar, one methyl group must be cis and the other trans to the carbonyl oxygen, and if rotation is slow about the $-\text{CO}-\text{N}'$ bond then the protons of each methyl group will give rise to a separate resonance line. As has already
/been

been pointed out, the methyl resonance of N,N-dimethylformamide is a doublet at room temperature. As the temperature is raised, however, the rate of rotation about the $\text{-CO-N}\langle$ bond becomes progressively larger and the two lines of the methyl resonance first broaden, then coalesce to form a single broad line that gradually becomes a single narrow line.^{25,27,28,22.}

Methods of obtaining exchange rates from spectral line shapes have already been described in some detail in Chapter 2. The present example involves the collapse of a chemical shift and corresponds to the case of equal site populations and mean lifetimes that is, in the notation of Chapter II, $p_A = p_B$ and $\tau_A = \tau_B$.

Considerable work^{25,27,28,22} has been done to determine the activation parameters for rotation about the $\text{-CO-N}\langle$ bond of N,N-dimethylformamide (I) and the values obtained are given in table (3-7), together with the corresponding values for N,N-dimethylacetamide (III) and related compounds (IV-XIV). No satisfactory explanation has been put forward for the considerable variation in the reported values (table(3-7)) of the activation parameters for internal rotation in N,N-dimethylformamide.

TABLE 3-7

Activation Parameters for Hindered Internal Rotation about Bonds with

Partial Double Bond Character

No.	Compound	E_a or ΔH^\ddagger ^a kcal./mole	b	$\log_{10} A$	ΔG^\ddagger ^c kcal./mole	Tc(°K)	Solvent	ref.
I	N,N-dimethyl- formamide	--	--	--	24 (453°K)	453		22
		7 (± 3)	5 (± 2)	22 (372°K)	372	Pure Liquid	27	
		18.3(± 0.7)	10.8(± 0.4)	21.0	421.6		25	
		9.6(± 1.5)	6.5	--	--		28	
II	N,N-dimethyl- formamide (conjugate acid)	12.7(± 1.5)	8.0	--	403	100% H_2SO_4	28	
		12 (± 2)	8.5(± 1.5)	--	325		27	
IV	N,N-dimethyl- trifluoroacetamide	10.6(± 0.4)	7.8(± 0.2)	17.4	360.3		25	
		9.3(± 0.6)	6.8(± 0.4)	17.6	367.9	Pure Liquid		
V	N,N-dimethyl- trichloroacetamide	9.9(± 0.3)	9.1(± 0.2)	14.9	287.1			

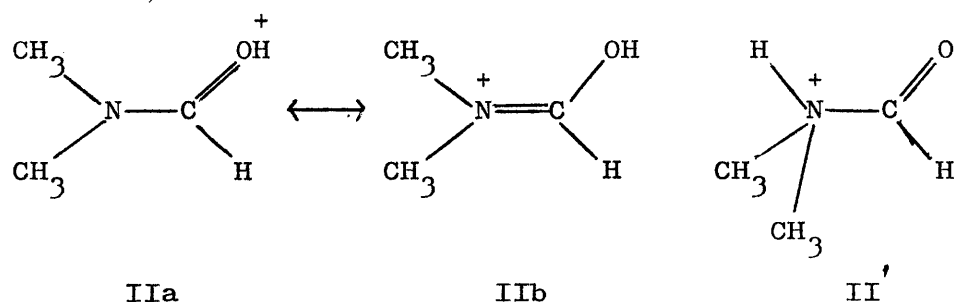
VI	N,N-dimethyl-acrylamide	6.8(±0.7)	6.0(±0.5)	16.1	--	
VII	N,N-dimethylbenzamide	7.7(±0.5)	7.2(±0.4)	15.3	284.9	CH ₂ Br ₂
VIII	N,N-dimethylpropionamide	9.2(±0.7)	7.3(±0.5)	16.7	334.4	Pure liquid
	N,N-dimethylpropionamide	6.7(±0.7) ^e	5.4(±0.5)	16.7	338.3	CH ₂ Br ₂
	N,N-dimethylpropionamide	6.3(±0.4) ^f	5.7(±0.3)	16.0	316.4	CCl ₄
IX	N,N-dimethylcarbonyl chloride	7.3(±0.5)	6.1(±0.3)	16.5	326.0	Pure liquid
	N,N-dimethylcarbonyl chloride	7.3(±0.6) ^g	6.0(±0.4)	16.5	325.9	CH ₂ Br ₂
	N,N-dimethylcarbonyl chloride	6.8(±0.2) ^h	5.9(±0.2)	16.2	317.4	CCl ₄
X	N,N-dibenzylacetamide	7.3(±0.5)	6.1(±0.3)	16.5	343.7	CH ₂ Br ₂
	N,N-dibenzylacetamide	6.4(±0.6)	5.5(±0.4)	16.3	334.5	CCl ₄
XI	formamide	18 (±3)				(CH ₃) ₂ C=O
XII	N-methyl-N-benzylformamide	12 (±2)	7			
XIII	N-methyl-N-methylbenzylformamide	11(±1.5)	7			
XIV	N-methyl-N-diphenylmethylformamide	11(±1.5)	8			
XV	N,N-dimethylthioformamide	27.9(±1.1)	13.6(±0.1)			Pure liquid
	N,N-dimethylthioformamide	36.2(±1.7)	19.1(±0.2)			O-Cl ₂ C ₆ H ₄
XVI	N,N-diisopropylthioformamide	31.8(±2.8)	14.9(±0.2)			Pure liquid

	N,N-diisopropylthioformamide	24.2(±5.6)	12.8(±0.6)			O-Cl ₂ C ₆ H ₄
XVII	(CH ₃) ₂ N-CH=CH-CHO	14.9(±1.5)	12	15.8	308	
XVIII	(CH ₃) ₂ N-CH=CH-C=O C ₆ H ₅	11.7(±1.5)	10	15.2	293	CHCl ₃
XIX	(CH ₃) ₂ N-CH=CH-C=O OC ₂ H ₅	4.6(±1.5)	5	14.8	273	
XX	methyl nitrite	9.0(±2)			230(±3)	Toluene
	methyl nitrite	10.5(±2)	12.1		235	Pure liquid
XXI	ethyl nitrite	9.0(±2)			227(±3)	Toluene
XXII	n-propyl nitrite	9.0(±2)			227(±3)	Toluene
XXIII	iso-propyl nitrite	6.0(±2)			233(±3)	Toluene
XXIV	iso-butyl nitrite	--		10(215°K)	215	Pure liquid
XXV	N,N-dimethyl-nitrosamine	23	12.8	22.8	453	Pure liquid
	N,N-dimethyl-nitrosamine	--		25(488°K)	488	Pure liquid
XXVI	diazoacetone	9.5(±4)	8.5(±0.5)	--	--	
XXVII	C ₆ H ₅ ClBN(CH ₃) ₂	18(±2)	--	--	391	CDCl ₃
XXVIII	C ₆ H ₅ B(N(CH ₃) ₂) ₂	10	--	--		
XXIX	benzaldehyde	--	--	7.9(150°K)	150	vinyl chloride
	benzaldehyde	6.37(±0.2) ^{ti}				Pure liquid
	benzaldehyde	6.69(±0.2) ^{ti}				Pure liquid
	benzaldehyde	4.66 ^{ti}	--	--	--	Pure liquid
XXX	4-N,N-dimethylamino-benzaldehyde-3,5-d ₂			10.8(202°K)	202	CH ₂ Cl ₂

XXXX	Compound	Activation Energy (kcal/mole)	Temperature (K)	Solvent	Page
XXXXI	p-methoxybenzaldehyde	--	9.2(174°K)	vinyl chloride	34
XXXXII	p-chlorobenzaldehyde	4.87(±0.2) [†]	--	nujol	33
XXXXIII	p-tolualdehyde	6.39(±0.2) [†]	--	Pure liquid	
XXXXIV	N-methyl-2,4,6-trinitroaniline	14.5(±0.3)	15.1	CH ₂ Cl ₂	35
XXXXV	2,2-diphenyl-1-picrylhydrazine	12.5(±0.2)	10.8	CH ₂ Cl ₂	

- a † indicates ΔH^\ddagger
- b logarithm to the base 10 of the Arrhenius frequency factor
- c the values apply to the free energy of activation at 298°K unless another temperature is indicated in brackets
- d the temperature of coalescence
- e concentration dependent, refers to 10.2 mole% amide solution
- f concentration dependent, refers to 11.1 mole% amide solution
- g concentration dependent, refers to 10.7 mole% amide solution
- h concentration dependent, refers to 11.0 mole% amide solution
- i determined by infra red spectroscopy

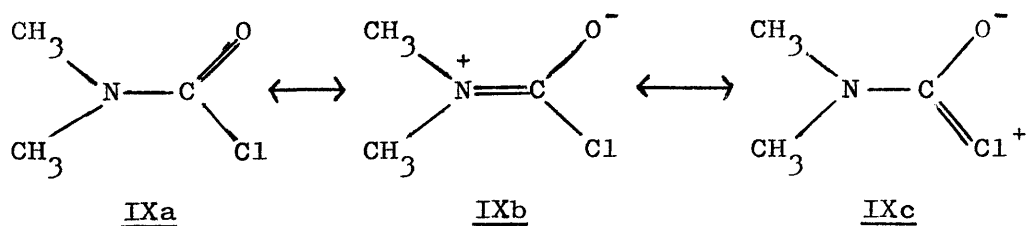
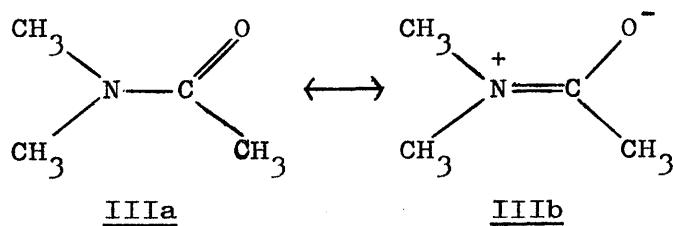
Fraenkel and Franconi²⁸ found an increase in barrier height for internal rotation on passing from N,N-dimethylformamide (I) in the pure liquid ($E_a = 9.6(\pm 1.5)$ kcal./mole) to the conjugate acid (II) in 100% sulphuric acid ($E_a = 12.7(\pm 1.5)$ kcal./mole). On a basis of this result the above workers deduced that the predominantly formed salt was the oxygen-protonated form II and not the nitrogen-protonated form II',



since oxygen protonation would lead to an increase in barrier height due to greater double bond character in the central C-N bond of II compared with I, whereas addition of a proton to nitrogen would destroy the double bond character of the central C-N bond and reduce the barrier to rotation to the very low value expected for a C-N single bond. It was later unambiguously established by Gillespie and Birchall⁹⁸ that compound I and other amides protonate mainly on oxygen, a new peak having been found to appear in the

PMR spectra recorded at low temperatures of solutions of the amides in fluorosulphuric acid which could be assigned with certainty to the >C=OH^+ group.

Rogers and Woodbrey²⁵ found that the barrier height is significantly smaller in N,N-dimethylacrylamide (VI), $E_a = 6.8(\pm 0.7)$ kcal./mole, and in N,N-dimethylcarbonyl chloride (IX), $E_a = 7.3(\pm 0.3)$ kcal./mole, than in N,N-dimethylacetamide (III), $E_a = 10.6(\pm 0.4)$ kcal./mole. The change in barrier height in these compounds has been interpreted in terms of cross-conjugation as represented by structure IXc (for example) which would be expected to reduce the double bond



character of the central C-N bond by competing with

/the resonance

the resonance form IXb (analogous to IIIb) to which the major portion of the energy barrier is attributed.

The barriers for N,N-dimethylpropionamide (VIII) and N,N-dimethylcarbonyl chloride (IX) were found to be concentration dependent, the form of the dependence varying with the polarity of the solvent.²⁶ A

qualitative explanation in terms of the relative stabilities of the ground state as compared with a less polar transition state has been put forward.

Sunners, Piette and Schneider²⁹ have investigated internal rotation about the C-N bond in formamide.

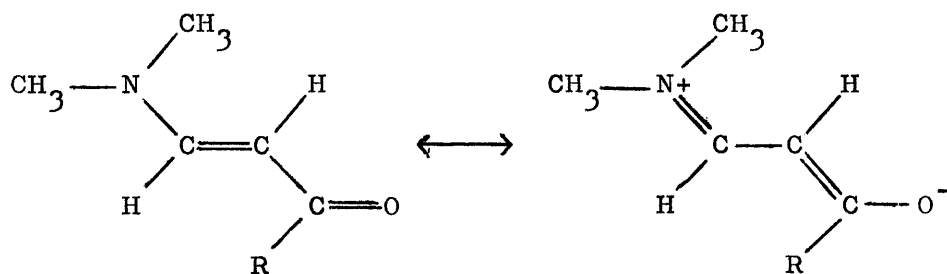
The complication due to quadrupole broadening of the resonance signals by the N¹⁴ nucleus was eliminated by substitution of the isotopic nucleus N¹⁵ and from the observed changes in the proton spectra as a function of temperature the barrier hindering rotation (measured in a 10 mole% solution of formamide-N¹⁵) was found to be 18 ± 3 k.cal./mole.

Loewenstein and coworkers⁹⁹ have investigated hindered rotation in N,N-dimethylthioformamide (XV) and N,N-diisopropylthioformamide (XVI) and found that the barriers hindering rotation about the central C-N bond are significantly higher (table (3-7)) than for the amides. An important factor contributing to

/this increase

this increase in barrier height on passing from the amides to the thioamides may be the greater conjugative electron withdrawing power (-M effect) of the C=S group compared with the C=O group.¹⁰⁰

In a study of hindered internal rotation in β -dimethylamino-acraldehyde (XVII) and related compounds XVIII and XIX, Kramer



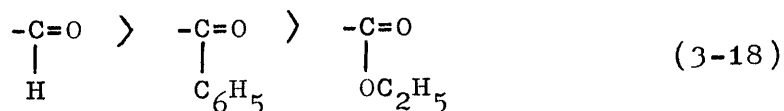
XVII: R = H

XVIII: R = C₆H₅

XIX: R = OC₂H₅

and Gompper found appreciable barriers hindering rotation about the (CH₃)₂N-C bonds.¹⁰¹

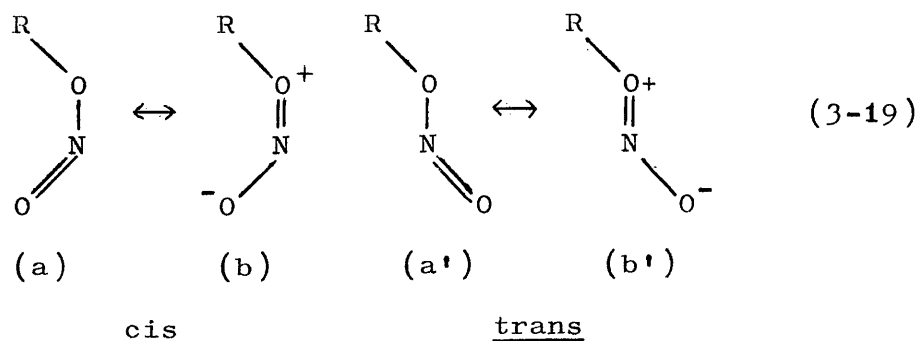
As the mesomeric electron attracting power (-M effect)¹⁰⁰ of the -COR group decreases,



the height of the potential barrier hindering rotation
/falls

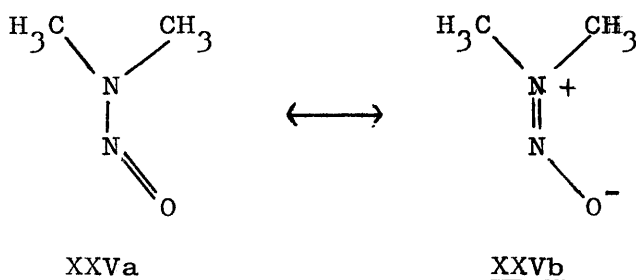
falls sharply, E_a being 14.9 (± 1.5) kcal./mole for XVII, 11.7 (± 1.5) kcal./mole for XVIII, and 4.6 (± 1.5) kcal./mole for XIX. Since the amount of double bond character in the $(\text{CH}_3)_2\text{N}-\text{C}$ bond will decrease with the -M effect of the -COR group, a critical dependence of barrier height on the amount of double bond character in the bond can be clearly inferred. Kramer and Gompper were able to show^{101,102} that β -dimethylaminoacetaldehyde protonates mainly on the carbonyl oxygen atom, though some protonation also takes place on nitrogen and at the α -carbon atom.

The existence of stable rotational isomers for alkyl nitrites was first inferred from doublings of the $\text{N}=\text{O}$ stretching and $\text{O}-\text{N}=\text{O}$ bending frequencies in the infra-red spectra of this class of compounds.¹⁰³ Several^{23,22,24} NMR studies have been carried out to measure potential barriers in alkyl nitrites and the values obtained are given in table (3-7). The barrier to rotation may arise, in part, from contributions such as (3-19b) and (3-19b'),

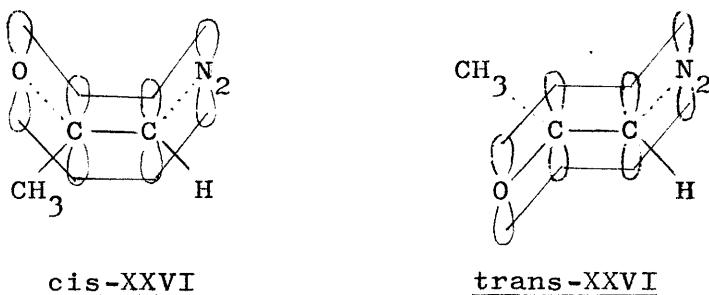


to the electronic structure of these molecules, but repulsion between non-bonding electrons on the nitrogen and -O- oxygen atom may contribute significantly.

Looney, Phillips and Reilly²¹ found a barrier height E_a of 23 kcal./mole for internal rotation about the N-N bond in N,N-dimethylnitrosamine (XXV). The magnitude of this value indicates that the zwitterionic form XXVb makes a substantial contribution to the electronic structure of XXV.



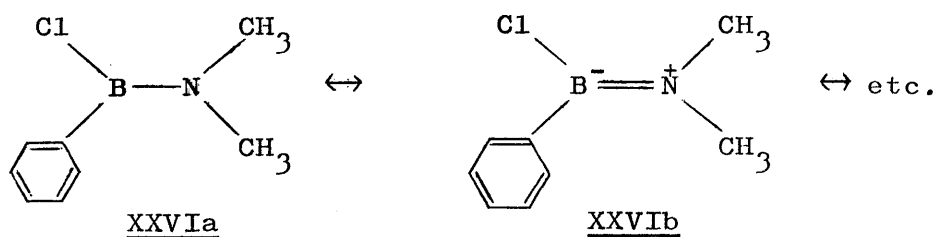
A study by Kaplan and Meloy¹⁰⁴ of the temperature dependence of the NMR spectrum of diazoacetone (XXVI) in chloroform-d has clearly revealed the presence of two conformational isomers, a cis isomer (cis-XXVI) and a trans isomer (trans-XXVI).



The isomers cis- and trans-XXVI result from a

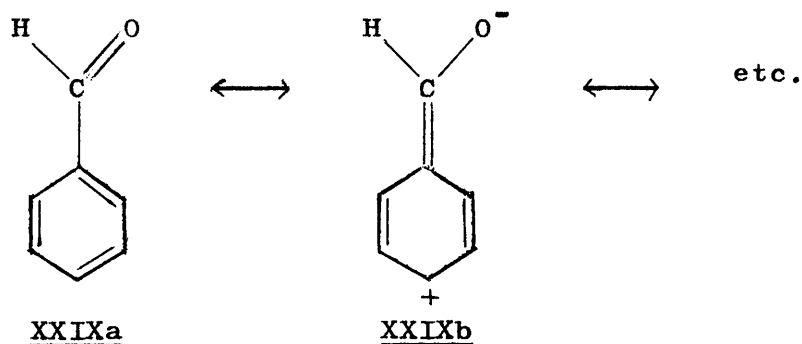
barrier to free rotation about the central C-C bond and the height of this barrier E_a was found to be 9.5 (± 4) kcal./mole. The free energy difference ΔG between the isomers at 241°K was determined by line intensity measurements and the value obtained was 1.14 kcal./mole.

Barfield, Lappert and Lee¹⁰⁵ have investigated hindered rotation about B-N bonds. The barrier height E_a for rotation about the B-N bond in PhClBN(CH₃)₂ (XXVI) was found to be 18 ± 2 kcal./mole, and the magnitude of this value was taken to indicate that forms such as XXVIb, having a positive charge on nitrogen and a negative charge on boron, make an appreciable contribution to the electronic structure of the molecule.



Quite recently activation parameters for internal rotation about the Ar-CHO bond in some aromatic aldehydes (XXIX-XXXIII) have been measured by means of /infra-red

infra-red^{31,33} and proton spectroscopy³⁴ and the values obtained are given in table (3-7). The magnitude of the barrier in benzaldehyde (table (3-7), compound XXIX) is in marked contrast to the triple cosine barrier of 1.15 kcal./mole in acetaldehyde¹⁰⁶ and suggests that the barrier is due to the overlap of the π orbitals of the ring with those of the carbonyl group.



The change in barrier height brought about by introducing a group X into a position para to the formyl function can be explained in terms of the inductive and mesomeric effects of the group X.^{33,34}

The existence of appreciable barriers hindering internal rotation about the Ar-NH- bond in N-methyl-2,4,6,-trinitroaniline (XXXIV) and in 2,2-diphenyl-1-picrylhydrazine (XXXV) has been established³⁵ by studying the PMR spectra of the aromatic protons of

/these

these compounds as a function of temperature using methylene chloride as solvent. Parameters for the internal rotation of XXXIV and XXXV are given in table (3-7).

CHAPTER IV

EXPERIMENTAL AND RESULTS

Chapter IV. Experimental and Results

4.1. Materials

4.2. Preparation of Solutions

4.3. Instrumental

4.4. Measuring Techniques

4.5. Infrared and Ultraviolet Spectra

4.6. Proton Magnetic Resonance Results for
p-Nitroso-N,N-dimethylaniline

4.7. Proton Magnetic Resonance Results for the
Conjugate Acid of p-Nitroso-N,N-dimethylaniline

4.8. Results for Proton Transfer in Aqueous Dioxane

4.9. Determination of Association Constants by
Proton Magnetic Resonance Spectroscopy

4.10. Kinetic Results for Proton Transfer in
Aqueous Dioxane

4.1. Materials

All reagents used were commercially available except p-nitroso-N,N-dimethylaniline hydrochloride which was prepared as described below. Melting points and boiling points agreed with literature values. The p-nitroso-N,N-dimethylaniline (British Drug Houses Ltd.) was recrystallised from light petroleum (b.p. 60-80°C) before use.

The hydrochloride of p-nitroso-N,N-dimethylaniline was prepared by passing dry hydrogen chloride gas into a solution of the aniline in methanol. The colour of the solution changed rapidly from dark green to orange-yellow. The solution was then concentrated in vacuo and a yellow precipitate was obtained which, on recrystallisation from AnalaR-grade methanol, yielded yellow needles melting sharply with decomposition at 177°C (literature m.p. 177°C (decomp.)¹⁰⁸).

Trifluoroacetic acid (Eastman Kodak) was used without further purification. Solvent acetone was of AnalaR-grade and was dried over CaSO₄ before being used. AnalaR-grade dioxane was dried by refluxing it with sodium for 9 hours, after which time the metal remained bright. The solvent was then fractionally distilled from the sodium, the first 10% being discarded and the

next 40% being used to prepare solutions. Karl Fischer titration indicated that the water content of solvent dioxane prepared in this way was less than 0.008M. Piperidine (Hopkin and Williams Ltd.) was thoroughly dried over potassium hydroxide and distilled before use. The water used in preparing solutions was purified by ion-exchange resins. 2,6-Di-t-butyl-phenol (Eastman Kodak) was purified by sublimation in vacuo before being used.

4.2. Preparation of Solutions

All solutions were prepared by standard quantitative techniques. Stock solutions of dioxane-water and dioxane-piperidine were prepared for convenience. The required quantities of the solution components were weighed out into graduated flasks which were then made up to the mark and reweighed. The rate measurements were made only on freshly prepared solutions. In the case of samples containing 2,6-di-t-butylphenol the kinetic measurements were made within about two hours of preparation. All measurements were made using air-saturated solutions.

4.3. Instrumental

All proton spectra were measured at a frequency of 60 Megacycles per second. The instrument used for rate measurements was an Associated Electrical Industries Ltd. R.S.2. model high-resolution NMR spectrometer. Spectra were recorded on a Hellige recorder with variable chart speed, and were calibrated by the side-band technique.¹⁰⁹

A modified sample probe was provided by A.E.I. for variable temperature work and has already been described by Anderson.¹¹⁰ The gas used for controlling the temperature was dry nitrogen which was conducted to the probe by a series of silvered vacuum-jacketed transfer tubes. To obtain sample temperatures below room temperature ($27 \pm 2^\circ\text{C}$) the dry nitrogen was cooled by passage through a copper coil immersed either in a dry ice-acetone bath or a liquid nitrogen bath depending upon the temperature range required. Temperature was controlled by carefully adjusting the rate of nitrogen flow. Sample temperatures above room temperature were obtained by heating the dry nitrogen by passage through a glass tube containing glass beads (to aid heat transfer) which was wound with heating
/tape.

tape. The temperature was controlled by careful adjustment of both the current flowing through the heating tape (by means of a rheostat) and the nitrogen flow rate.

Temperatures above room temperature were measured by placing a sample of ethylene glycol in the probe. It has been found¹¹¹ that the variation with temperature of the separation of the two proton resonances of ethylene glycol provides a convenient method of temperature measurement from room temperature to about 200°C. The temperature T in °C is given to an accuracy of about 2°C by the equation $T = 173 - 1.483\Delta\nu$, where $\Delta\nu$ is the separation of the CH_2 and OH resonances in c.sec.^{-1} at 60Mc.sec.^{-1} . In a typical temperature measurement above room temperature the ethylene glycol sample was allowed at least twenty minutes to come to thermal equilibrium at a particular temperature, and then the separation of the two resonances was measured using the oscilloscope of the spectrometer by superposing the side-band of one resonance on the other, the intensity of the side-band being adjusted so that it is equal to the intensity of the signal on which it is being superposed. Superposition was taken to correspond to the most pronounced

/'wobble'

'wobble' pattern following a sweep through the combined signal. When the peaks were superimposed, the frequency separation was read from the audio-frequency oscillator and the temperature found using the above equation. The ethylene glycol sample was then replaced by the sample under investigation which was allowed at least twenty minutes to reach thermal equilibrium. Temperatures in the range from room temperature down to about -40°C were measured in an analogous manner to that described above using the variation with temperature of the separation of the CH_3 and OH proton resonances of methanol. The methanol sample used contained a trace of concentrated hydrochloric acid which was added to aid superposition of signals by completely collapsing the fine structure of the methanol resonances due to spin-spin coupling. Varian Associates¹¹² have prepared a calibration graph, the chemical shift between the CH_3 and OH resonances being plotted against temperature. Temperature measurement below about -40°C involved the use of two copper-constantan thermocouples. One of these was a permanently-sealed thermocouple in the probe and had one junction close to, but separated by a thin glass wall from, the sample tube. This

/thermocouple

thermocouple gave readings on a potentiometer supplied by A.E.I. and the potentiometer was calibrated in degrees Centigrade as follows. One junction of another copper-constantan thermocouple was placed directly in a sample tube in the probe containing a suitably low-freezing liquid such as hexa-1,5-diene (m.p. -141°C), the reference junction being at 0°C . The potential of this thermocouple was measured using a Croydon Precision Instrument type P4 portable thermocouple potentiometer and the sample temperature was found from a plot of thermocouple potential against temperature.¹¹³ Further details of the methods used to measure temperatures below room temperature are given by Anderson.¹¹⁰

Over the entire temperature range -70°C to $+60^{\circ}\text{C}$ the temperature control was probably good to only $\pm 1^{\circ}\text{C}$ due to slight variations in the nitrogen flow rate. A reasonable estimate of the accuracy of temperature determination is $\pm 2^{\circ}\text{C}$.

A few proton spectra were recorded on a Perkin-Elmer model R10 NMR spectrometer operating at 60 Megacycles per second.

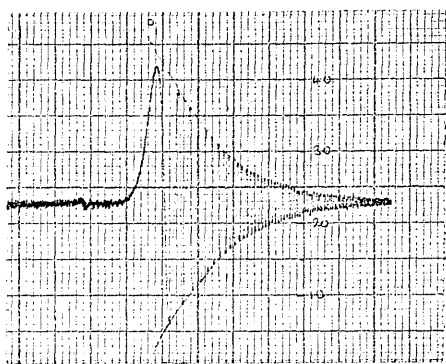


Figure 4-1. A typical exponential decay pattern produced by rapidly sweeping through the sharp dioxane signal. This spectrum corresponds to a sweep rate of about 15c. sec.^{-2}

4.4. Measuring Techniques

In the measurement of line positions by the side-band technique¹⁰⁹ for the determination of association constants, side-bands of an internal reference peak, for example the dioxane resonance, were placed above and below the resonance whose position was to be measured, and within 20 c.sec.⁻¹ of it. The line position was then obtained by linear interpolation between the side-bands. Each of the line positions used in the determination of association constants was obtained by averaging the results of about ten spectra.

The field homogeneity was carefully adjusted and checked at frequent intervals. The effective relaxation time T_2 corresponding to the field homogeneity was calculated, by applying the method of Jacobsohn and Wangsness,⁵³ from the decay of the 'wiggles' following a fast sweep through the sharp acetone or dioxane signal (see Figure 4-1). The effective T_2 was measured at the beginning and end of each record. Measurements were rejected if $1/T_2$ changed by more than 20% during a measurement.

Slow passage width measurements were carried out, the sweep rate $d\nu/dt$ used being less than or equal to

$$/1/8\pi T_2'^2$$

$1/8\pi T_2'^2$ for a line with line width parameter T_2' , in order to avoid the formation of 'wiggles' and signal broadening by distortion (see Section 2.5). Typically the value of the full-width at half-height $\Delta\nu_{\frac{1}{2}}$ used in kinetic measurements was the average of about six line-width determinations, an equal number of upfield and downfield measurements being used in the average to help to compensate for any magnetic field drift. In the case of a single broadened line the transverse relaxation time T_2' can be found directly using the relation $1/T_2' = \pi\Delta\nu_{\frac{1}{2}}$. On the other hand, in the case of a group of unresolved or partly resolved lines, the transverse relaxation time T_2' corresponding to the individual components must be found indirectly from slow-passage measurements. An example of an indirect method of determining T_2' is given in Section 4.6.

The separation J of the lines of the quartet or doublet of acetaldehyde 2.85 c.sec.^{-1} , or the separation of suitably placed side-bands served as suitable frequency calibrations for the measurement of sweep rates.

In the kinetic measurements suitably low r.f. power levels were selected which gave adequate signal intensity without causing any appreciable signal

/distortion

distortion due to saturation.

Standard thin-walled sample tubes with an outer diameter of 5 mm. (supplied by Messrs. Jencons Ltd.) were used. The sample tubes were sealed with light tightly-fitting rubber caps (supplied by Vicarey, Davidson and Co.) in order to exclude atmospheric moisture and carbon dioxide.

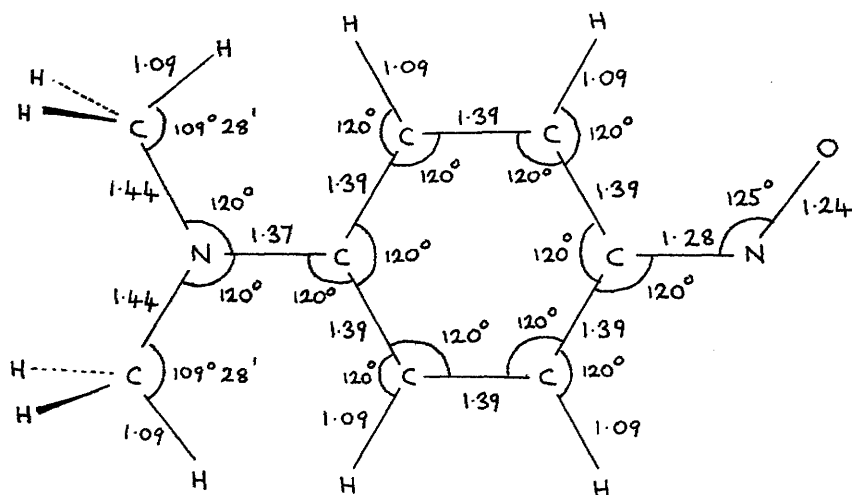


Figure 4-2. The structure used in the calculation by Pitzer's¹¹⁴ method of the reduced moment for the torsion of the NO group of p-nitroso-N,N-dimethylaniline. Bonds which lie in the plane of the paper are represented by —, while bonds lying above and below the plane of the paper are represented by — and ----- respectively.

4.5. Infrared and Ultraviolet Spectra

The torsional vibration of the polar NO group of p-nitroso-N,N-dimethylaniline is expected to be strongly active in the far infrared region. Absorption in the range 110-180 cm.^{-1} was very kindly measured for the author by G. E. Campagnaro. In benzene solution a strong relatively sharp band ($\Delta\nu_{\frac{1}{2}} = 15 \text{ cm.}^{-1}$) occurs at 166 cm.^{-1} and can almost certainly be assigned to the torsional fundamental. For the correlation of this frequency to the barrier opposing rotation a reduced moment of 9.67 a.m.u. \AA^2 is used. This reduced moment was calculated by Pitzer's¹¹⁴ method for a structure (shown in Figure 4-2) whose dimensions were inferred from other known structures, particularly those of p-nitroaniline¹¹⁵ and p-iodonitrosobenzene.¹¹⁶

The infrared spectrum of a saturated solution of p-nitroso-N,N-dimethylaniline hydrochloride in chloroform in the range 3150-3650 cm.^{-1} was measured with a Unicam S.P. 100 double-beam infrared spectrophotometer. The only band in the above range occurs at 3630 cm.^{-1} ($\Delta\nu_{\frac{1}{2}} = 37 \text{ cm.}^{-1}$). The chloroform used was of AnalaR grade and was dried by repeated passage through a column of blue silica gel immediately before use.

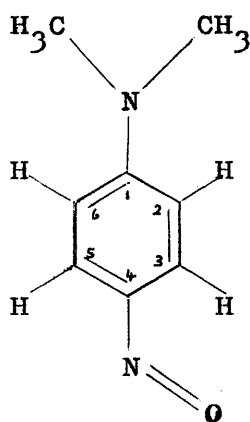
/The absorption

The absorption spectra of solutions of p-nitroso-N,N-dimethylaniline (0.017 to ~0.5 M) in trifluoroacetic acid in the range 600-850 m μ were measured with a Unicam S.P. 800 spectrophotometer. Matched, stoppered, fused silica cells with a 1 cm. path were used. In the above range there is no absorption assignable to the $n \rightarrow \pi^*$ transition of a nitroso group.

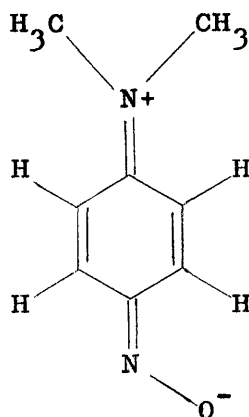
4.6. Proton Magnetic Resonance Results for

p-Nitroso-N,N-dimethylaniline

In p-nitroso-N,N-dimethylaniline (I) rotation of the N=O group by 180° about the axis of the bond joining it to the aromatic ring interconverts identical configurations. The existence of a relatively high barrier hindering this rotation, reflecting the contribution of structure (II) has been inferred from dipole moment,¹¹⁷ infrared,¹¹⁸ and ultraviolet measurements.¹¹⁹ The compound is monomeric in the solid state¹¹⁹ and in solution¹²⁰ so that no complications arise out of its dimerisation.



(I)



(II)

At room temperature, the aromatic protons of (I) give rise to a typical A_2X_2 spectrum in which the

/relative

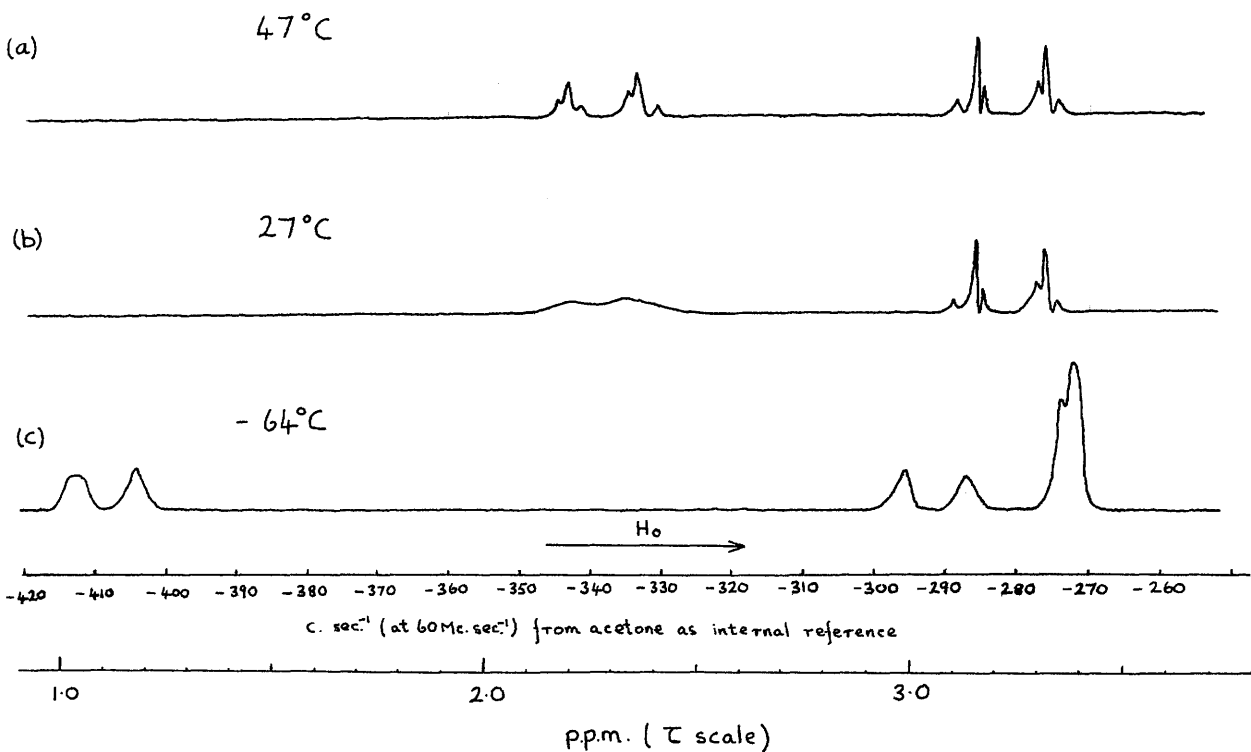


Figure 4-3. NMR spectra recorded at 60 Mc.sec.⁻¹ of the aromatic protons of p-nitroso-N,N-dimethylaniline (ca. 0.5M in acetone) at the following temperatures: (a) 47°C; (b) 27°C; (c) -64°C. Spectra (a) and (b) have the same intensity scale but this scale is different from the intensity scale of spectrum (c).

relative shift of the A and X protons is about 1.0 p.p.m. (see Figure 4-3b). The signal at lower field, marking the protons at the 3- and 5- positions is then quite broad though not structureless. Lowering the temperature first wipes out all spin splitting, then divides the spectrum into three broad signals instead of two, and finally brings about the reappearance of spin splittings. At this point the aromatic resonance covers a range of about 2.3 p.p.m. as shown in Figure 4-3c. Above room temperature the H_3 , H_5 signal sharpens up (see Figure 4-3a) so that motional narrowing is virtually complete at about 60° . These observations show that at low temperature the torsion of the NO group is hindered by the potential barrier so that the spectrum corresponds to the individual form (I), with non-equivalent aromatic protons. Near and above room temperature the interconversion is sufficiently fast to average out the difference between H_3 and H_5 , and H_2 and H_6 . Internal rotation of the NMe_2 group has no effect either on chemical shifts or on coupling constants and leaves no mark in the spectrum.

Analysis of the "averaged" high-temperature spectrum gives the coupling constants and shifts

/shown

TABLE 4-1

Chemical Shifts and Coupling Constants for the Aromatic
Hydrogens of p-Nitroso-N,N-dimethylaniline (Acetone
Solution)

Spin system	T, °K	Shift ^a	Coupling Constant
		H ₅ ,H ₆ 272.2 ± 0.4	
A ₂ KX	< 250°	H ₂ 291.5 ± 0.8	J ₂₃ = J ₅₆ = 9.1
		H ₃ 408.9 ± 0.4	J ₂₆ = J ₃₅ = 2.5
A ₂ X ₂	> 300°	H ₂ ,H ₆ 281.1 ± 0.2	J ₂₅ = J ₃₆ = 0
		H ₃ ,H ₅ 338.8 ± 0.4	

^ac.sec.⁻¹ (at 60 Mc.sec.⁻¹) from acetone. Add
 125 c.sec.⁻¹ to obtain shift from TMS.

shown in the lower portion of table (4-1.) The coupling constants were then used in a calculation by the method of Wallace¹²¹ of a trial spectrum which was compared with the low temperature spectrum. The theoretical spectrum comprises about 28 significant lines not all of which could be resolved experimentally. A satisfactory fit in regard to line position and intensity was obtained with the set of shifts given in the upper portion of table (4-1) and with all coupling constants taken as positive in sign. Strictly, the aromatic hydrogens form an ABKX system but in practice the AB shift is so small that the spectrum is indistinguishable from A₂KX. Likewise, no evidence was found to suggest that $J_{23} \neq J_{56}$ or $J_{26} \neq J_{35}$ in the low temperature spectrum. From the parameters of the "cold" spectrum one calculates that the shifts expected for the coalesced signals at higher temperature (observed at 281 and 339 c.sec.⁻¹) are 282 and 341 c.sec.⁻¹

Rate constants were obtained either in the region of slight exchange broadening or motional narrowing and were calculated by standard methods for slow and fast exchange respectively. The effects observed are due solely to the averaging of chemical shifts for,

/since

TABLE 4-2

Kinetic Data for Internal Rotation in
p-Nitroso-N,N-dimethylaniline

Method	T, °K	$10^3 T^{-1}$, °K ⁻¹	$10^{-3} k$, sec. ⁻¹	$\log_{10} \left(\frac{k}{T} \right)$	ΔG^\ddagger kcal./ mole.
exchange broadening	211	4.739	0.0026	-1.91 (±0.3)	11.8 (±0.5)
	215	4.651	0.0064	-1.52 (±0.5)	
motional narrowing	300	3.333	6.95	1.36 (±0.3)	12.1 (±0.5)
	320	3.125	35.1	2.04 (±0.1 ₅)	
	330	3.030	64.5	2.29 (±0.1 ₅)	

since $J_{23} = J_{56}$ and $J_{26} = J_{35}$ in the "cold" spectrum, the isomerization does not bring about coalescence of spin splittings.

The fact that the spin splittings are lost at intermediate temperatures is due to general increase in line width associated with one or other of the coalescences H_3, H_5 or H_2, H_6 . These coalescences, however, are difficult to analyse kinetically and attempt to obtain rate constants at intermediate temperatures were not satisfactory. Results are given in table (4-2). In the region of exchange broadening, the mean lifetime $2\tau = k^{-1}$ of a given configuration was determined by matching the envelope of the H_3 spin multiplet to one of a set of shapes calculated for several different values of the line width parameter T_2' . The calculated envelope was a superposition of curves, one for each component of the H_3 multiplet. Once T_2' had been determined in this way, $\tau (= \frac{1}{2}T_A)$ was obtained by means of equation (2-42). In this region the relaxation time T_2 corresponding to the field inhomogeneity was calculated from the decay envelope of the 'wiggles' following a fast sweep through the acetone signal.

Motional narrowing was analysed in essentially the same manner by means of equation (2-49). The

second moment of the coalescing multiplets ∇ was calculated using expression (2-52). This expression gives the value of ∇ to a good approximation in the present case owing to the large H_3, H_5 chemical shift. In the fast exchange region T_2 was found by means of slow-passage line width measurements on the two most intense lines of the H_2, H_6 resonance. Two methods were employed to determine T_2' . The first of these involved slow-passage line width measurements on the two principal lines of the H_3, H_5 resonance. The second method involved peak height measurements on the four strongest lines of the A_2X_2 spectrum, conditions of slow passage and negligible saturation being employed. The ratio of the height of the inner strong line of the H_2, H_6 resonance to the height of the inner strong line of the H_3, H_5 resonance and the corresponding ratio for the two outer strong lines were calculated. These ratios were found to be equal to a constant value for a given set of peak heights and this value was equated¹²² to the ratio of the transverse relaxation times T_2/T_2' . Once the ratio T_2/T_2' had been measured in this way substitution of the value of T_2 allowed T_2' to be calculated.

/Owing

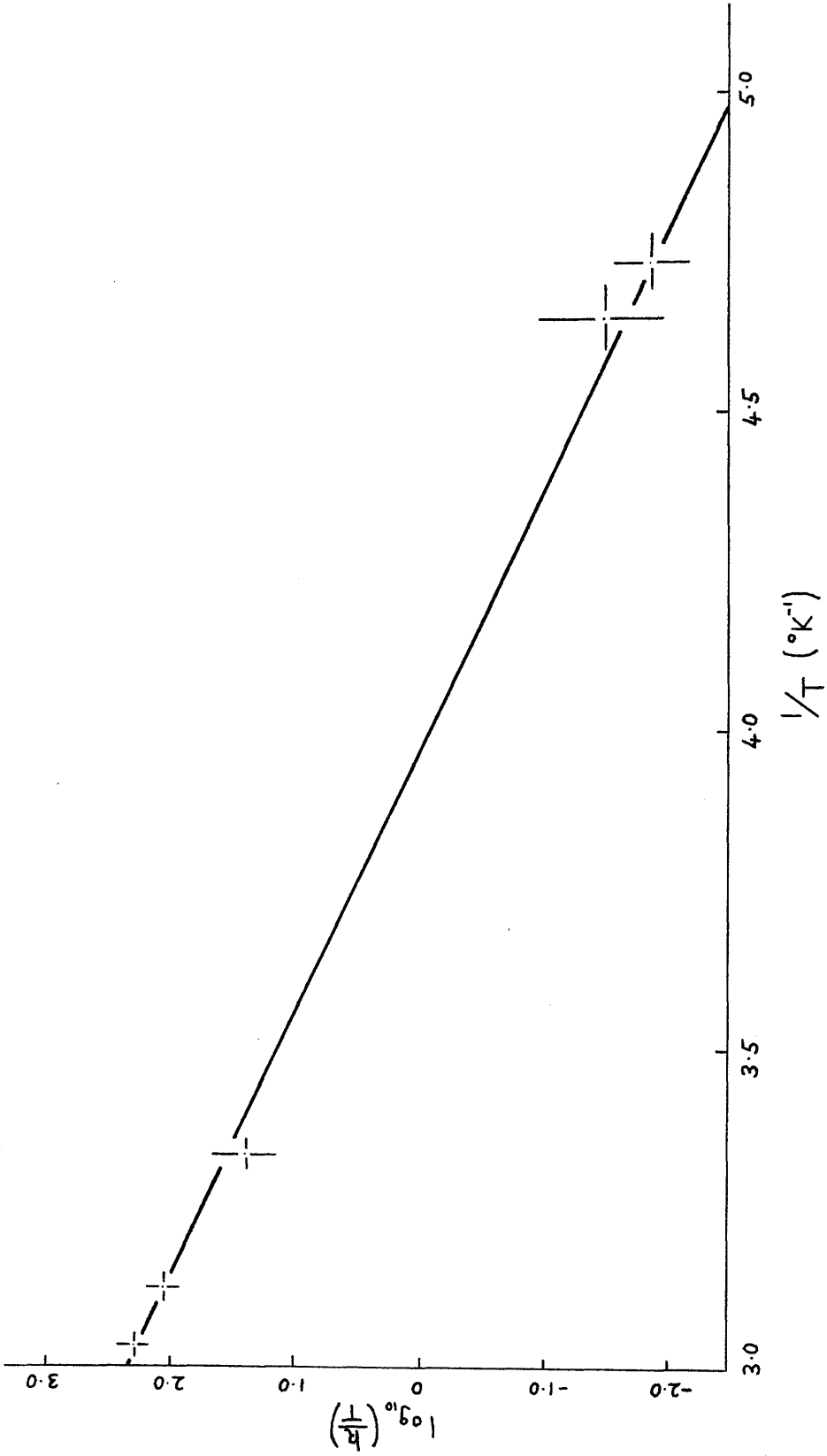


Figure 4-4.

Owing to the large H_3 , H_5 shift there is a considerable range of temperature, from about -60 to $+25^\circ\text{C}$ where neither the slow nor the fast exchange approximation is valid. However, the measurements encompass a ratio of about 25,000 in rates and were analysed by the equation

$$\log_{10}\left(\frac{k}{T}\right) = 10.319 + \Delta S^\ddagger/4.59 - (\Delta H^\ddagger/4.59)/T$$

giving $\Delta H^\ddagger = 11.2 (\pm 1.1)$ kcal.mole $^{-1}$ and $\Delta S_{298}^\ddagger = -3.0 (\pm 5)$ cal.mole $^{-1}$ deg. $^{-1}$. The above equation is obtained from equation (2-75) of Section 2.7 by substituting the appropriate numerical values¹²³ of the universal constants into equation (2-75) and by taking the transmission coefficient κ as equal to unity. A plot of $\log_{10}(k/T)$ against $1/T(^{\circ}\text{K}^{-1})$ is shown in Figure 4-4.

4.7. Proton Magnetic Resonance Results for the
Conjugate Acid of p-Nitroso-N,N-dimethylaniline

In the solvent trifluoroacetic acid, p-nitroso-N,N-dimethylaniline (I) is expected on the basis of a calculation using the acidity function H_o ,¹²⁴ to be converted almost completely to the corresponding trifluoroacetate salt owing to the marked acidic properties of the aniline, the pK_a of the conjugate acid of (I) being 3.52.¹²⁶ In the case of a 0.5 M solution of (I) in trifluoroacetic acid, the absence of observed absorption in the range 600-850 $m\mu$ (see Section 4.5) attributable to the $n \rightarrow \pi^*$ transition of the nitroso group ($\lambda_{max}^{EtOH} 670m\mu, \epsilon 62.5$)¹¹⁹ allows an upper limit to the concentration of the unionised aniline to be set at about 2×10^{-4} M. Kolthoff and Bruckenstein¹²⁷ have emphasised that it is necessary to represent base dissociation as occurring in two steps, ionisation and dissociation, especially in solvents of low dielectric constant. In the above solution, owing to the low dielectric constant of trifluoroacetic acid ($\epsilon = 8.2$ at $25^\circ C$),¹²⁸ the amount of salt which exists in the form of solvated free ions is expected to be small, the bulk of the salt being present in the form of ion pairs and higher ionic

/aggregates.

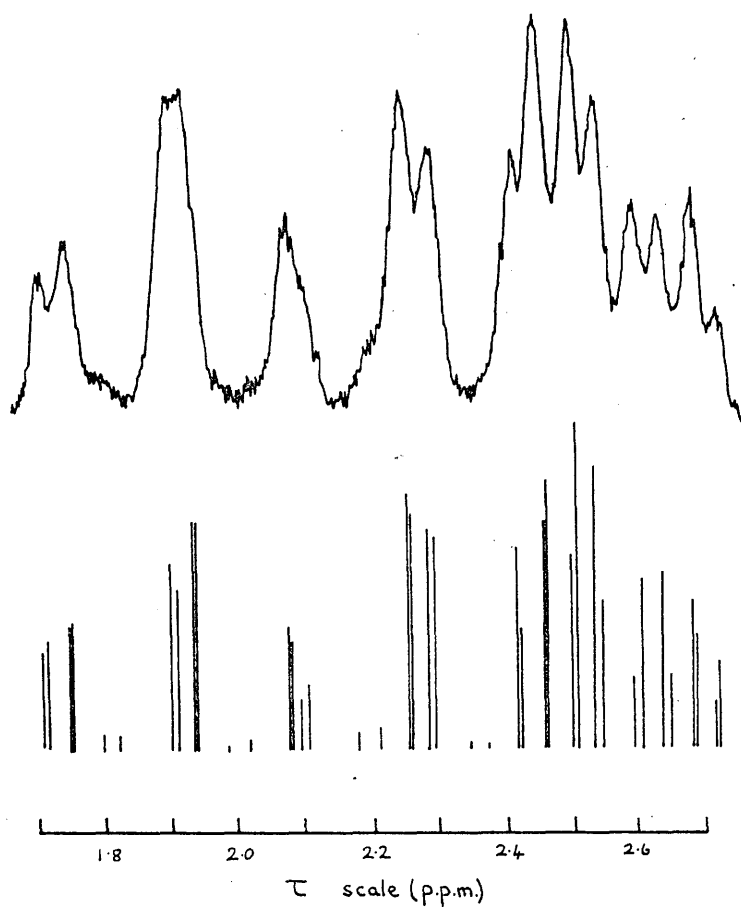
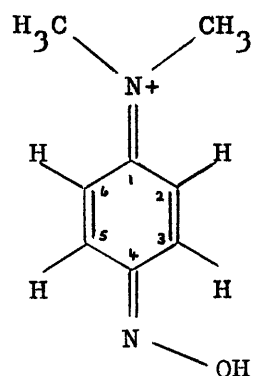


Figure 4-5. Observed (upper) and calculated (lower) PMR spectra (at 60 Mc.sec.⁻¹) of the ring protons of the conjugate acid of p-nitroso-N,N-dimethylaniline (ca. 0.5M in trifluoroacetic acid) at 33.5°C.

aggregates.¹²⁹

The PMR measurements were made at $33.5 (\pm 1)^{\circ}\text{C}$ using a solution similar in composition to that described above except that it contained a small concentration ($< 0.05 \text{ M}$) of tetramethylsilane, this having been added as an internal reference. The four ring protons of the conjugate acid (III) of p-nitroso-N,N-dimethylaniline give rise to an ABCD spectrum which is shown in the upper part of Figure 4-5. Analysis of the ABCD spectrum using a



(III)

refinement method devised by Wallace¹²¹ yielded the set of chemical shifts and coupling constants given in table (4-3). The theoretical spectrum comprises about 40 significant lines and is shown beneath the experimental spectrum in Figure 4-5. As can be seen

/from

TABLE 4-3

Chemical Shifts and Coupling Constants
for the Ring Hydrogens of the Conjugate
Acid of p-Nitroso-N,N-dimethylaniline
in Trifluoroacetic Acid

Spin system	T, °K	Shift ^a	Coupling Constant
ABCD	306.5°	H ₆ 445.5 ± 1.0	J ₂₃ = + 11.18 J ₅₆ = + 10.77
		H ₂ 449.7 ± 1.0	J ₂₆ = + 2.27
		H ₅ 468.8 ± 1.0	J ₃₅ = + 1.99
		H ₃ 490.2 ± 1.0	J ₂₅ = - 0.51 J ₃₆ = - 0.49

^ac.sec.⁻¹ (at 60Mc.sec.⁻¹) downfield from tetramethylsilane.

from the Figure the fit with respect to line position and intensity is satisfactory. Justification for the formulation of the conjugate acid as the oxygen-protonated form (III) will be given in Chapter 5.

Since the ring protons of the conjugate acid give rise to an ABCD spectrum, as described above, it is apparent that rotation about the C₄-N bond is not sufficiently rapid to cause collapse of the H₂, H₆ shift or the H₃, H₅ shift. Rotation about the C₄-N bond at 33.5°C therefore corresponds to the region of exchange broadening. An analogous method to that employed for the slow exchange measurements in Section 4.6 was used to determine $(1/T_2' - 1/T_2)$ and the value obtained was 4.7 (± 1.6) radians sec.⁻¹ The reorientation process may not be the sole cause of this broadening since, for example, there may be an increment to line width due to incompletely collapsed nuclear quadrupolar coupling with the nitrogen nuclei. However, if all the broadening is taken as being due to the internal rotation, equation (2-42) allows an upper limit to the first-order rate constant for the reorientation process to be set at 6.3 sec.⁻¹ Hence, by means of equation (2-77), a lower limit to the free

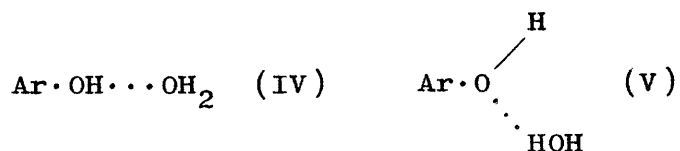
/energy

energy of activation ΔG^\ddagger for rotation about the C_4-N bond at 33.5°C was found to be 16.9 kcal./mole.

4.8. Results for Proton Transfer in Aqueous Dioxane

In mixed solvents the rates of reactions that generate ions are sensitive to the mole fraction of water in the solvent, a "medium effect" of this type being ordinarily attributed to changes in solvation and/or dielectric constant. In order to learn more about its origin the rate of proton exchange between a phenol and base (piperidine) in dioxane-water mixtures containing 0-0.05 mole fraction of water was measured.

2,6-Di-*t*-butylphenol was chosen for detailed study. To analyse the results in aqueous media, the association constants of the phenol with dioxane (1:1- and 2:1- complexes) and the association constant of the phenol with water in aqueous dioxane were determined from the proton spectrum as described in Section 4.9. Since the phenolic oxygen atom is screened by the alkyl groups, this phenol acts only as proton donor in hydrogen-bond formation; thus its complex with water is represented by (IV) and not (V),¹³⁰



and its self-association is very weak.¹³¹

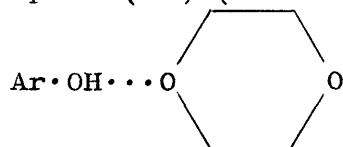
4.9. Determination of Association Constants by Proton
Magnetic Resonance Spectroscopy

Nuclear magnetic resonance spectroscopy can be used to study the phenomenon of hydrogen-bonding in solution and can allow accurate determination of the extent of association between the complexing agents.¹³²

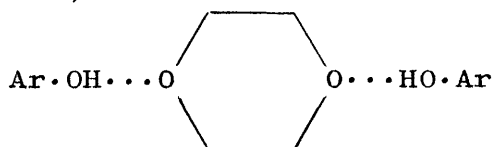
This application of nuclear magnetic resonance spectroscopy is based on the marked effect of hydrogen-bonding on the resonance frequencies of protons.

Where the hydrogen involved is bonding to an oxygen or nitrogen atom the proton resonance signal moves downfield relative to that of the uncomplexed signal.¹³²

The present section describes results for the association of 2,6-di-t-butylphenol with dioxane to form the complexes (VI) and (VII), and the association of the phenol with water in aqueous dioxane to form complex (IV) (see Section 4.8).



(VI)



(VII)

To investigate the association of 2,6-di-t-butylphenol with dioxane the position of the phenolic -OH proton resonance was measured (using a 0.1 M solution /of the phenol

TABLE 4-4

Chemical Shift Data for the Phenolic -OH Proton of 2,6-Di-t-butylphenol in Solvent Media ranging from pure Cyclohexane, through various Cyclohexane-Dioxane Mixtures, to pure Dioxane

$[D]^a$	δ_{CH}^b	δ^c	$10^{-3} \times \frac{[D]}{\delta}$
0	208.8 \pm 0.3		
0.100	225.0 \pm 0.2	16.2 \pm 0.4	6.17 \pm 0.15
0.195	233.9 \pm 0.2	25.1 \pm 0.4	7.77 \pm 0.12
0.400	244.5 \pm 0.2	35.7 \pm 0.4	11.20 \pm 0.13
0.521	248.2 \pm 0.2	39.4 \pm 0.4	13.22 \pm 0.13
0.701	253.3 \pm 0.3	44.5 \pm 0.4	15.75 \pm 0.14
0.903	258.5 \pm 0.3	49.7 \pm 0.4	18.17 \pm 0.15
1.0	260.2 \pm 0.3 ^d	51.4 \pm 0.4	19.46 \pm 0.15

^aThe mole fraction of dioxane in the solvent.

^bThe chemical shift of the -OH proton of 2,6-di-t-butylphenol in c.sec.⁻¹ (at 60Mc./sec.) downfield from cyclohexane as internal reference. The concentration of 2,6-di-t-butylphenol used was 0.1M.

^cThe downfield shift in c./sec. (at 60Mc./sec.) of the phenolic -OH proton resonance relative to the position of the -OH proton resonance of the phenol in pure cyclohexane.

^dThis value was obtained by addition of the relative separation of the dioxane and cyclohexane resonances (127.8 \pm 0.1 c./sec.) to the chemical shift of the phenolic -OH proton in c./sec. (at 60Mc./sec.) downfield from dioxane (as internal reference). The above relative separation of the dioxane and cyclohexane resonances (at 60Mc./sec.) was measured using a dioxane-cyclohexane mixture which had the mole fraction of dioxane equal to 0.9.

of the phenol) in a series of solvent media ranging from pure cyclohexane through cyclohexane-dioxane mixtures to pure dioxane. Pertinent results are shown in table (4-4). The phenolic -OH resonance moves progressively to lower fields with increasing mole fraction of dioxane owing to the fact that complex formation between the phenol and dioxane becomes more extensive as the mole fraction of dioxane increases. To obtain equilibrium constants from the PMR measurements a suitable mathematical expression was derived as follows:

For a solution of the phenol in a cyclohexane-dioxane mixture, or in pure dioxane, the relevant equilibria are



and



with equilibrium constants given respectively by

$$2K = \frac{[PD]}{[P][D]} \quad (4-3)$$

and

$$K/2 = \frac{[P_2D]}{[P][PD]} \quad (4-4)$$

where P, D, PD and P_2D refer respectively to uncomplexed 2,6-di-t-butylphenol, uncomplexed dioxane, complex (VI)

/and

complex (VII). Brackets of the type [] refer to mole fractions. The equilibrium constant for (4-2) is assumed equal to one-fourth of that for (4-1) owing to statistical considerations. This assumption is consistent with the results of a study by McGlashan and Rastogi¹³³ of complex formation (1:1- and 1:2-complexes) between dioxane and chloroform, it having been found that the presence of one chloroform molecule has only a small effect on the addition of the second.

Material balance gives

$$[P]_0 = [P] + [PD] + 2[P_2D] \quad (4-5)$$

where $[P]_0$ is the mole fraction of the phenol in all its subspecies. Making use of equations (4-3) and (4-4), equation (4-5) can be transformed into

$$[P]_0 = [P] \{1 + 2K[D] + 2K^2[P][D]\} \quad (4-6)$$

If the position of the -OH proton resonance of unassociated 2,6-di-t-butylphenol is arbitrarily taken as zero, then one may write

$$[P]_0 \delta = [PD] \delta_c + 2[P_2D] \delta_c \quad (4-7)$$

where δ is the observed -OH chemical shift, and δ_c is the shift of the -OH proton of associated 2,6-di-t-butylphenol. Combining equations (4-3), (4-4) and (4-7) gives

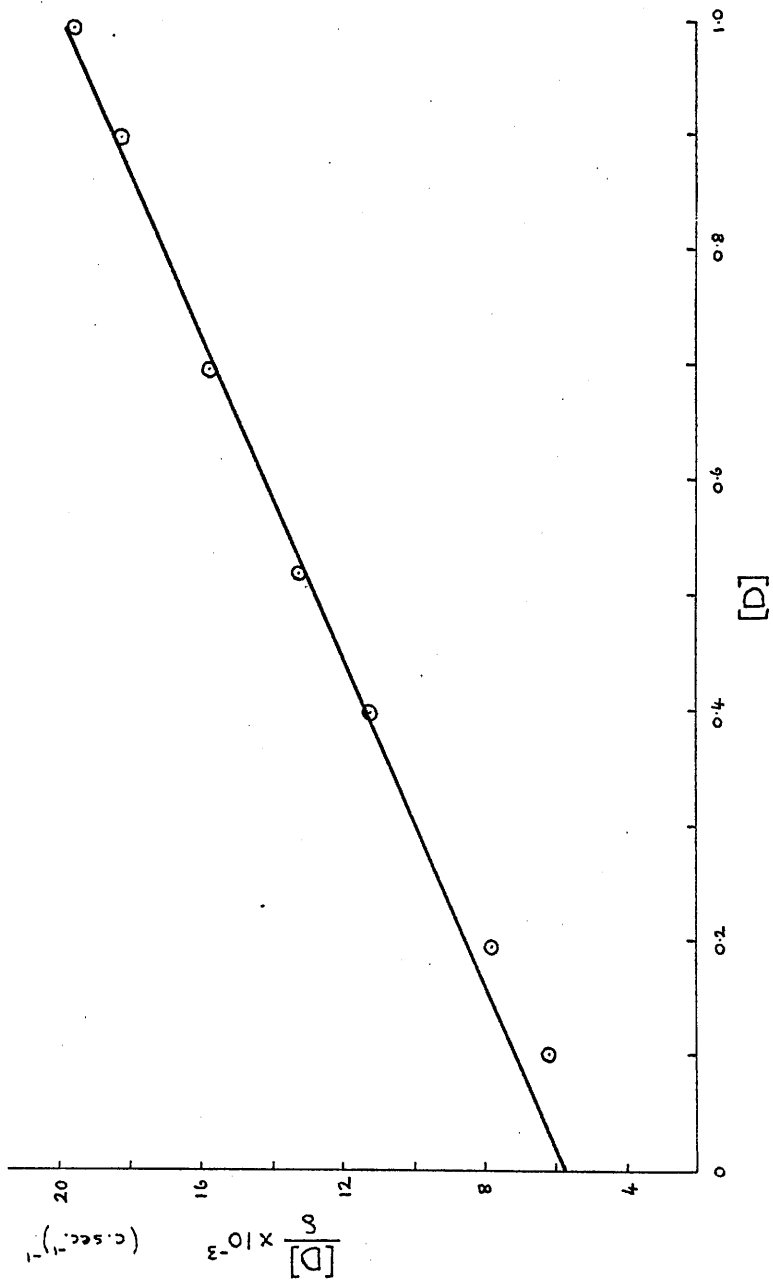


Figure 4-6.

$$[P]_0 \delta = [P] \{2K[D] + 2K^2[P][D]\} \delta_c \quad (4-8)$$

Dividing equation (4-6) by equation (4-8) yields

$$\frac{1}{\delta} = \frac{1 + 2K[D] + 2K^2[P][D]}{\{2K[D] + 2K^2[P][D]\} \delta_c} \quad (4-9)$$

and hence, by rearranging equation (4-9), one obtains

$$\frac{[D]}{\delta} = \frac{1}{2K\{1 + K[P]\} \delta_c} + \frac{[D]}{\delta_c} \quad (4-10)$$

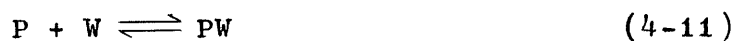
The data in table (4-4) were analysed by equation (4-10) giving $K = 1.1_8$ and $\delta_c = 72_0 \text{ c. sec.}^{-1}$. The slope and intercept of a plot of $[D]/\delta$ against $[D]$ (Figure 4-6) were used in the calculation of the above values of K and δ_c . In the above analysis and in the following analysis it was assumed that $[D] \approx [D]_0$, $[D]_0$ being the stoichiometric mole-fraction of dioxane in the solvent.

To investigate the association of 2,6-di-*t*-butylphenol with water in aqueous dioxane the position of the phenolic -OH proton resonance was measured (using a 0.1 M solution of the phenol) in dioxane-water mixtures. The phenolic -OH and water resonances being separate, the position of the former can be measured directly. Pertinent results are given in table (4-5). From the data given in the table it can be seen that the

/phenolic

phenolic -OH resonance moves to lower fields as the mole fraction of the water in the solvent increases. This progressive downfield movement of the phenolic -OH resonance with increasing mole fraction of water in the solvent indicates increasing formation of complex (IV). To obtain the equilibrium constant for the formation of complex (IV) from the PMR chemical shift measurements, a suitable mathematical expression was derived as follows.

The important equilibria governing the variation in position of the phenolic -OH resonance in dioxane-water mixtures are equilibria (4-1) and (4-2) with association constants as defined above, and the equilibrium



with equilibrium constant K' defined by

$$K' = \frac{[PW]}{[P][W]} \quad (4-12)$$

where W and PW refer respectively to water and complex (IV), the other symbols having the same significance as before.

Material balance gives

$$[P]_0 = [P] + [PD] + 2[P_2D] + [PW] \quad (4-13)$$

and hence, combining equations (4-3), (4-4), (4-12)

/and

and (4-13), one obtains

$$[P]_o = [P]\{1 + 2K[D] + 2K^2[P][D] + K'[W]\} \quad (4-14)$$

If the position of the -OH proton resonance of unassociated 2,6-di-*t*-butylphenol is arbitrarily taken as zero, then one may write

$$[P]_o \delta' = [PD]\delta_c + 2[P_2D]\delta_c + [PW]\delta_w \quad (4-15)$$

where δ' is the observed chemical shift of the phenolic -OH proton, δ_w is the chemical shift of the phenolic -OH proton in complex (IV), and δ_c is as defined earlier. Combination of equations (4-3), (4-4), (4-12) and (4-15) yields

$$[P]_o \delta' = [P]\{2K[D]\delta_c + 2K^2[P][D]\delta_c + K'[W]\delta_w\} \quad (4-16)$$

Dividing equation (4-14) by equation (4-16) gives

$$\frac{1}{\delta'} = \frac{\{1 + 2K[D] + 2K^2[P][D] + K'[W]\}}{\{2K[D]\delta_c + 2K^2[P][D]\delta_c + K'[W]\delta_w\}} \quad (4-17)$$

The corresponding equation for cyclohexane-dioxane mixtures is equation (4-9) which can be recast in the form

$$\{2K[D] + 2K^2[P][D]\} \delta_c = \delta \{1 + 2K[D] + 2K^2[P][D]\} \quad (4-18)$$

Now for the same mole fraction of dioxane, substitution of (4-18) into (4-17) gives

$$\frac{1}{\delta'}$$

TABLE 4-5

Chemical Shift Data for the Phenolic -OH Proton of
2,6-Di-*t*-butylphenol in Dioxane and in Aqueous Dioxane

$[W]_0^a$	δ_D^b	δ'^c	$10^{-2} \times (\delta' - \delta) \frac{\{1 + 2K[D] + 2K^2[PH][D]\}}{[W]}$
0	132.4 \pm 0.2	51.4 \pm 0.4	
0.050	134.7 \pm 0.2	53.7 \pm 0.4	2.42 \pm 0.38
0.100	136.7 \pm 0.2	55.7 \pm 0.4	2.05 \pm 0.18
0.200	139.5 \pm 0.2	58.5 \pm 0.4	1.63 \pm 0.08
0.300	141.5 \pm 0.2	60.5 \pm 0.4	1.38 \pm 0.05

^aStoichiometric mole fraction of water

^bThe observed chemical shift of the phenolic -OH proton of 2,6-di-*t*-butylphenol in c./sec. (at 60Mc./sec.) downfield from dioxane as internal reference. The concentration of 2,6-di-*t*-butylphenol used was 0.1M.

^cThe downfield shift in c./sec. (at 60Mc./sec.) of the phenolic -OH proton resonance of 2,6-di-*t*-butylphenol relative to the position of the -OH proton resonance of unassociated 2,6-di-*t*-butylphenol relative to dioxane, which was used in the evaluation of δ' , was calculated by subtraction of the dioxane-cyclohexane separation (see footnote d of table 4-4) from the relative separation of the cyclohexane and phenolic -OH resonances in pure cyclohexane.

$$\frac{1}{\delta'} = \frac{\{1 + 2K[D] + 2K^2[P][D] + K'[W]\}}{\delta\{1 + 2K[D] + 2K^2[P][D]\} + K'[W]\delta_W} \quad (4-19)$$

and hence, by rearranging equation (4-19), it can be shown that

$$(\delta' - \delta) \frac{\{1 + 2K[D] + 2K^2[P][D]\}}{[W]} = K'\delta_W - \delta'K' \quad (4-20)$$

The data in table (4-5) were analysed by equation (4-20) giving $K' = 15.2$ (± 5), the slope of a plot of $(\delta' - \delta)\{1 + 2K[D] + 2K^2[P][D]\}/[W]$ against δ' (Figure 4-7) having been used in the calculation of K' .

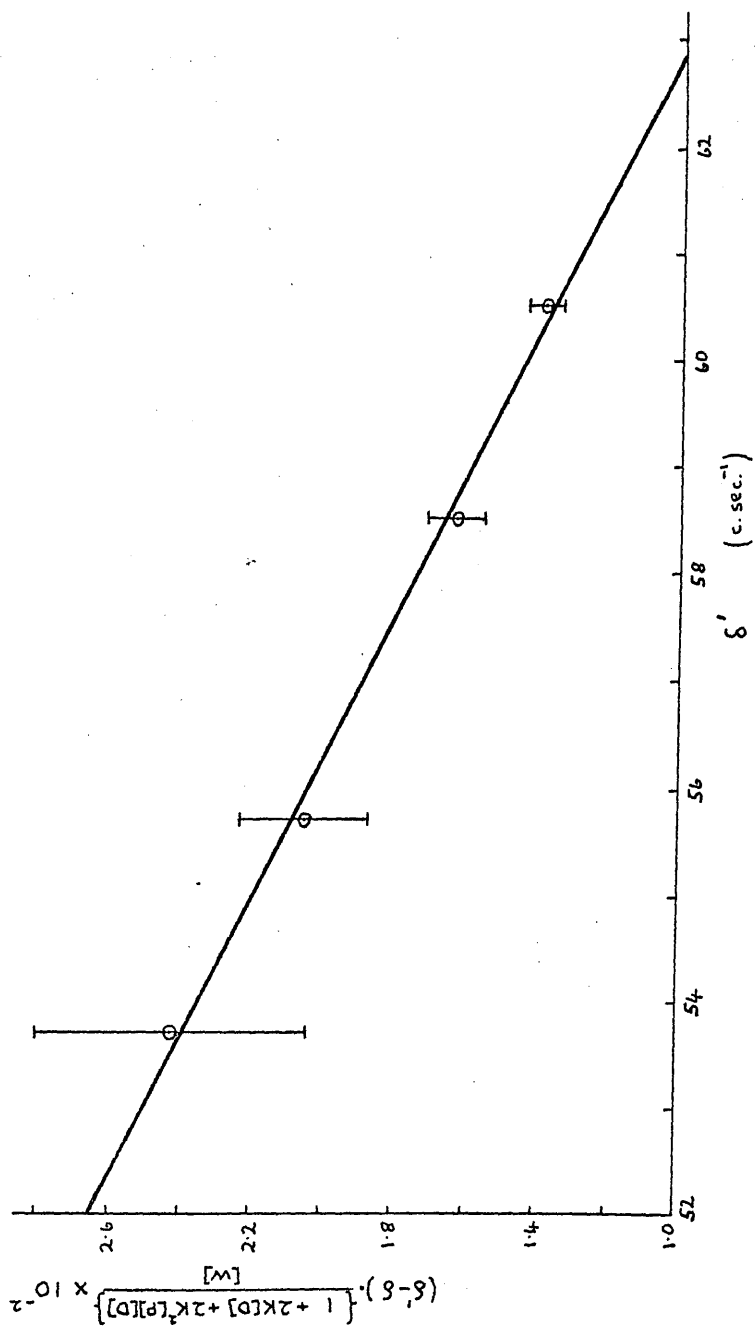


Figure 4-7.

4.10. Kinetic Results for Proton Transfer in Aqueous
Dioxane

To investigate the kinetics and mechanism of proton exchange between 2,6-di-t-butylphenol and piperidine in aqueous dioxane three main series of PMR rate measurements were made:

- (a) a study of the rate of proton transfer as a function of piperidine concentration, the concentrations of phenol and water being held constant throughout (table (4-6));
- (b) a study of proton transfer rate as a function of water concentration with the concentrations of the phenol and piperidine held constant (table (4-7));
- (c) a study of proton transfer rate as a function of the concentration of the phenol with the concentrations of piperidine and water held constant (table (4-8)).

In addition, two brief complementary studies were made:

- (d) a study of proton exchange between 2,6-di-t-butylphenol and piperidine in dry dioxane;
- (e) a study of proton exchange between water and piperidine in dioxane (in the absence of the phenol).

/In series (a)

TABLE 4-6

Kinetic Data for Series (a)

$10^3 \times$ $(\rho)_0$ (M)	$10^4 \times$ $(\rho)(P)(W)^b$ (M ³)	$\frac{1}{T_2}$ (sec ⁻¹)	$\left(\frac{1}{T_2'}\right)_{\text{PhOH}}$ (sec ⁻¹)	$\left(\frac{1}{T_2'}\right)_{\text{H}_2\text{O}}$ (sec ⁻¹)	$\frac{1}{T}$ PhOH (sec ⁻¹)	$\frac{1}{T}$ H_2O (sec ⁻¹)	R' (M sec ⁻¹)	\dagger
0.73	0.541	1.30	3.80 ± 0.19	2.92 ± 0.24	2.50 ± 0.23	1.62 ± 0.27	1.24 ± 0.21	
1.53	1.134	1.42	5.59 ± 0.46	5.25 ± 0.66	4.17 ± 0.48	3.83 ± 0.68	2.93 ± 0.52	
3.15	2.334	1.28	8.28 ± 1.07	8.99 ± 0.64	7.00 ± 1.08	7.71 ± 0.65	5.89 ± 0.50	
4.63	3.431	1.43	11.29 ± 0.71	17.12 ± 2.37	9.86 ± 0.72	15.69 ± 2.38	11.99 ± 1.82	
5.94	4.401	1.43	16.12 ± 0.21	23.56 ± 4.97	14.69 ± 0.25	22.13 ± 4.97	16.91 ± 3.80	
7.72	5.720	1.29	22.31 ± 1.38		21.02 ± 1.39			

$(\rho)_0$ denotes the stoichiometric concentration of piperidine in moles per litre.

Brackets of the type () refer to concentrations in moles per litre, the other symbols having the same significance as in Section 4.9. For the series $(D)_0 = 8.750$ M and $(W)_0 = 0.382$ M, these being stoichiometric concentrations.

For the values in this column, the error was taken as ± 10%.

Where $\frac{1}{T'}_{\text{PhOH}} = \left(\frac{1}{T_2'}\right)_{\text{PhOH}} - \frac{1}{T_2}$ (equation (2-42)). Since $(P)_0 = 1.00$ M for the present series, the values given in this column are numerically equal to the rates of proton exchange R (in M sec.⁻¹) measured from the phenolic -OH resonance, R being given by the expression $R = \frac{1}{T'}_{\text{PhOH}} (P)_0$.

\dagger Where $\frac{1}{T'}_{\text{H}_2\text{O}} = \left(\frac{1}{T_2'}\right)_{\text{H}_2\text{O}} - \frac{1}{T_2}$ (equation (2-42)).

\dagger The rate of proton exchange measured from the water resonance where $R' = 2 \times \frac{1}{T'}_{\text{H}_2\text{O}} (W)_0$. The factor of two in the expression for R' allows for the fact that the water molecule has two protons.

TABLE 4-7

Kinetic Data for Series (b)

^a (W) ₀ (M)	(D) ₀ (M)	(P) (M)	(W) (M)	$10^4 \times$ (ρ) ₀ (P)(W) (M ³)	^c $\frac{1}{T_2}$ (sec ⁻¹)	$\left(\frac{1}{T_2'}\right)_{\text{PhOH}}$ (sec ⁻¹)	$\left(\frac{1}{T_2'}\right)_{\text{H}_2\text{O}}$ (sec ⁻¹)	^d $\frac{1}{\tau_{\text{PhOH}}}$ (sec ⁻¹)	^e $\frac{1}{\tau_{\text{H}_2\text{O}}}$ (sec ⁻¹)	^f R' (M sec ⁻¹)
0	8.770	0	0	0	1.13	3.66 ±0.31		2.53 ±0.33		
0.095	8.690	0.307	0.063	0.865	1.08	4.71 ±0.28		3.63 ±0.30		
0.191	8.555	0.298	0.127	1.702	1.87	7.78 ±0.82		5.91 ±0.84		
0.382	8.750	0.281	0.264	3.342				10.75 ±1.00	13.35 ±1.00	10.20 ±0.76
0.479	8.715	0.274	0.331	4.096	1.35	17.96 ±0.80	17.02 ±1.47	16.61 ±0.81	15.67 ±1.48	15.01 ±1.42
0.575	8.755	0.268	0.402	4.856	2.18	20.99 ±2.84	16.57 ±0.51	18.81 ±2.85	14.39 ±0.56	16.55 ±0.64

^a The symbols W, D, etc., have the same significance as in table 4-6.

^b For the values in this column the error was taken as ±10%.

^c For the present series (ρ)₀ = 0.0045₁M.

^d Where $\frac{1}{\tau_{\text{PhOH}}} = \left(\frac{1}{T_2'}\right)_{\text{PhOH}} - \frac{1}{T_2}$ (equation (2-42)). Since (P)₀ = 1.00M

for the present series, the values given in this column are numerically equal to the rates of proton exchange R (in Msec.⁻¹) measured from the phenolic-OH resonance, R being given by the expression $R = \frac{1}{\tau_{\text{PhOH}}}$ (P)₀.

^e Where $\frac{1}{\tau_{\text{H}_2\text{O}}} = \left(\frac{1}{T_2'}\right)_{\text{H}_2\text{O}} - \frac{1}{T_2}$ (equation (2-42)).

^f The rate of proton exchange measured from the water resonance where

$R' = 2 \times \frac{1}{\tau_{\text{H}_2\text{O}}} (W)_0$. The factor of two in the expression for R' allows for

the fact that the water molecule has two protons.

TABLE 4-8

Kinetic Data for Series (c)

(P) ₀ ^a (M)	(D) ₀ (M)	$\frac{1}{T_2}$ ^b (sec. ⁻¹)	$\left(\frac{1}{T_2'}\right)_{\text{PhOH}}$ (sec. ⁻¹)	$\left(\frac{1}{T_2'}\right)_{\text{H}_2\text{O}}$ (sec. ⁻¹)	$\frac{1}{T}$ ^c PhOH (sec. ⁻¹)	$\frac{1}{T}$ ^d H ₂ O (sec. ⁻¹)	R ^e (M sec. ⁻¹)	R' ^f (M sec. ⁻¹)
0.256	10.80	1.38	9.61 ±0.55	4.84 ±0.26	8.23 ±0.57	3.46 ±0.30	2.11 ±0.15	2.64 ±0.23
0.499	9.90	1.55	9.01 ±0.32	5.91 ±0.46	7.46 ±0.36	4.36 ±0.49	3.72 ±0.18	3.33 ±0.37
1.000	8.75				7.53 ±0.75	9.34 ±0.93	7.53 ±0.75	7.14 ±0.71

^a For the present series, (W)₀ = 0.382 M and (ρ)₀ = 0.00316 M, the symbols having the same significance as in table 4-6.

^b For the values in this column the error was taken as ±10%.

^c Where $\frac{1}{T'}_{\text{PhOH}} = \left(\frac{1}{T_2'}\right)_{\text{PhOH}} - \frac{1}{T_2}$ (equation (2-42)).

^d Where $\frac{1}{T'}_{\text{H}_2\text{O}} = \left(\frac{1}{T_2'}\right)_{\text{H}_2\text{O}} - \frac{1}{T_2}$ (equation (2-42)).

^e The rate of proton exchange measured from the phenolic -OH resonance

$$\text{where } R = \frac{1}{T'}_{\text{PhOH}}(P)_0.$$

^f The rate of proton exchange measured from the water resonance where

$R' = 2 \times \frac{1}{T'}_{\text{H}_2\text{O}}(W)_0$. The factor of two in the expression R' allows for the fact that the water molecule has two protons.

In series (a) the concentrations of the phenol and water were 1.000 M and 0.382 M respectively, and the piperidine concentration varied from 10^{-3} to 10^{-2} M. Throughout this range of piperidine concentration the phenolic -OH and water resonances are separate so that the proton spectrum provides two measures of the proton exchange rate. In order to aid the interpretation of the line width measurements given in table (4-6), it is worthwhile examining the proton spectrum of a solution having the same stoichiometric phenol and water concentrations as employed in series (a) but containing no piperidine. Values of some relevant chemical shifts are given in table (4-9). In the absence of piperidine the width of the water line corresponds to the inhomogeneity of the magnetic field but the phenolic -OH resonance is significantly (ca. 0.5 c.sec.^{-1}) broader than the width due to the field inhomogeneity. It is noteworthy that this increase in the width of the phenolic -OH resonance cannot be due to proton exchange between the phenolic -OH and water sites since the water resonance is not broadened accordingly. It follows, therefore, that in this solution proton exchange

/between

between the phenol and water is slow (in the sense of the present studies). The excess width of the phenolic -OH resonance is ascribed to spin-spin coupling of the phenolic -OH proton with the protons of the phenolic ring (see below).

As can be seen from table (4-6), both the phenolic -OH resonance and the water resonance broaden significantly upon the addition of piperidine. It is of interest to consider the possible causes of this broadening.

In Chapter 2 it was pointed out that increases in line width can arise from spin-spin splitting of a proton resonance by O^{17} (spin $I = 5/2$) which is only partially averaged out by proton exchange. A detailed study⁵⁴ of proton transfer in water at the natural abundance of O^{17} (0.037%) has shown, however, that the maximum extent of broadening due to this effect is about 0.13 radians per sec. It is reasonable to take this value as an upper limit to the broadening of water in dioxane due to O^{17} coupling. If it is assumed that the coupling constant for the O^{17} -H interaction in 2,6-di-t-butylphenol is similar to that for water, 580 radians per sec.,⁵⁴ the maximum broadening of the phenolic -OH resonance due to O^{17} coupling must also

/be about

be about 0.13 radians per sec. Since the experimental error in measuring line widths is considerably greater than the maximum possible broadening due to 0^{17} coupling, no correction was made for this effect.

Another possible source of broadening of the phenolic -OH resonance arises from spin-spin splitting of the phenolic -OH resonance by the ring protons of the phenol. To estimate the extent of this broadening, the simplifying assumption is made that the phenolic -OH proton is coupled significantly only with the H_3 , H_5 ring protons so that the analogue of equation (2-66) is

$$\frac{1}{T_2'} - \frac{1}{T_2} = \frac{J^2\tau}{2} \left(1 + \frac{1}{1 + \delta^2\tau^2} \right) \quad (4-21)$$

where δ is the chemical shift (in radians per sec.) between the two kinds of protons causing the spin splitting J , that is, in the present case, the chemical shift between the phenolic -OH proton and the H_3 , H_5 protons of the phenolic ring (table (4-9)). The value of the coupling constant J is probably less than 0.6 radians per second. Although strictly τ in equation (4-21) is defined by an expression analogous to equation (2-65), for the present purpose it is quite

/adequate

TABLE 4-9
Chemical Shift Data

System	Shift ^a
A solution of 2,6-di-t-butylphenol in aqueous dioxane with $(P)_o^b = 1.000$ M and $(W)_o^c = 0.382$ M	t-butyl $\underline{\text{C}}\text{H}_3$ +129.8 ± 2.0
	$\underline{\text{H}}_2\text{O}$ + 55.8 ± 2.0
	phenolic $\underline{\text{O}}\text{H}$ -132.2 ± 2.0
	protons of the } H_4 -187.0 ± 2.0 phenolic ring } H_3, H_5 -210.8 ± 2.0
A solution of piper- idine in dry dioxane with $(\rho)_o^d = 1.01$ M	piperidine $\underline{\text{N}}\text{H}$ +110.5 ± 2.0 $(\Delta\nu_{\frac{1}{2}} = 2.5_4 \text{ c. sec.}^{-1})$
A solution of water in dioxane with $(W)_o^c = 0.50\text{M}$	$\underline{\text{H}}_2\text{O}$ + 53.7 ± 2.0
A solution of piper- idine in aqueous dioxane with $(\rho)_o^d = 0.99\text{M}$ and $(W)_o^c = 0.51\text{M}$	Coalesced $\underline{\text{H}}_2\text{O}$ - piperidine $\underline{\text{N}}\text{H}$ signal + 73.0 ± 2.0 $(\Delta\nu_{\frac{1}{2}} = 1.31 \text{ c. sec.}^{-1})$

TABLE 4-9

- ^a All line positions are in c. sec.^{-1} (at 60Mc./sec.) from dioxane as internal reference. Positive values correspond to resonances upfield from dioxane and negative values correspond to resonances downfield from the reference line.
- ^b The stoichiometric concentration of the phenol in moles per litre.
- ^c The stoichiometric concentration of water in moles per litre.
- ^d The stoichiometric concentration of piperidine in moles per litre.

adequate to take τ as the mean residence time of a proton on the phenolic -OH group. Substitution of typical values of τ (see below) into equation (4-21) shows that the broadening of the phenolic -OH resonance due to the present effect is insignificant for series (a).

In view of the above considerations it is apparent that exchange of protons between different chemical positions must be the main cause of the broadening of the phenolic -OH and water resonances, that is, collapse of spin multiplets cannot be a significant cause of line width in series (a). Similar conclusions hold for series (b) and (c).

Throughout series (a), (b) and (c), the proton spectra of solutions containing both water and the phenol show separate phenolic -OH and water resonances so that rates of proton exchange can be found by means of the usual "lifetime broadening" equation (2-42),

$$\frac{1}{T_2'} - \frac{1}{T_2} = \frac{1}{\tau} \quad (4-22)$$

The value of T_2' used in the above equation was obtained by means of slow passage line width measurements, and T_2 , the transverse relaxation time corresponding to the field inhomogeneity was calculated

/from

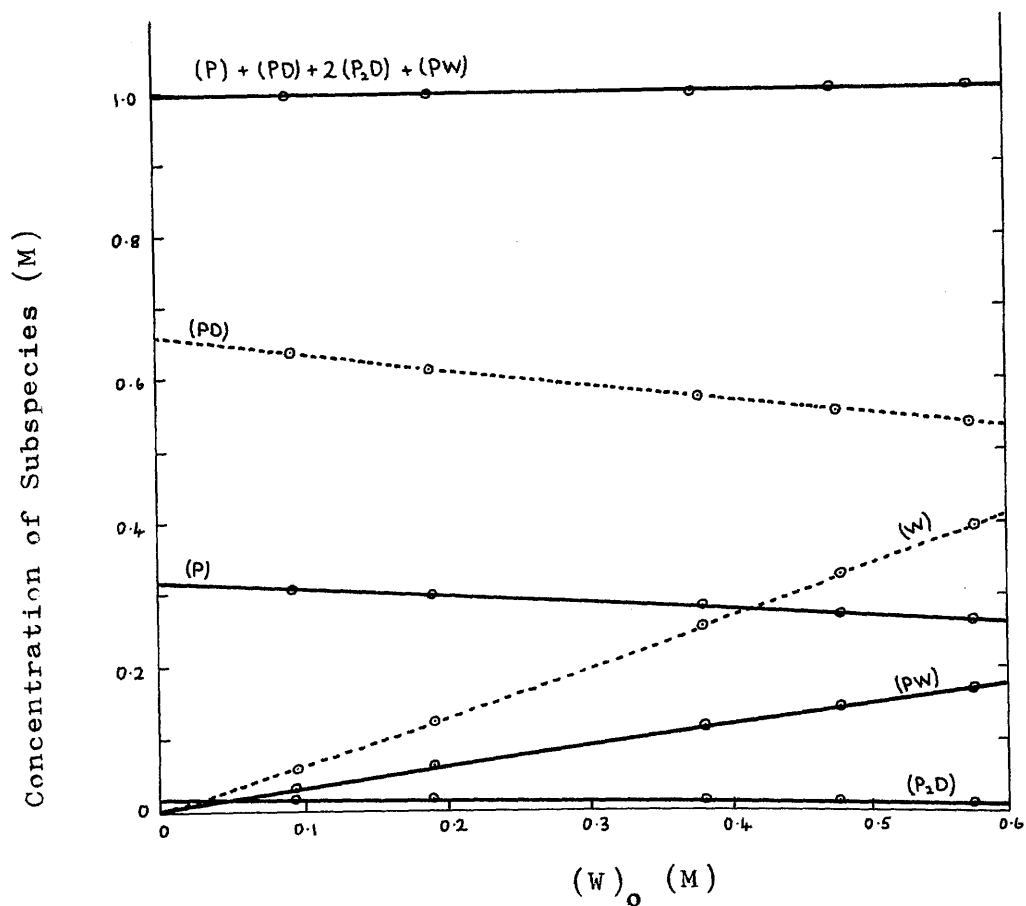


Figure 4-8. The data in this Figure are for a stoichiometric concentration of 2,6-di-*t*-butylphenol $(P)_0$ of 1.00 moles per litre.

from the decay of the "wiggles" following a rapid sweep through the dioxane signal.

The rates were analysed on the assumption that the dioxane-phenol complexes (VI) and (VII) (see Section 4.9) are kinetically inactive, the phenolic hydrogen being shielded from the base during the lifetime of the complex. Using the values of the equilibrium constants $2K$, $K/2$ and K' determined in Section 4.9, the concentrations in moles per litre of the species P , PD , P_2D , W and PW (figure 4-8) were calculated for series (a) and series (b) by means of a computer, the symbols having the same significance as before.

In series (a) (table 4-6), the rate of proton exchange measured from the phenolic -OH resonance, $R = \frac{1}{T} (P)_{PhOH}$, and the rate of proton exchange measured from the water resonance, $R' = \frac{1}{T} (W)_{H_2O} \times 2$ (the factor of two allows for the fact that the water molecule has two protons), were found to be given, within the limits of experimental error, by the rate law

$$R = R' = k_1(P)(W)(\rho)_o \quad (4-23)$$

with $k_1 = 3.3_3 \times 10^4 M^{-2} sec.^{-1}$

where $(\rho)_o$ denotes the stoichiometric concentration of

/piperidine

piperidine. The rate constant k_1 was calculated from the slope of a combined plot (figure 4-9) of R and R' against the product $(P)(W)(\rho)_o$. It is of interest to note that this plot passes through the origin, this being consistent with the fact that proton exchange between the phenol and water is slow in the absence of piperidine (see page 129).

In series (b) (table 4-7), the rate of proton exchange measured from the phenolic -OH resonance, $R = \frac{1}{T_{\text{PhOH}}} (P)_o$, was found to be represented, within the limits of experimental error, by the rate law

$$R = 2.0_o + k_1'(P)(W)(\rho)_o \quad (4-24)$$

with

$$k_1' = 3.06 \times 10^4 \text{ M}^{-2} \text{ sec.}^{-1}$$

The experimental rate law (4-24) was derived from a graphical plot of R against the product $(P)(W)(\rho)_o$ (see figure 4-10).

It is difficult to calculate the uncertainty in these rate constants but a reasonable estimate of the error may be about $\pm 20\%$.

The remainder of this Section is concerned with studies (d) and (e). The investigation of proton exchange between 2,6-di-t-butylphenol and piperidine in dry dioxane involved the measurement of the proton

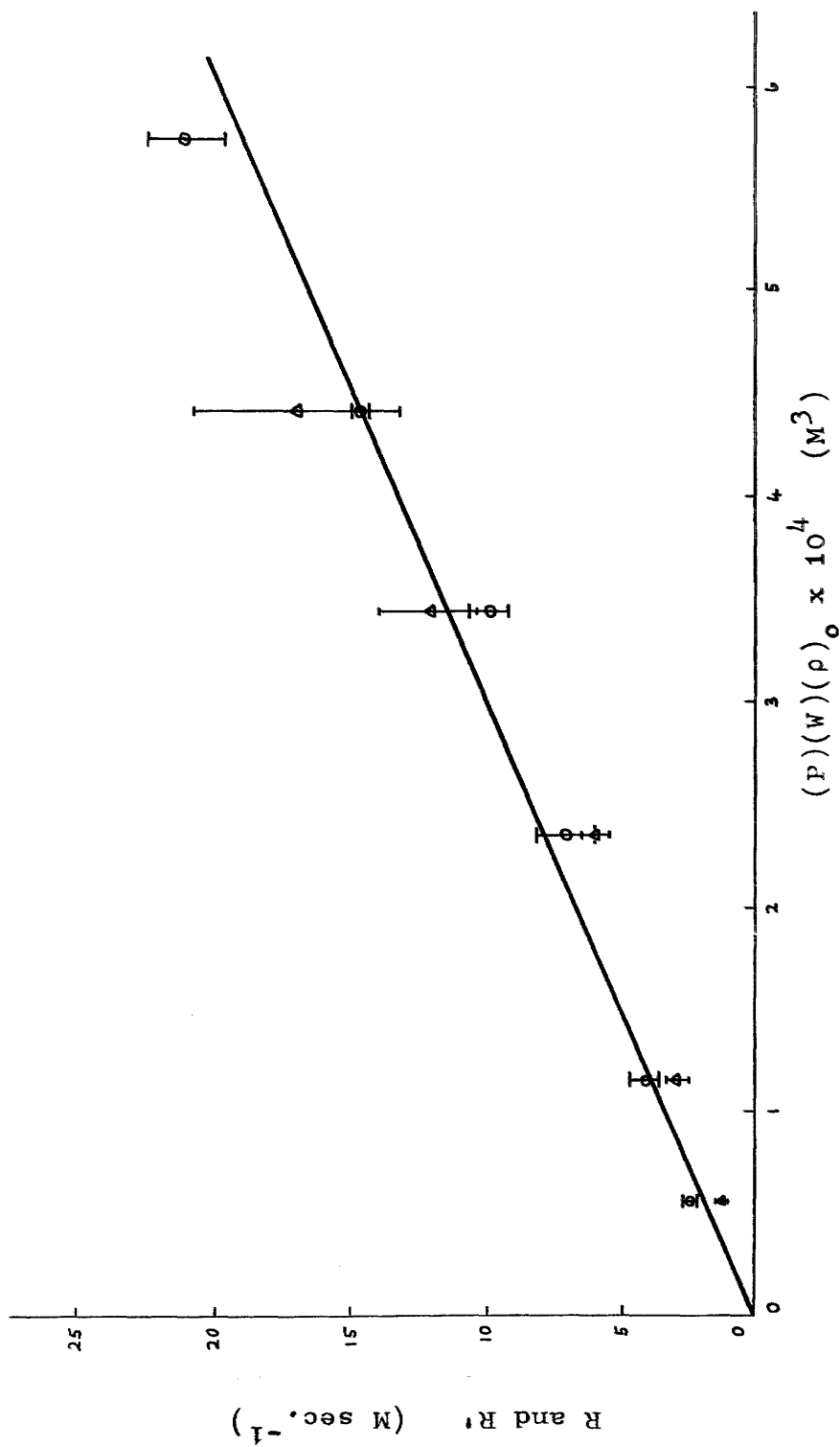


Figure 4-9. Circles \odot denote rates measured from the phenolic -OH resonance (R) and triangles denote rates measured from the water resonance (R').

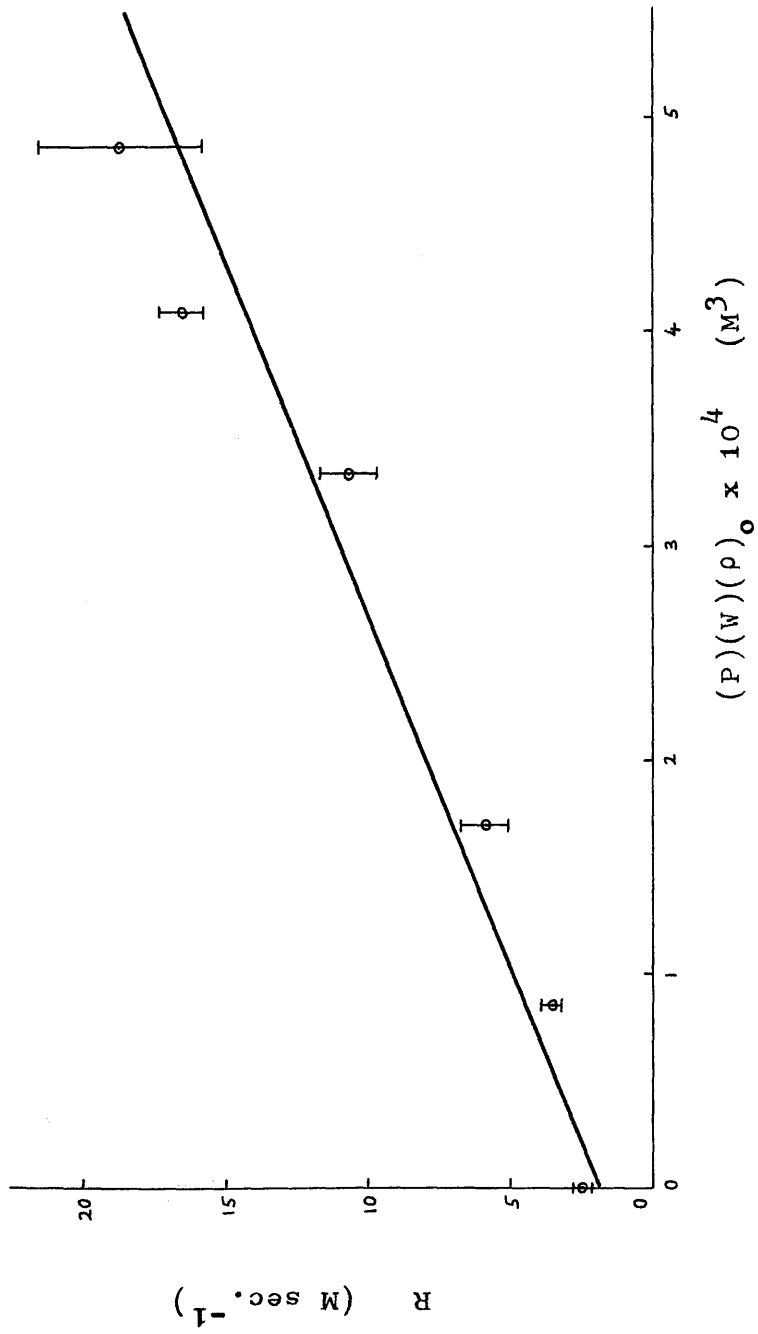
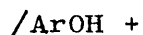
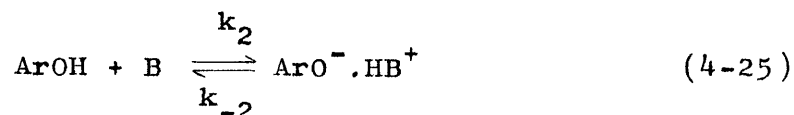


Figure 4-10.

spectrum of a dioxane solution containing 1.00 moles/litre of the phenol and 1.00 moles/litre of piperidine. In this spectrum no signal arising from either the phenolic -OH protons or the piperidine >NH protons is visible, indicating that proton exchange is sufficiently rapid to cause collapse of the individual signals, yet not rapid enough to produce an observable combined signal at the weighted mean position. This spectrum was taken to correspond to the coalescence point and was analysed accordingly, by means of equation (2-63) giving τ , the mean lifetime of a proton on either type of site between exchanges, equal to $1.8_5 \times 10^{-3}$ sec. (It should be pointed out, perhaps, that τ in equation (2-63), unlike here, denotes half the mean lifetime of either site). Owing to the relatively large separation of the resonances which have coalesced, 243 c. sec.^{-1} (see table 4-9) there is considerable difficulty in judging the exact point of coalescence so that some reservation must be placed on the accuracy of the above value of τ . This value is, however, probably correct to within a factor of two.

There is little doubt that proton exchange is brought about by the reversible ionization process,





where ArOH and B denote 2,6-di-*t*-butylphenol and piperidine respectively and $\text{ArO}^{\ominus} \cdot \text{HB}^{\oplus}$ represents an intimate ion pair in which the anion and cation are linked by a hydrogen bond. Dissociation of the ion pair $\text{ArO}^{\ominus} \cdot \text{HB}^{\oplus}$ to give solvated free ions is not expected to be extensive in view of the low dielectric constant of the solvent medium.¹³⁵ It is noteworthy that throughout the present studies on proton transfer reactions occurring in solvents of low dielectric constant, no evidence could be found to suggest that solvated free ions (as opposed to short-range ion pairs) play a kinetically significant role. The second-order rate constant k_2 for the ionization step of the reversible cycle (4-25) was related to τ by means of the expression

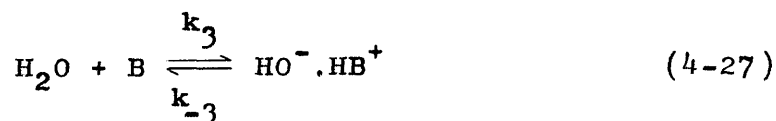
$$2 \times \frac{1}{\tau} (\text{ArOH})_0 = k_2 (\text{ArOH})_0 (\text{B})_0 \quad (4-26)$$

giving $k_2 = 1.1 \times 10^3 \text{M}^{-1} \text{sec}^{-1}$. The factor of two in equation (4-26) was introduced for statistical reasons, it being assumed that the mean lifetime of the hydrogen bond linking the phenoxide ion and the piperidinium ion is short compared with the lifetime of the ion pair. There being no direct evidence to

support this assumption, the value of k_2 given above is probably best regarded as a lower limit to the second-order rate constant for the ionization process.

Proton exchange between piperidine and water in aqueous dioxane was studied in essentially the same manner as described above. Values of some pertinent chemical shifts are given in table (4-9). In this case the proton spectrum of a dioxane solution containing 0.99 moles/litre of piperidine and 0.51 moles/litre of water was measured and was found to show a combined signal arising from the piperidine NH and water protons. This spectrum clearly corresponds to the "exchange narrowing" region of exchange rates, the combined signal being $0.91 (\pm 0.2)$ c.sec.⁻¹ broader than the width due to the field inhomogeneity. The broadening of the combined signal was analysed using equation (2-53), giving τ_w the mean lifetime of a water proton between exchanges, equal to 1.96×10^{-4} sec.

It is reasonable to suppose that proton exchange is brought about by the reversible cycle,



where B denotes piperidine and $\text{HO}^- \cdot \text{HB}^+$ represents an intimate ion pair in which the hydroxide ion and the

/piperidinium

piperidinium ion are linked by a hydrogen bond. The second-order rate constant k_3 for the ionization step of the reversible cycle (4-27) was related to τ_w by means of the relationship

$$2 \times \frac{1}{\tau_w} (\text{H}_2\text{O})_o = k_3 (\text{H}_2\text{O})_o (\text{B})_o \quad (4-28)$$

giving $k_3 = 1.0 \times 10^4 \text{M}^{-1} \text{sec.}^{-1}$ Equation (4-28) being the analogue of equation (4-26), the above value of k_3 is probably best regarded as a lower limit to the second-order rate constant for the formation of the ion pair $\text{HO}^- \cdot \text{HB}^+$.

CHAPTER V

DISCUSSION

Chapter V. Discussion

5.1. Hindered Internal Rotation

5.2. Proton Exchange in Aqueous Dioxane

TABLE 5-1

Activation Parameters for Internal Rotation in p-Nitroso-N,N-dimethylaniline
and Parameters for the Internal Rotation in three other related Compounds

Compound	Solvent	ΔG^\ddagger_{298} kcal./mole	ΔH^\ddagger kcal./mole	ΔS^\ddagger cal. mole ⁻¹ deg. ⁻¹	ref.
p-nitroso-N,N-dimethylaniline	acetone	12.1 \pm 0.5 11.8 \pm 0.5 ^a	11.2 \pm 1.1	-3.0 \pm 5	
N,N-dimethylnitrosamine	none	22.8	22.1	-2.5	134
p-N,N-dimethylaminobenzaldehyde	vinyl chloride	10.8 ^a			34
N,N-dimethylformamide	none	21.0	18.3 \pm 0.7	-9.1	25

a refers to free energy change at 202°K

5.1. Hindered Internal Rotation

Activation parameters for internal rotation in p-nitroso-N,N-dimethylaniline, and parameters for the internal rotation of three other related compounds are given in table (5-1). In all four examples there is little doubt the barrier results from conjugation between $-NMe_2$ and NO and CHO. NO and CHO seem about equally effective in this conjugation, though NO may be slightly more effective. The phenyl ring attenuates the conjugation, cutting the barrier to approximately one half on passing from N,N-dimethylnitrosoamine to p-nitroso-N,N-dimethylaniline.

If the barrier to rotation is assumed to have the simple form

$$V = \frac{1}{2}V_2(1 - \cos 2\theta) \quad (5-1)$$

it can be shown that the first few energy levels of the NO torsion obey the equation

$$(E_v - E_0)/hc = v\sigma_0 - \frac{1}{2}v(v+1)\sigma_1 \quad (5-2)$$

with $\sigma_1 = h/8\pi^2 c I_r$. Setting $V_2 = \Delta H^\ddagger = 11.2$ kcal./mole and $^{114} I_r = 9.67$ a.m.u. \AA^2 one obtains

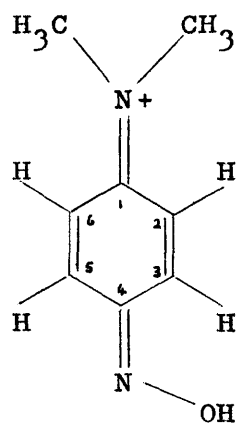
$$\sigma_0 = 165.3 \quad \text{and} \quad \sigma_1 = 1.75 \text{ cm.}^{-1}$$

Frequencies calculated for the fundamental and lower "hot" bands are then 164 (1-0 transition), 162

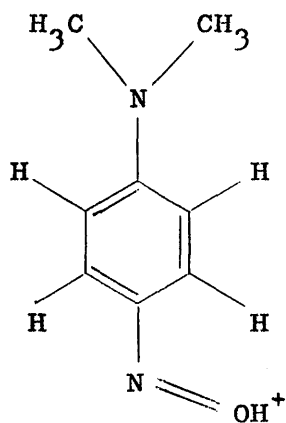
$$(2-1),$$

(2-1), 160 (3-2) and 158 (4-3) cm.^{-1} etc., in good agreement with the observation in solution of a relatively sharp infra-red peak at 166 cm.^{-1}

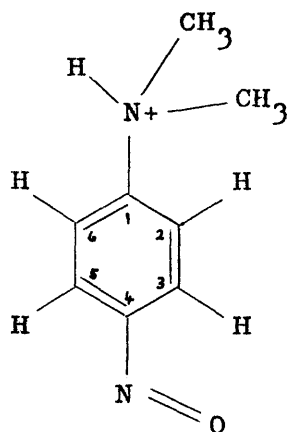
Interesting information about the structure of the ion formed when p-nitroso-N,N-dimethylaniline (I) accepts a proton can be derived from data given in Chapter IV, it being possible to discriminate between the oxygen-protonated form (III) and the nitrogen-protonated form (III').



(a)
(III)



(b)
(III')



(III')

In Chapter IV, a lower limit to the free energy of activation ΔG^\ddagger for internal rotation about the C_4 -N bond in the conjugate acid of p-nitroso-N,N-dimethylaniline was found to be $16.9 \text{ kcal.mole}^{-1}$ at 33.5°C . This lower limit is substantially greater than the free energy of activation for the analogous internal rotation in the unprotonated aniline ($\Delta G^\ddagger = 12.1 \pm 0.5 \text{ kcal.mole}^{-1}$ at 33.5°C). Assuming the entropy of activation does not differ greatly for these two internal rotations, it follows that there is an increase in barrier height on passing from p-nitroso-N,N-dimethylaniline to its conjugate acid. This increase in barrier height indicates that oxygen-protonation /predominates,

predominates, since oxygen-protonation would lead to an increase in partial double-bond character in the C_4-N bond¹⁰⁰ and so would cause an increase in barrier to internal rotation about this bond, whereas addition of a proton to the dimethylamino nitrogen atom would lead to a decrease in π -character in the C_4-N bond¹⁰⁰ and so would cause a decrease in barrier.

It is noteworthy that solutions of p-nitroso-N,N-dimethylaniline in trifluoroacetic acid show no absorption (in the range 600-850m μ) attributable to the $n \rightarrow \pi^*$ transition of a nitroso group, this absence of absorption being fully consistent with predominant oxygen-protonation.

Further confirmation that protonation occurs predominantly on oxygen can be obtained from the infra-red spectrum of a saturated solution of p-nitroso-N,N-dimethylaniline hydrochloride in dry chloroform in the range 3150-3650 $cm.^{-1}$. The only band in this range occurs at 3630 $cm.^{-1}$ ($\Delta\nu_{\frac{1}{2}} = 37 \text{ cm.}^{-1}$) and can almost certainly be assigned¹³⁶ to the stretching fundamental of the OH group of the oxygen-protonated cation (III).

It is of interest to note that the ortho coupling constants J_{23} and J_{56} increase significantly on

/passing

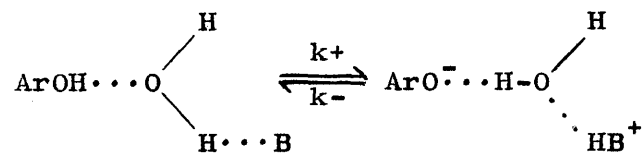
passing from unionised p-nitroso-N,N-dimethylaniline ($J_{23} = J_{56} = + 9.1 \text{ c. sec.}^{-1}$) to the conjugate acid of the aniline in trifluoroacetic acid ($J_{23} = +11.18 \text{ c. sec.}^{-1}$, $J_{56} = + 10.77 \text{ c. sec.}^{-1}$). The markedly increased coupling between H_2 and H_3 and between H_5 and H_6 , attributable to increased partial double-bond character in the C_2-C_3 and C_5-C_6 bonds, indicates that the quinonoid canonical form (IIIa) makes a relatively large contribution to the actual electronic structure of the oxygen-protonated cation (III).

5.2. Proton Exchange in Aqueous Dioxane

In series (a) (Section 4.10), the rate of exchange of the phenolic -OH protons R and the rate of exchange of the water protons R' were found to be equal within the limits of experimental error. This result indicates that water is involved in some fundamentally important way in the piperidine-catalysed protolysis of 2,6-di-*t*-butylphenol in aqueous dioxane.

A possible mechanism for proton exchange in aqueous dioxane can be formulated as follows:

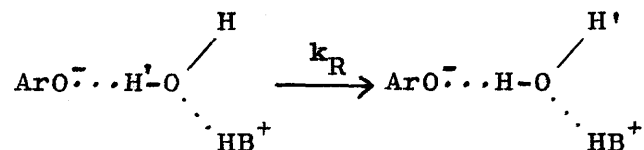
- (a) reversible ionization to produce a caged ion pair in which the phenoxide ion and the piperidinium ion are separated by a water molecule



(VIII)

(5-3)

- (b) reorientation of the water molecule within the ion pair



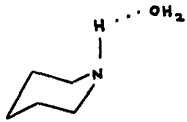
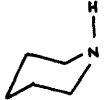
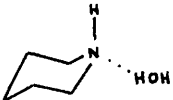
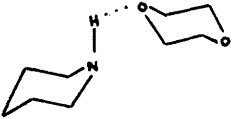
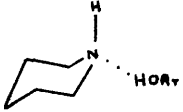
/Processes

Processes analogous to the forward and reverse steps of the reversible cycle (5-3a) are well established and have been described in some detail in Section 3.1. The forward step of cycle (5-3a) may be a concerted process involving simultaneous (or nearly simultaneous) transfer of the proton from the phenol to the hydrogen-bonded water molecule, and from the water molecule to the hydrogen-bonded piperidine molecule.

It is very important to note that the reversible cycle (5-3a) does not lead to proton exchange unless reorientation of the water molecule (process (5-3b)) occurs during the lifetime of the ion pair, that is, if the reverse step of cycle (5-3a) takes place when the water molecule has the same orientation as when the pair was formed, the cycle will lead only to momentary escape of the phenolic OH proton and not to exchange. Clearly, therefore, the rate of proton exchange between the phenolic OH and water sites is dependent not only upon the rate constant for the forward step of cycle (5-3a) (k_+ sec.⁻¹) but also upon the relative magnitudes of the rate constants for the reverse step of cycle (5-3a) (k_- sec.⁻¹) and the reorientation process (k_R sec.⁻¹). However, to obtain a molecular explanation of the medium effect in series (a), (b) and (c) the rate constants k_+ , k_- , and k_R will be assumed to be independent of the medium and

/an attempt

TABLE 5-2 Possible 1:1- Complexes of Piperidine^c

1:1- complex ^a	Symbol	Equilibrium ^b
	ρW_1	$(\rho W_1) = K_1(\rho)(W)$
	ρ	
	ρW_2	$(\rho W_2) = K_2(\rho)(W)$
	ρD	$(\rho D) = K_3(\rho)(D)$
	ρP	$(\rho P) = K_4(\rho)(P)$

^a In the preferred form of piperidine, the nitrogen lone pair occupies an equatorial position.¹³⁷

^b ρ denotes piperidine and the symbols P, W, and D have the same significance as in Section 4.9., viz:
P = 2:6-di-t-butylphenol; W = water; D = dioxane.

^c Owing to the low concentrations of piperidine employed in series (a), (b) and (c) the formation of dimers and higher polymers of piperidine has been neglected.

an attempt will be made to explain the rates in terms of the changing concentration of the complex (VIII).

It is instructive to consider the equilibria forming sub-species of piperidine. Assuming the principal sub-species of piperidine to be complex (VIII) (also denoted by $PW\rho$) and the 1:1-complexes listed in table (5-2), material balance gives

$$(\rho)_o = (\rho) + (\rho W_1) + (\rho W_2) + (\rho D) + (\rho P) + (PW\rho) \quad (5-4)$$

The concentration of the complex (VIII), $(PW\rho)$, can be expressed in terms of the concentrations (P) , (W) , and (ρ) by means of the relationship

$$(PW\rho) = K_5(P)(W)(\rho) \quad (5-5)$$

Hence, combining equations (5-4) and (5-5) and the expressions given in table (5-2), one obtains

$$(\rho)_o = (\rho) \left\{ 1 + K_1(W) + K_2(W) + K_3(D) + K_4(P) + K_5(P)(W) \right\} \quad (5-6)$$

and, therefore,

$$(\rho) = \frac{(\rho)_o}{\left\{ 1 + [K_1 + K_2 + K_5(P)](W) + K_3(D) + K_4(P) \right\}} \quad (5-7)$$

Substituting the expression (5-7) for (ρ) into equation (5-5) gives

$$(PW\rho) = \frac{K_5(P)(W)(\rho)_o}{\left\{ 1 + [K_1 + K_2 + K_5(P)](W) + K_3(D) + K_4(P) \right\}} \quad (5-8)$$

From equation (5-8), it follows that the observed

/rate

rate of exchange, taken as proportional to the concentration of the complex (VIII), should conform to the relationship

Observed rate \propto
of exchange

$$\frac{(P)(W)(\rho)_o}{\{1 + [K_1 + K_2 + K_5(P)](W) + K_3(D) + K_4(P)\}} \quad (5-9)$$

When it is recalled that the stoichiometric concentrations of the phenol and water are constant throughout series (a), it is apparent that the denominator of the relationship (5-9) will be effectively constant throughout this series, only small changes in the concentrations (P), (W) and (D) being expected (Figure 4-8). The observed rate (measured from either the phenolic -OH resonance R or the water resonance R') is therefore expected to be proportional to the product (P)(W)(ρ)_o, this being consistent with the experimental rate law (4-23),

$$R = R' = k_1(P)(W)(\rho)_o$$

with

$$k_1 = 3.3_3 \times 10^4 \text{ M}^{-2} \text{ sec.}^{-1}$$

In series (b), the experimental rate law describing the rate of exchange R of the phenolic -OH protons was

/found

found to have the form (4-24),

$$R = 2.0 + k_1'(P)(W)(\rho)_0$$

with

$$k_1' = 3.06 \times 10^4 \text{ M}^{-2} \text{ sec.}^{-1}$$

The intercept of a plot (Figure 4-10) of R against the product $(P)(W)(\rho)_0$, corresponding to the first term of the rate expression (4-24), indicates that protolysis of the phenol occurs at a significant rate even in the absence of water, this being consistent with the findings of study (d) (see page 134). If it is assumed that the rate of proton exchange between piperidine >NH and phenolic -OH sites in dry dioxane obeys a rate law which is second-order, that is, first-order in each of piperidine and the phenol, then using equation (4-26) the broadening of the phenolic -OH resonance in series (b) for dry dioxane, corresponding to the value of the intercept, can be calculated. The extent of this broadening (in excess of the field inhomogeneity) can be easily found to a good approximation by means of Meiboom's dominant line treatment, equation (2-56), since the concentration of piperidine >NH sites ($4.5_1 \times 10^{-3} \text{ M}$) is much smaller than the concentration of phenolic -OH sites (1.00 M) in series (b). The value of the broadening calculated

/by the

by the above method (2.2 radians per second) is in good agreement with the observed value of the intercept of the plot of R against the product $(P)(W)(\rho)_0$ (Figure 4-10) which corresponds to a broadening of the phenolic -OH resonance of 2.0 radians per second.

It is of interest to recall that proton exchange was found to occur between piperidine >NH and water sites (in the absence of phenol) in study (e) (page 137). However, in studies (a), (b) and (c) no evidence could be found to suggest that proton exchange between piperidine >NH and water sites gives rise to a significant contribution to the width of the water line, this being consistent with the low concentrations of piperidine employed in these studies.

The form of the second term of the rate equation (4-24), (c.f. (4-23)), suggests that this term arises from the rate process for which the reaction mechanism (5-3) has been proposed. For (5-3) to be accepted as a possible mechanism in series (b), however, it must be shown that the second term of (4-24), $k_1'(P)(W)(\rho)_0$, is consistent with the relationship (5-9),

/Observed

Observed rate
of exchange \propto

$$\frac{(P)(W)(\rho)_o}{\{1 + [K_1 + K_2 + K_5(P)](W) + K_3(D) + K_4(P)\}}$$

In series (b), although (D) and (P) change relatively slightly, marked variation in (W) occurs (see Figure 4-8 and table (4-7)), it being therefore apparent that the denominator of the above relationship need not be effectively constant for this series. Unfortunately, the values of the equilibrium constants K_1 , K_2 , K_3 , K_4 and K_5 are unknown so that the variation of the denominator cannot be calculated. However, if it is assumed that (W) is sufficiently low throughout series (b) for the inequality (5-10) to hold.

$$[K_1 + K_2 + K_5(P)](W) \ll 1 + K_3(D) + K_4(P) \quad (5-10)$$

then it is possible that any tendency of the denominator to decrease with increasing stoichiometric water concentration $(W)_o$, due to decrease in $(K_3(D) + K_4(P))$ (see Figure 4-8 and table (4-7)), may be approximately cancelled by a reverse tendency of $[K_1 + K_2 + K_5(P)](W)$ to increase the denominator, so that the denominator as a whole would be relatively insensitive to change in the stoichiometric concentration of water. The rate of proton exchange corresponding to complex (VIII) would then be expected to be

proportional to the product $(P)(W)(\rho)_o$ as observed. It is of particular importance to note that the values of the rate constants k_1 and k'_1 in equations (4-23) and (4-24) respectively are equal within the limits of experimental error, this tending to confirm the proposed interpretation of the kinetic data.

The process (5-3a) of mechanism (5-3), it is worth noting, corresponds to maximum economy in the use of water molecules to solvate the dipolar transition state.

Glossary of Symbols for Chapters IV and V

c	velocity of light
D	dioxane
h	Planck's constant
J	coupling constant
K	equilibrium constant
k	rate constant
k	Boltzmann's constant
P	2:6-di-t-butylphenol
T	absolute temperature
W	water
ΔG^\ddagger	free energy of activation
ΔH^\ddagger	enthalpy of activation
ΔS^\ddagger	entropy of activation
$\Delta \nu_{\frac{1}{2}}$	full-width at half-height of a spectral line
δ	chemical shift
K	transmission coefficient in transition-state theory
ρ	piperidine

References

1. De Maeyer and Kustin, *Ann. Rev. Phys. Chem.*,
1963, 14, 5.
2. Grunwald and Price, *J. Amer. Chem. Soc.*,
1964, 86, 2965.
3. Grunwald and Price, *J. Amer. Chem. Soc.*,
1964, 86, 2970.
4. Grunwald and Price, *J. Amer. Chem. Soc.*,
1964, 86, 4517.
5. Grunwald and Cocivera, *Discussions Faraday Soc.*,
1965, in the press.
6. Grunwald and Cocivera, *J. Amer. Chem. Soc.*,
1965, 87, 2070.
7. "Bronsted, *Rec. trav. chim.*, 1923, 42, 718;
Lowry, *Chem. and Ind.*, 1923, 42, 43.
8. Hantzsch and Veit, *Ber.*, 1899, 32, 615;
Wynne-Jones, *J. Chem. Phys.*, 1934, 2, 381;
Maron and La Mer, *J. Amer. Chem. Soc.*, 1938, 60, 2588;
Bell and Norris, *J. Chem. Soc.*, 1941, 118;
Bell and Clunie, *Proc. Roy. Soc.*, 1952, A212, 16.
9. Lewis and Seaborg, *J. Amer. Chem. Soc.*,
1939, 61, 1894.
10. Pearson, *J. Amer. Chem. Soc.*, 1948, 70, 204.

11. Wiberg, Chem. Rev., 1955, 55, 715.
12. Westheimer, Chem. Rev., 1961, 61, 429.
13. Bell, "Acid-Base Catalysis", Clarendon Press, Oxford, 1941.
14. Delahay, "New Instrumental Methods in Electrochemistry", Interscience Publishers, Inc., New York, 1954, ch. V.
15. Eigen, Discussions Faraday Soc., 1954, 17, 194.
16. Weller, Z. Elektrochem., 1952, 56, 662;
1954, 58, 849; 1956, 60, 1144; 1957, 61, 956;
Weller, Z. physik. Chem. (Frankfurt), 1955, 3, 238.
17. Eigen and de Maeyer, Z. Elektrochem., 1955, 59, 986.
18. Onsager, J. Chem. Phys., 1934, 2, 599;
Debye, Trans. Electrochem. Soc., 1942, 82, 265.
19. Kreevoy and Mead, J. Amer. Chem. Soc.,
1962, 84, 4596.
20. Wilson in "Advances in Chemical Physics",
ed. Prigogine, vol. II, Interscience Publishers, Inc.,
New York, 1959, pp. 367-393.
21. Looney, Phillips and Reilly, J. Amer. Chem. Soc.,
1957, 79, 6136.
22. Phillips, Looney and Spaeth, J. Mol. Spectroscopy,
1957, 1, 35.
23. Piette and Anderson, J. Chem. Phys., 1959, 30, 899.

24. Gray and Reeves, J. Chem. Phys., 1960, 32, 1878.
25. Rogers and Woodbrey, J. Phys. Chem., 1962, 66, 540
26. Woodbrey and Rogers, J. Amer. Chem. Soc.,
1962, 84, 13.
27. Gutowsky and Holm, J. Chem. Phys., 1956, 25, 1228.
28. Fraenkel and Franconi, J. Amer. Chem. Soc.,
1960, 82, 4478.
29. Sunners, Piette and Schneider, Canad. J. Chem.,
1960, 38, 681.
30. Franconi, Z. Elektrochem., Ber. Bunsenges.
Physik. Chem., 1961, 65, 645.
31. Fateley, Harris. Miller and Witkowski,
Spectrochim. Acta, 1965, 21, 231.
32. Aston, Szasz, Wolley and Brickwedde,
J. Chem. Phys., 1948, 14, 67.
33. Silver and Wood, Trans. Faraday Soc., 1964, 60, 5.
34. Anet and Ahmad, J. Amer. Chem. Soc., 1964, 86, 119.
35. Heidberg, Weil, Janusonis and Anderson,
J. Chem. Phys., 1964, 41, 1033.
36. Ramsey, "Nuclear Moments", Wiley and Sons, Inc.,
New York, 1953.
37. Pake, Solid State Phys., 1956, 2, 1.

38. Andrew, "Nuclear Magnetic Resonance", Cambridge University Press, London and New York, 1956, p. 9.
39. Purcell, Torrey and Pound. Phys. Rev. 1946, 69, 37.
40. Bloch, Hansen and Packard, Phys. Rev., 1946, 69, 127.
41. Andrew, "Nuclear Magnetic Resonance", Cambridge University Press, London and New York, 1956, p. 35-73.
42. Pople, Schneider and Bernstein, "High-Resolution Nuclear Magnetic Resonance", McGraw-Hill, New York, 1959, p. 50-86.
43. Ramsey and Purcell, Phys. Rev., 1952, 85, 143.
44. Jackman, "Applications of Nuclear Magnetic Resonance Spectroscopy in Organic Chemistry", Pergamon Press, London, Oxford, New York and Paris, 1959, p. 20.
45. Jackman, "Applications of Nuclear Magnetic Resonance Spectroscopy in Organic Chemistry", Pergamon Press, London, Oxford, New York, and Paris, 1959, p. 25.
46. Bloembergen, Purcell and Pound, Phys. Rev., 1948, 73, 679.
47. Pople, Schneider and Bernstein, "High-Resolution Nuclear Magnetic Resonance", McGraw-Hill, New York, 1959, ch. 9.

48. Pople, Schneider and Bernstein, "High-Resolution Nuclear Magnetic Resonance", McGraw-Hill, New York, 1959, p. 30.
49. Bloch, Phys. Rev., 1946, 70, 460.
50. See, for example, Pople, Schneider and Bernstein, "High-Resolution Nuclear Magnetic Resonance", McGraw-Hill, New York, 1959, p. 31-34.
51. Gutowsky, McCall and Slichter, J. Chem. Phys., 1953, 21, 279.
52. McConnell, J. Chem. Phys., 1958, 28, 430.
53. Jacobsohn and Wangsness, Phys. Rev., 1948, 73, 942.
54. Meiboom, J. Chem. Phys., 1961, 34, 375.
55. Loewenstein and Meiboom, J. Chem. Phys., 1957, 27, 1067.
56. Anbar, Loewenstein and Meiboom, J. Amer. Chem. Soc., 1958, 80, 2630.
57. Grunwald, Loewenstein and Meiboom, J. Chem. Phys., 1957, 27, 630.
58. Takeda and Stejskal, J. Amer. Chem. Soc., 1960, 82, 25.
59. Arnold, Phys. Rev., 1956, 102, 136.
60. Pople, Schneider and Bernstein, "High-Resolution Nuclear Magnetic Resonance", McGraw-Hill, New York, 1959, ch. 6.

61. Grunwald, Jumper and Meiboom, J. Amer. Chem. Soc., 1962, 84, 4664.
62. Pople, Schneider and Bernstein, "High-Resolution Nuclear Magnetic Resonance", McGraw-Hill, New York, 1959, p. 24.
63. Solomon and Bloembergen, J. Chem. Phys., 1956, 25, 261.
64. Kaplan, J. Chem. Phys., 1958, 28, 278.
65. Grunwald, Jumper and Meiboom, J. Amer. Chem. Soc., 1963, 85, 522.
66. Emerson, Grunwald and Kromhout, J. Chem. Phys., 1960, 33, 547.
67. Glasstone, Laidler and Eyring, "The Theory of Rate Processes", McGraw-Hill, New York, 1941.
68. Albery, Ann. Reports, 1963, 60, 40.
69. "A General Discussion on the Kinetics of Proton Transfer Processes", Discussions Faraday Soc., 1965, in the press.
70. Loewenstein and Connor, Ber. Bunsenges. Physik. Chem., 1963, 67, 280.
71. Grunwald, Loewenstein and Meiboom, J. Chem. Phys., 1956, 25, 382.
72. Grunwald, Karabatsos, Kromhout and Purlee, J. Chem. Phys., 1960, 33, 556.

73. Loewenstein, J. Phys. Chem., 1963, 67, 1728.
74. Grunwald, J. Chem. Phys., 1963, 67, 2208.
75. Silver and Luz, J. Amer. Chem. Soc., 1961, 83, 786.
76. Eigen and de Maeyer, in "Rates and Mechanisms of Reactions", Friess, Lewis and Weissberger, ed., part II, Interscience Publishers, Inc., New York, 1963, p. 1031-1050.
77. Grunwald, J. Phys. Chem., 1963, 67, 2211.
78. Emerson, Grunwald, Kaplan and Kromhout, J. Amer. Chem. Soc., 1960, 82, 6307.
79. Swain and Labes, J. Amer. Chem. Soc., 1957, 79, 1084.
80. Swain, McKnight and Kreiter, J. Amer. Chem. Soc., 1957, 79, 1088.
81. Luz and Meiboom, J. Chem. Phys., 1963, 39, 366.
82. Cocivera, Grunwald and Jumper, J. Phys. Chem., 1964, 68, 3234.
83. Krakower and Reeves, Trans. Faraday Soc., 1963, 59, 2528.
84. Grunwald and Meiboom, J. Amer. Chem. Soc., 1963, 85, 2047.
85. Grunwald and Jumper, J. Amer. Chem. Soc., 1963, 85, 2051.
86. Feldbauer and Weller, Z. Physik. Chem. (Frankfurt), 1962, 32, 263.

87. Luz and Meiboom, J. Amer. Chem. Soc., 1963, 85, 3923.
88. Luz and Meiboom, J. Amer. Chem. Soc., 1964, 86, 4764.
89. Luz and Meiboom, J. Amer. Chem. Soc., 1964, 86, 4766.
90. Luz and Meiboom, J. Amer. Chem. Soc., 1964, 86, 4768.
91. Sheinblatt, J. Chem. Phys., 1962, 36, 3103.
92. Sheinblatt, J. Chem. Phys., 1963, 39, 2005.
93. Sheinblatt and Gutowsky, J. Amer. Chem. Soc.,
1964, 86, 4814.
94. Dannhauser and Bahe, J. Chem. Phys., 1964, 40, 3058;
Dannhauser and Cole, J. Amer. Chem. Soc.,
1952, 74, 6105.
95. Phillips in "Determination of Organic Structures by
Physical Methods", Nachod and Phillips, ed., vol. 2,
Academic Press, New York and London, 1962, p. 437-445.
96. Pople, Schneider and Bernstein, "High-Resolution
Nuclear Magnetic Resonance", McGraw-Hill,
New York, 1959, ch. 13.
97. Phillips, J. Chem. Phys., 1955, 23, 1363.
98. Gillespie and Birchall, Canad. J. Chem.,
1963, 41, 148.
99. Loewenstein, Melera, Rigny and Walter,
J. Phys. Chem., 1964, 68, 1597.
100. Ingold, "Structure and Mechanism in Organic
Chemistry", Bell and Sons Ltd., London, 1953, ch. 2.

101. Kramer and Gompper, Z. Physik. Chem., (Frankfurt),
1964, 43, 292.
102. Kramer and Gompper, Z. Physik. Chem., (Frankfurt),
1964, 43, 349.
103. Tarte, J. Chem. Phys., 1952, 20, 1570.
104. Kaplan and Meloy, Tetrahedron Letters, 1964, 2427.
105. Barfield, Lappert and Lee, Proc. Chem. Soc.,
1961, 421.
106. Kilb, Lin and Wilson, J. Chem. Phys., 1957, 26, 1695.
107. Leffler and Grunwald, "Rates and Equilibria of
Organic Reactions", Wiley and Sons, Inc., New York, 1963.
108. Baeyer and Caro, Ber., 1874, 7, 963.
109. Pople, Schneider and Bernstein, "High-resolution
Nuclear Magnetic Resonance", McGraw-Hill, New York,
1959, p. 74.
110. Anderson, Ph.D. Thesis, Glasgow University, 1964.
111. Brown, Varian Associates, private communication.
112. Cook, Varian Associates, private communication.
113. Chelton and Mann, "Cryogenic Data Book", National
Bureau of Standards, Cryogenic Engineering Laboratory,
Boulder, Colorado, 1956.
114. Pitzer, J. Chem. Phys., 1946, 14, 239.
115. Donohue and Trueblood, Acta Cryst., 1956, 2, 960.
116. Webster, J. Chem. Soc., 1956, 2841.

117. Pesteiner and Brück, in Landolt-Bornstein,
"Tabellen, Zahlenwerte und Funktionen", I Band,
3 Teil (Molekeln II), Springer-Verlag, Berlin, 1951.
118. Lüttke, J. Phys. Radium, 1954, 15, 633; Lüttke,
Z. Elektrochem., 1957, 61, 302; Tarte, Bull. Soc.
chim. belges, 1954, 63, 525; Mason and Dunderdale,
J. Chem. Soc., 1956, 754.
119. Nakamoto and Rundle, J. Amer. Chem. Soc.,
1956, 78, 1113.
120. Keussler and Lüttke, Z. Elektrochem., 1959, 63, 614.
121. Wallace, Ph. D. Thesis, Glasgow University, 1964.
122. Pople, Schneider and Bernstein, "High-Resolution
Nuclear Magnetic Resonance", McGraw-Hill, New York,
1959, p. 39.
123. Brand and Speakman, "Molecular Structure: the
Physical Approach", Arnold (Publishers) Ltd.,
London, 1960, p. 8.
124. Paul and Long, Chem. Revs., 1957, 57, 1.
125. Randles and Tedder, J. Chem. Soc., 1955, 1218.
126. Davis and Addis, J. Chem. Soc., 1937, 1622.
127. Kolthoff and Bruckenstein, J. Amer. Chem. Soc.,
1956, 78, 1.
128. Dannhauser and Cole, J. Amer. Chem. Soc.,
1952, 74, 6105.

129. Bell, "The Proton in Chemistry". Methuen and Co. Ltd., London, 1959, ch. IV.
130. Bellamy, Eglinton and Morman, J. Chem. Soc., 1961, 4762.
131. Somers and Gutowsky, J. Amer. Chem. Soc., 1963, 85, 3065.
132. Pople, Schneider and Bernstein, "High-Resolution Nuclear Magnetic Resonance", McGraw-Hill, New York, 1959, ch. 15.
133. McGlashan and Rastogi, Trans. Faraday Soc., 1958, 54, 496.
134. Looney, Phillips and Reilly, J. Amer. Chem. Soc., 1957, 79, 6136; Leffler and Grunwald, "Rates and Equilibria of Organic Reactions", Wiley and Sons, Inc., New York, 1963, p. 116.
135. Fuoss and Kraus, J. Amer. Chem. Soc., 1933, 55, 1019.
136. Bellamy, "The Infra-red Spectra of Complex Molecules", Methuen and Co. Ltd., London, 1958.
137. Costain and Parkin, Proc. XXth Conference on Molecular Spectroscopy, Columbus, Ohio, 1965.

Relevant Publications

"Internal Rotation in p-Nitrosodimethylaniline",
by D. D. MacNicol, R. Wallace and J. C. D. Brand,
Trans. Faraday Soc., 1965, 61, 1.

"Proton Transfer in Aqueous-Organic Solvents",
by J. C. D. Brand, D. D. MacNicol and
D. G. Williamson, Chem. Comm., 1965, 123.